THE UNIVERSITY OF CHICAGO

THE EVOLUTIONARY ANATOMY, BIOMECHANICS, AND DIVERSIFICATION DYNAMICS OF REPEATEDLY EVOLVED MASSETER MUSCLES IN RODENTS

A DISSERTATION SUBMITTED TO

THE FACULTY OF THE DIVISION OF THE BIOLOGICAL SCIENCES

AND THE PRITZKER SCHOOL OF MEDICINE

IN CANDIDACY FOR THE DEGREE OF

DOCTOR OF PHILOSOPHY

COMMITTEE ON EVOLUTIONARY BIOLOGY

BY

DALLAS KRENTZEL

CHICAGO, ILLINOIS

JUNE 2019

Table of Contents

List of Figures

List of Tables

Acknowledgements

I have to thank my committee for their many, many, many hours of work in meetings helping me along the way all of these years. Getting a Ph.D. had been my passion since I was a sophomore in high school, but Ken Angielczyk, Graham Slater, Callum Ross, Mike Coates, and Bruce Patterson made sure that it would actually be a dream come true. They kept me honest, focused, and put me back on task when I was off studying porcupines for fun.

The graduate students in the Darwin Cluster deserved my utmost thanks for keeping me sane and making sure that my experience here was memorable, enjoyable, and most of all filled the loving relationships of true friendship.

My family was instrumental in getting me here today. We didn't grow up easy, but my mom, Theresa Glavin, always made sure to support my curiosity and intellect and always told me to follow my goals. My sister paved each step of the way, as she is 17 months older than I and demonstrated time after time that getting an education was possible and worthwhile.

I was fortunate to meet a number of excellent mentors that guided me to a path of science. My high school AP Biology teach Mrs. Bronwyn Young recognized my interests and passions and made sure I was trained in an actual scientific lab setting before I graduated high school. That's how I came to work with Dr. Tammy Dugas, who trained me along with her graduate students for 3 years learning the basics of experimentation, data analysis, and what it took to make it in academia. My college advisors Dr. Cynthia Brame, Dr. Beth Leuck, Dr. Jeff Agnew, and Dr. Scott Chirhart went out of their ways to support my academic development and connect me to opportunities outside of Louisiana. Working with Dr. John Flynn and Dr. Christian Kammerer at

the AMNH was the essential step that brought me into my preferred field and the opportunities that the gave me were invaluable and life changing.

Finally, I have to thank my partner, Andrea DaViera, for supporting me throughout the end my Ph.D. Without her I may have never have gotten to this point and fulfilled this life long dream.

Abstract

Explaining large scale transitions in discrete morphology is one of the most challenging problems in biology, requiring input from anatomy, biomechanics, ecology, paleontology, development, and genomics to appropriately contextualize evolutionary events. Rodents evolved discrete masseter muscle arrangements including novel muscle units that evolve homoplastically in clades of diverse ecological strategies and differing levels of species richness. These derived conditions, sciuromorphy, hystricomorphy, and myomorphy, differ from the primitive condition, protrogomorphy, in the anterior attachment of novel masseter muscles that have been thought represent specializations for gnawing or chewing mechanics. Here I test the hypotheses that these novel muscles function optimally at particular bite points and bias clade histories towards more gnawing or chewing intensive ecologies. I examine the functional ecomorphology of rodent dentition relative to masseter conditions, the biomechanics of individual muscles in different chewing positions, and the detailed anatomy of these muscles in key taxa with extreme cranial modifications, using a dataset comprised of over 200 rodent species. These studies reveal that sciuromorphy and hystricognathy are associated with gnawing and chewing specializations, respectively. In contrast, clades characterized by myomorphy demonstrate limited morphological and biomechanical evolution at lower evolutionary rates despite their high rates of taxonomic diversification and wide range of ecological habits compared to other groups. Strikingly, non-myomorph arid adapted rodents with large auditory bullae and reduced size of the temporalis muscle demonstrate major jaw muscle rearrangements, but arid-adapted myomorphs with temporalis reduction fail to demonstrate similar compensatory adaptations, implying that dual anterior attachments of derived masseter muscles are sufficient to conduct most major functional

roles of the masticatory system. These data suggest that at least sciuromorphy and myomorphy conform to the typical hypotheses of muscle function and gnawing specialties, and are consistent with myomorphy serving as a key innovation in rodent dietary and functional evolution. These studies demonstrate that masseter conditions have profound impacted the functional and ecological evolution of rodents and baised clades toward differing histories that favor gnawing, chewing, or both strategies for ingestion. These studies demonstrate that masseter conditions have profoundly impacted the functional and ecological evolution of rodents and baised clades toward differing histories that favor gnawing, chewing, or both strategies for ingestion. Furthermore, this study has shown that detailed examination of masseter anatomy in rodents can still reveal previously undocumented morphologies, and that the functional flexibility of myomorphy significantly affects the dynamics of rodent macroevolution.

Introduction

The evolution of novel anatomies and large saltatorial jumps in the evolution of morphology presents key challenges in modern evolutionary theory. Understanding the drivers of large, discrete morphological transitions in evolution requires an integrative approach utilizing ecology, biomechanics, paleontology, development, and genomics to appropriately delineate the key factors influencing phenotype. For example, subsequent to the Cambrian Explosion, arthropods demonstrate an inordinate variety of bodyplans and become dominant ecologically across marine systems. However, a subgroup of arthropods, insects, fail to experiment with bodyplan evolution, retaining the same patterns of tagmatization across nearly all species despite exhibiting the highest diversity of all animal by far. Novelties and discrete morphological transitions thus likely play complex roles in influencing macroevolution that require similarly complex consideration in order to properly contextualize.

Rodents demonstrate a number of discrete and complex morphological transitions from the mammalian bauplan that limit our understanding of their evolutionary morphology, biomechanics, and the details of the evolutionary anatomy, but retain these structure seemingly as they are soon after their early evolutionary establishment. Given their diversity, rodents can thus be considered the “insects of mammals,” diversifying and occupying vast and diverse ecological space using the same novel toolkits over and over again. Unlike all other mammals, rodents do not occlude their entire dental arcade simultaneously, but instead when they occlude their cheekteeth their incisors are separated, and to occlude their incisors to gnaw they must thrust their mandible anteriorly, misaligning the cheekteeth and preventing their occlusion. This novel mechanical relationship would conceivably reduce the constraints on the masticatory

apparatus to vary more substantially anteroposteriorly, as the the gnawing and chewing systems would be quasi-independent functionally and thus allowed to be more independent developmentally.

Subsequent to the evolution of this functionally novel masticatory system, rodents repeatedly evolved novel units of masseter muscles in new arrangements on the skull (Swanson et al. 2019; Fabre et al. 2011). These include sciuromorphy, in which the anterior deep masseter (ADM), a division of the deep masseter, originates on a large attachment surface on the cranium called the zygomatic plate anterior to the eye on the rostrum (Fig. I.1). This condition has been thought to be adapted to gnawing mechanics, with at least some comparative biomechanical data to support this contention (Druzinsky 2010a,b; Cox et al. 2012). Hystricomorphy is defined by the penetration of the infra-orbital foramen by an anterior unit of the zygomaticomandibularis (ZMIO), which originates on the rostrum and inserts laterally on the mandible after making a near 90 degree turn in some cases after passing through the infra-orbital foramen (Fig. I.1). It has been speculated to be important for chewing functions (Cox et al. 2012, Cox 2017). Myomorphy combines these latter features, with a medial ZMIO and a lateral ADM (Fig. I.1). It has been suggested to be a more efficient masseter system that can perform better at both chewing and gnawing intensive diets (Wood 1965, Cox et al. 2012).

Here, I aim to test these hypotheses of rodent masseter configuration adaptations and functions, as well as the hypothesis that these masseter conditions have remained mostly static in qualitative features of their morphology since the Eocene. I will do this by conducting a detailed comparative analysis of functional and dietary metrics across hundreds of rodent species across each individual evolution of derived masseter configuration, as well as a comparative biomechancial analysis of individual muscle units in the feeding system as they relate to

important functional metrics of the jaw. In each case I will take a phylogenetic perspective by modeling the tempo and mode of character evolution across the latest iteration of the rodent phylogeny (Upham et al. 2019) to test whether masseter configuration affect the evolutionary trajectories of functional metrics and biomechanical performance. Finally, I will conduct a detailed analysis of the three dimensional muscle morphology of select species of rodent with and without large auditory bullae to assess how the loss of the temporalis, usually a major feeding muscle, induces compensatory adaptations across masseter muscle conditions.

References

Cox, P.G. (2017). The jaw is a second-class lever in *Pedetes capensis* (Rodentia: Pedetidae). PeerJ 5, e3741.

Cox, P.G., and Jeffery, N. (2011). Reviewing the Morphology of the Jaw-Closing Musculature in Squirrels, Rats, and Guinea Pigs with Contrast-Enhanced MicroCt. The Anatomical Record: Advances in Integrative Anatomy and Evolutionary Biology 294, 915–928.

Cox, P.G., Rayfield, E.J., Fagan, M.J., Herrel, A., Pataky, T.C., and Jeffery, N. (2012). Functional Evolution of the Feeding System in Rodents. PLoS ONE 7, e36299.

Druzinsky, R.E. (2010a). Functional Anatomy of Incisal Biting in *Aplodontia rufa* and Sciuromorph Rodents - Part 1: Masticatory Muscles, Skull Shape and Digging. Cells Tissues Organs 191, 510–522.

Druzinsky, R.E. (2010b). Functional Anatomy of Incisal Biting in *Aplodontia rufa* and Sciuromorph Rodents – Part 2: Sciuromorphy Is Efficacious for Production of Force at the Incisors. Cells Tissues Organs 192, 50–63.

Fabre, P.-H., Hautier, L., Dimitrov, D., and Douzery, E.J.P. (2012). A glimpse on the pattern of rodent diversification: a phylogenetic approach. BMC Evolutionary Biology 12, 88.

Swanson, M., Oliveros, C.H. and Esselstyn, J. (2019). A phylogenomic rodent tree reveals the repeated evolution of masseter architectures. Proceedings of the Royal Society B: Biological Sciences. 286, 20190672.

Wood, A.E. (1965). Grades and Clades Among Rodents. Evolution 19, 115–130.

Figures

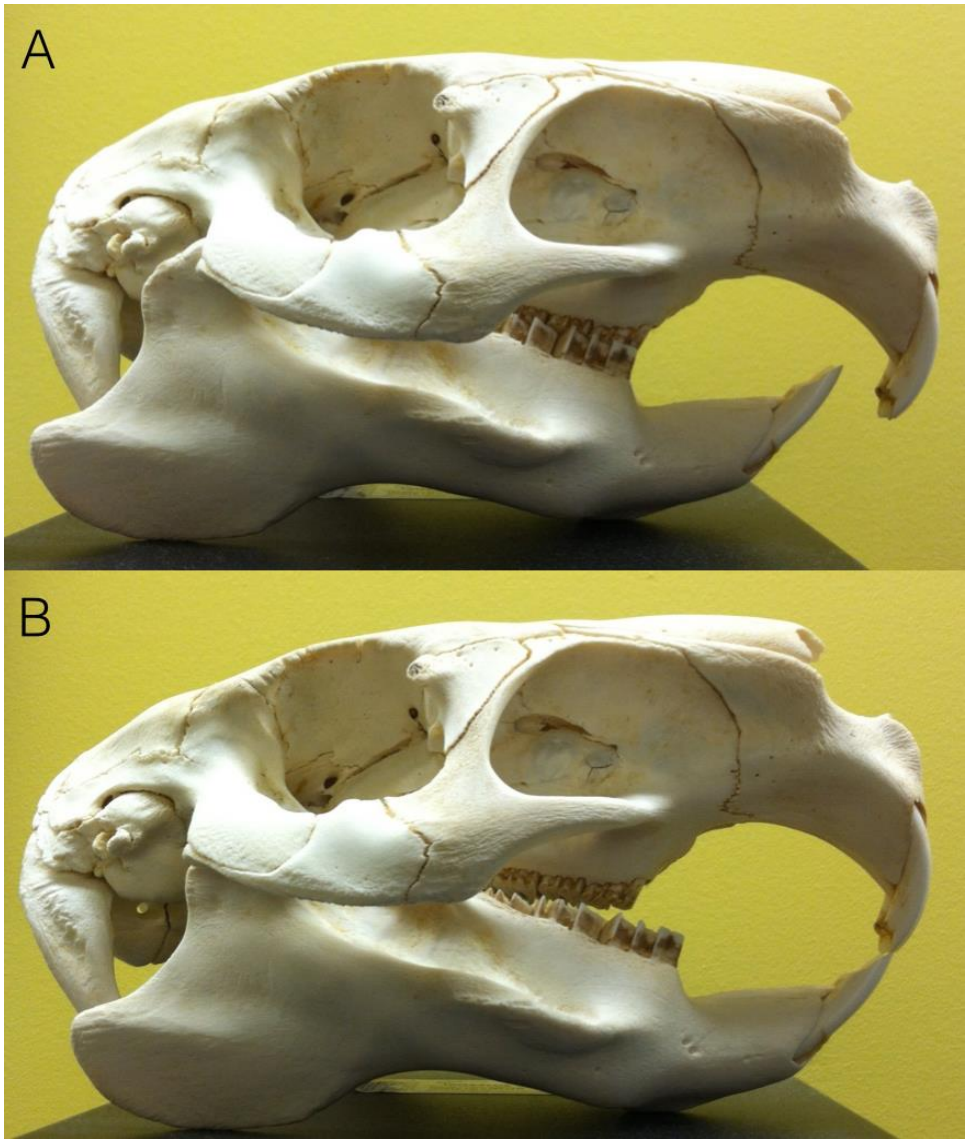

Figure I.1. Skull of capybara in gnawing and chewing positions. Capybara, *Hydrochoerus hydochaeris*, skull in A) chewing and B) gnawing positions. Notice the gap between the incisors in (A) and between the cheekteeth in (B), as well as the forward movement of the jaw joint in a static relationship with the rest of the mandible.

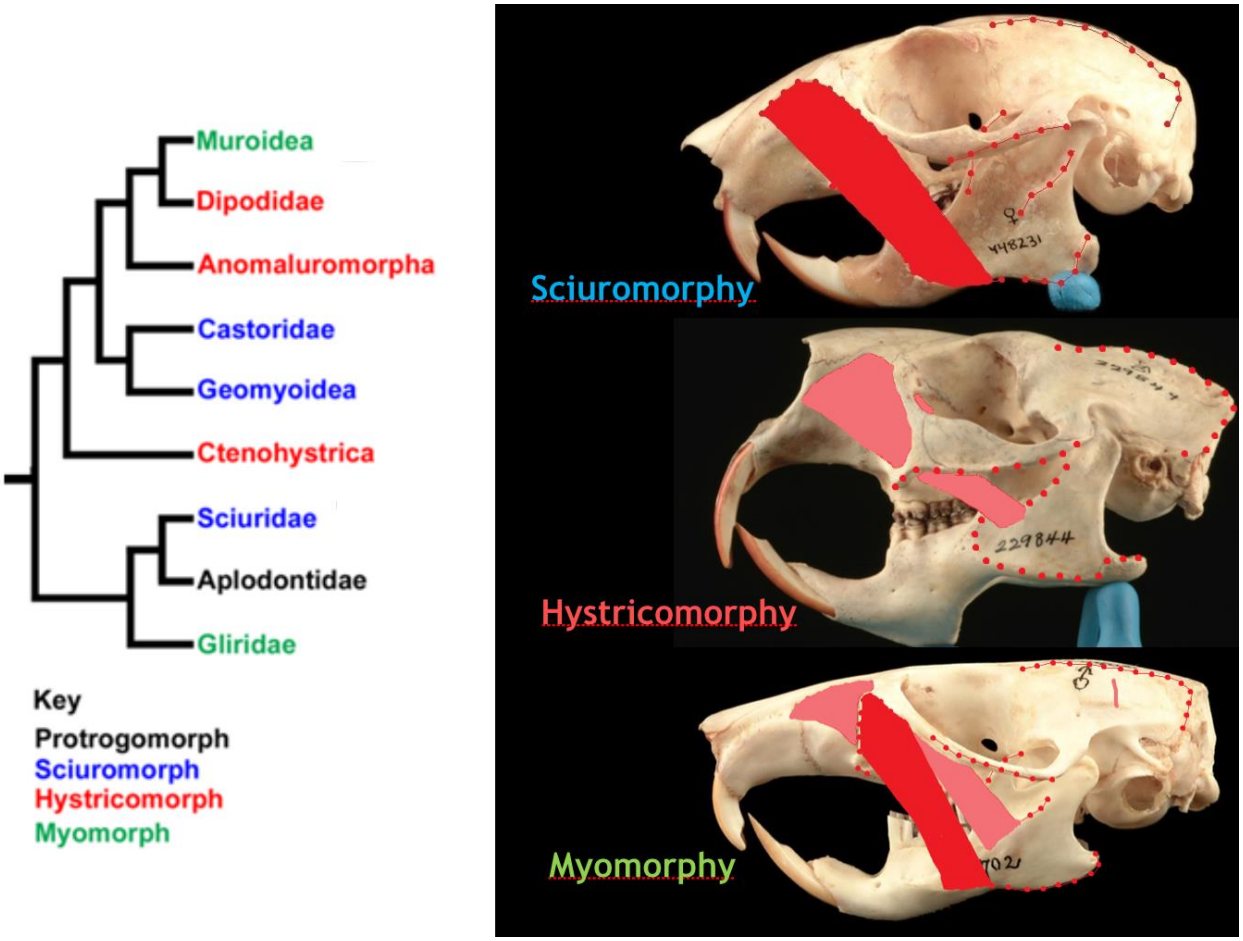

Figure I.2. Phylogeny of rodents and masseter conditions. Left: Phylogeny of rodents depicting multiple derivations of each masseter condition (modified from Cox and Jeffries 2011). Right: Representative skulls with illustrated muscle attachments and derived, diagnostic masserter units. Top: *Sciurus griseus*, sciuromorphy demonstrating the ADM, middle: *Erethizon dorsatum*, hystricomorphy, demonstrating ZMIO, and bottom: *Neotoma cinerea*, myomorphy, demonstrating dual ADM and ZMIO.

Chapter 1: Simple metrics of rodent dentition explain ecofunctional evolution and differentiate clades by masseter muscle configuration

Abstract

Studies of ecomorphology and functional morphology have provided important insight into the evolution of morphological variation across mammals. However, rodents have remained an understudied order despite their diversity and dominant ecological abundance in almost all terrestrial environments. Assessing rodent function and ecomorphology is limited by the uniqueness of the rodent masticatory apparatus, in which the incisors and cheekteeth do not occlude simultaneously during jaw closure and the masseter muscles have independently evolved novel divisions multiple times. Here I use simple metrics of the rodent incisor to argue that incisor depth and width are good predictors of functional and dietary signal across rodents. I then compare these functional and dietary predictors across masseter conditions to determine whether particular masseter conditions are biased in their evolutionary trajectories. I collected morphological data from the jaws of 275 rodent species spanning all independently-evolved masseter conditions to test the hypothesis that masseter conditions are optimized toward differing ecologies and functions, principally that sciuromorphy is adapted to gnawing intensive diets, hystricomorphy to chewing intensive diets, and myomorphy as a more generalized condition. Results demonstrate that dental allometry in rodents is similar across masseter conditions but some functionally-important outliers are apparent. Phylogenetic principal component analysis reveals that sciuromorph and some myomorph rodents evolve deep but thin incisors to gnaw on hard nuts and seeds, whereas hystricomorph taxa and some sciuromorphs are characterized by relatively small incisors when specializing in herbivory or faunivory. All subterranean taxa demonstrate similar incisor dimensions regardless of masseter condition, but only myomorphs

evolve specialized anteroposteriorly long but mediolaterally narrow cheekteeth rows associated with specialized grazing and folivory. Finally, evolutionary trait modeling demonstrates that myomorphs exhibit lower rates of evolution for dental characters despite exhibiting higher rates of phylogenetic species diversification, corroborating the hypothesis that myomorph rodents are successful because of an efficient, functionally flexible masticatory apparatus. This study is the first to compare functional and ecomorphological traits across rodent masseter conditions using a broad comparative approach, and crucially demonstrates key functional and dietary biases in these morphotypes and that are underlined by differential rates of trait evolution.

Introduction

The ecomorphology of the feeding system is a well studied topic in mammalogy (Janis and Ehrdhart 1988, Evans et al. 2007, Dumont et al. 2012, Santana et al. 2010, Slater et al. 2009), including in the most diverse order of mammals, Rodentia (Arregoitia et al. 2017, Samuels 2009, Galewski et al. 2005, Cano et al. 2017, Hautier et al. 2012). The uniqueness of the rodent feeding system's structure, biomechanics, and basic myology have been relatively unstudied in the context of ecomorphological evolution, however. Although the ecomorphology of the cheekteeth of rodents is generally comparable to trends seen in other diverse groups of mammals, such as carnivores, bats, and ungulates, the special role of the functionally independent, ever-growing incisor has received far less attention. Crucially, the major differences in the basic organization of the feeding muscles, primarily the masseters, are key to understanding how rodents differentially utilize their cheekteeth and incisors compared to other mammals.

The incisors of rodents are unique among extant mammals. Numerous other extant and extinct mammalian taxa have a single pair of incisors in the upper and lower jaw, including some

with ever-growing incisors. Rodents differ from all of these taxa in that their incisors never occlude during cheekteeth occlusion (chewing), in which the jaw is set posteriorly in the jaw joint, and their cheekteeth never occlude during incisor occlusion (gnawing), in which the jaw is shifted anteriorly with the mandibular condyle resting on the zygomatic process of the squamosal. This organization provides rodents with a functionally modularized feeding system, unlike that of any other mammals, in which the incisors never interfere with chewing behavior and the molars never interfere with gnawing behavior. I hypothesize that this separation of basic functionality decouples any existing evolutionary and developmental constraints that require precise occlusion of the entire tooth row, allowing each part of the jaw and dentition to develop and evolve at least quasi-independently. This scenario would allow rodents to easily evolve between gnawing and chewing specializations, making adaptations to both high-performance gnawing and chewing compatible in the same lineage.

Functionally modularized ever growing incisors are the primitive condition for rodents and are their most diagnostic feature (Meng et al. 2003, Druzinsky 2010a). The proliferation of masseter muscle diversity in rodents arose much later after the initial early divergences into major clades, with fossil data demonstrating that various rodent families retained the primitive jaw muscle arrangement protrogomorphy until the late Miocene, after which only the Aplodontidae remained (Hopkins 2008). The evolution of new masseter units and attachments occurred primarily in the mid to late Eocene and early Oligocene, with few such dramatic morphological changes happening thereafter (Marivaux 2004). I hypothesize that the elaboration of masseter musculature in rodents was a response to the biomechanical novelty of the modular masticatory system, facilitating new means of control over gnawing independent of molar occlusion and chewing independent of incisor occlusion. Derived masseter units promote more

efficient gnawing mechanics in gnawing specialists, and enhanced chewing mechanics in taxa with diets that require intense molar mastication, such as in high fiber specialist herbivores. If masseter configurations evolved to enhance the biomechanics of existing gnawing and chewing functions, we should expect to see differences between clades of differing masseter muscle configurations in terms of relative dental dimensions that are important for gnawing and chewing functions and ecomorphological correlates of diet.

Of the three derived masseter conditions, sciuromorphy has received the most biomechanical attention, with a variety of authors documenting enhanced gnawing proficiency compared to the modern protrogomorph Aplodontia rufa (sole surviving rodent species represented by the primitive masseter condition) and compared to other rodents (Druzinksy 2010a, 2010b; Cox et al. 2012). The insertion of the specialized anterior deep masseter unit in sciuromorphy is anterior to the rest of the jaw muscle insertion sites, granting it a high mechanical advantage necessary for maximizing force amplification in incisor bites. Hystricomorphy is diagnosed by a specialized insertion of the infraorbital portion of the zygomaticomandibularis (ZMIO) in a similar anterior position, however, the origin of this muscle on the cranium is far more complicated than for the origin of the anterior deep masseter in sciuromorphy, as the muscle bends at nearly a 90 degree angle to penetrate the infraorbital foramen and attach onto the lateral surface of the rostrum. Additionally, the insertion for the ZMIO is sometimes displaced laterally onto a bony shelf, as seen prominently in caviid rodents such as the guinea pig and capybara. Although the ZMIO could theoretically provide a similar role in maximizing mechanical advantage for the incisor, hystricomorphous taxa tend to be more herbivorous and the condition is far more associated with chewing proficiency. Cox et al. (2012) concluded that guinea pigs were more proficient chewers compared to gray squirrels based on

finite element analysis (FEA), and later Cox (2017) argued that the ZMIO provides for greater mechanical advantage at the cheekteeth using the springhare as model. These data suggest that hystricomorphy may be a condition well suited for enhancing chewing function, but this conclusion is based on only two individual taxa, making generalizable statements difficult.

Myomorphy subsumes both sciuromorphous and hystricomorphous conditions, with the ZMIO residing dorsomedially to the anterior deep masseter, with their origins separated by the bony maxillary wall of the zygomatic plate and ventrolateral wall of the infraorbital foramen. Myomorphs vary tremendously in the relative dimensions and heights of these origination sites, similar to sciuromorphs and hystricomorphs, such that some myomorphs effectively resemble one of the simpler conditions. Authors have generally treated myomorphy as a best-of-both-worlds condition, in which the anterior deep masseter can aid in gnawing proficiency and the ZMIO can aid in chewing proficiency. This idea was corroborated by Cox et al 2012 using an FEA model of a brown rat, but an in depth comparative approach is required to understand how this system functions over the enormous dietary and morphological variation of this taxonomically most diverse group of rodents. The vast majority (99+%) of myomorphic taxa are muroid rodents, with only some of the dormice (Gliridae) exhibiting full myomorphy (the genus Graphiurus is typically classified as a hystricomorph [Hautier et al. 2008]). Whether glirid myomorphy is structured and functions similarly to muroid myomorphy is still an open question. Here, I hypothesize that the myomorphic condition can provide for the proficiency of either gnawing or chewing, likely replacing other important aspects of the masticatory system due to its complexity.

This study's focus on functional adaptions of the incisors is based on the analysis of bite force predictors by Freeman and Lemen (2008). These authors used simple metrics of the lower

incisor and mandible to predict *in vivo* bite force measurements across a number of rodent taxa and found incisor "height," equivalent to incisor depth here, to be the most important predictor. Freemen and Lemen attributed this to their 2D finite element model conclusions, which found the stress to accumulate along the "height" dimension of the incisor, with an increase in height thus suitable to reenforce the incisor during chisel based gnawing behavior. Incisor width was a less important but still relevant feature in their analysis, while the mandible dimensions proximal to the incisor were mostly a redundant explanation for the incisor dimensions themselves. I have decided to test the importance of incisor "height" (which I will from here on refer to as incisor depth) and width as predictors of dietary behavior and functional adaptations in foraging across rodents. Incisor width will be measured as the total width of the incisor arcade as it is the functional unit that that rodents operate with during gnawing and thus reflects the width of the cropping surface used during foraging. I conducted this analysis in conjunction with cheekteeth dimensions and some measures of the mandible to more broadly assess ecological and biomechanical hypotheses of rodent feeding and masticatory behavior.

Here, I will measure gnawing proficiency as the relative labiolingual depth of the incisor based on the work of Freeman and Lemen (2008) demonstrating incisor depth to be the most important predictor of in vivo bite force in rodents. I will assume incisor width is an important feature for rodents that deal with complex food types and/or dig with their teeth, necessitating strength during mediolateral or torisional forces on the incisor. Following work from previous ecomorpholgical analyses in rodents and other mammals, I will use the relative occlusal area of the cheekteeth (OACT) as a measure of chewing oriented diets such as herbivory. Using these relative dental measures, I will test for the independent evolution of incisor depth and OACT in

all major clades and masseter muscle configurations, as well as for biases in these dimensions for each group demonstrating their proficiency for one feeding type in particular.

Finally, to test whether masseter condition biases the biomechanical evolution of each clade, I must also control for contingent affects of history and analyze how these important functional traits have evolved in each clade. If each clade of a differing masseter muscle configuration started out with differing relative dimensions of their incisors of OACT, than each group could be evolving as a random walk under a Brownian Motion model and still demonstrate overall, average differences that are unrelated to true functional differences and more related to differing history. On the other hand, if each clade is evolving according to an Ornstein-Uhlenbeck model, in which the trait's variance is constrained and consistently centered within a given range of values, this would demonstrate that these clades have true differences in the pressures selecting their relative dental dimensions, suggesting true functional differentiation and adaptation to particular modes of feeding. Alternatively, some clades of differing masseter configurations could follow one model while other clades another, suggesting that those condition are respectively functionally labile versus functionally stereotypical. Testing for these models of evolution will impart crucial information for how we understand how these potential differences in dental adaptations have arisen and been maintained from a functional perspective. Sciuromorphs could follow an OU model, in which their biomechanics is suited for particular dental dimensions, while myomorphs might demonstrate a BM model, in which their dentition can vary unconstrained by their labile and complex biomechanics.

I hypothesize that masseter condition will effect the rate and alpha parameters in the evolution of character traits, but not necessarily the model of evolution. Brownian Motion represents a neutral state of character evolution, which might be expected if clade histories are

particularly random and inhabit many different ecologies again and again such as rodent clades do, but not if the evolution of dental characters is predicted to be biased by masseter construction. If Brownian Motion is the best fit model across each masseter condition, it would demonstrate that masseter condition is not an important driver of incisor and cheekteeth functional evolution, calling into question whether masseter conditions evolved to perform at particular bite points whatsoever. OU models fitting the data would demonstrate that masseter conditions select for particular dental dimensions away from the ancestral state, conforming to the hypothesis that derived masseter units are adaptations to either gnawing or chewing mechanics.

The ADM in sciuromorphs should ultimately favor species with higher incisor depths and lower occlusal surface areas if sciuromorphy favors gnawing specialized ecologies. Hystricomorphy with a ZMIO that is supposedly well suited for chewing ecologies would also be biased toward low incisor depth and high occlusal area of the cheekteeth, while myomorphy should be somewhere in the middle of these optima if it equally contributes to both gnawing and chewing strategies. If myomorphy is a the most generalizable condition, I would hypothesize that it would demonstrate lower rates of character evolution, as its masseter system would already more efficiently utilize the existing dental dimensions compared to a similar sciuromorph or hystricomorph, which would theoretically need to evolve more extreme dental dimensions to inhabit the same ecologies. Finally, under the hypothesis that myomorphy is more generalizable and capable of more biomechanical opportunities, I would expect myomorphs to exhibit lower alpha parameters, or pulls back to the optimum of trait evolution in an OU model. Despite the predicted lower rates of evolution, myomorphy should not necessarily be tied to the optimum as closely as hystricomorphy and sciuromorphy, which are hypothetically more limited

biomechanically and would thus be more likely to continue to select for the same optimal dental dimensions. Myomorphs should be able to inhabit many very different dental dimensions and still perform, thanks to the complexity of their anterior masseter muscles. If myomorphs demonstrate a greater alpha parameter than sciuromorphs and hystricomorphs, however, it would hint that myomorphy is constrained to use its seemingly complex masseter system in particular ways, and thus would fail to fit the model of a biomechanically more flexible masseter arrangement.

Methods

Materials

Specimen data was collected from dry skulls in the Field Museum of Natural History (FMNH) Mammalogy collections using Mitutoyo (100 mm) calipers coupled with a foot pedal. Each individual linear measure was repeated 5 times and final measures were average across these five samples. Standard errors were checked to assure low variance across all measures before the averaged data was accepted. Specimens were sampled broadly across the rodent phylogeny to assure reasonably proportional coverage across the major clades and families, as well as to assure reasonable dietary diversity, including both generalist and specialist taxa. 278 species were sampled across 242 genera from 28 families. Each known instance of derived masseter conditions on the phylogeny were sampled, excluding the hystricomorphous dipodoids. Species were sampled using 1-3 specimens each and averaged across specimens to determine species average measures. Species for which few specimens existed were only sampled from one specimen.

Data Collected

Morphometric data was focused on the dentition and features of the mandible relevant to muscle attachments and the jaw joint. Dental measures include: lower incisor depth (measured as the linear distance from the anteroventral, or mesial, to posterodorsal, or distal side of the incisor, specifically a line between the two tangents on either side of the outline of the incisor's semi-circular shape, measured as close to the alveolus as possible without accessory bony or soft tissue interfering with the caliper), lower incisor width (measured as the linear distance from the lateral side of one incisor to the lateral side of the other incisor, measured as close to the alveoli as possible without accessory bony or soft tissue interfering with the caliper. This measure thus encompasses the width of the entire the lower incisor arcade), cheekteeth length (measured as the linear distance from the most anterior point of p4 or m1 to the most posterior point of m3, measured at the crown height that encompasses the longest possible distance between these two points), premolar and molar width and/or widest molar (measured as the widest possible linear distance mediolaterally for each cheektooth. Some specimens were only measured at their widest premolar/molar, which was used instead of an average of each width to calculate occlusal area of the cheekteeth), mandible length (measured as the linear distance from the mandibular condyle to the lateral surface of the incisor alveolus on the same side of the mandible, usually at the most distal bony point of the lateral margin of the alveolus that has an anteriorly facing convexity in most rodent species), mandible to inciscor tip length (measured as the linear distance between the mandibular condyle to the tip of the lower incisor), superficial masseter insertion length (measured as the linear distance from the apex of the concave saddle-like lower margin of the mandible to the posterior distal tip of the angular process), and temporalis insertion length (measured as the linear distance from the anterior base of the coronoid process at the toothrow to the most dorsal extent of the coronoid process). Occlusal area of the cheekteeth was estimated by

averaging the three to four premolar and molar widths (depending on the presence of p4, which is lost in all muroids and some select non-muroid species) of the cheekteeth and multiplying by the entire length of the cheekteeth row before finally taking the square root of this area measurement to reduce it's dimensionality. Dental and jaw metrics were size standardized into relative measures by dividing by mandible length (defined as the distance from the mandibular condyle to the lateral margin of the incisor alveolus).

Phylogeny Construction for Analyses

Upham et al 2019's phylogeny of mammals, the most comprehensive phylogeny of mammals to date, was used in all analyses for phylogenetic generalized least squares regressions and models of evolution. I used a version of this tree that only includes taxa with genetic data represented to assure an accurate topology and a lack of polytomies. This tree was further reduced to the 278 species sampled for this study using the drop.tip function from the package geiger in R. In some instances I increased the sample size by including species that were sampled in my data but did not have a genetically sampled representative in the Upham et al 2019 tree, I did this only where a congener from the tree could be substituted with the species from my dataset without loss of phylogenetic resolution. This was performed with only species per genus to preclude this type of substitution from creating an inaccurate or unknown topology or branching time between species. All other sampled species that were not represented by genetic data in the Upham et al tree or those species whose replacement with a congener would change known topology were excluded from the data set.

Allometric and functional regressions

All measures were log transformed. Phylogenetic generalized least squares (PGLS) were performed with the gls function from the NLME package (Pinheiro et al.2019) in R (R Core

Team 2013) along with the corPagel ("Pagel's lambda Correlation Structure") function from the ape package (Revell 2012) to simultaneously estimate phylogenetic signal in the residual error term (Revell 2010). The fit of the data were testing using a variety of modified PGLS models: 1) a PGLS across all taxa, 2) a PGLS that tests for differences in intercept between masseter morphotypes, and 3) and PGLS that tests for differences in intercept and slope between masseter morphotypes. These analyses were conducted to assess whether the data were best explained by a single phylogenetic regression or multiple phylogenetic regressions based on morphotype. The fit of these models was assessed by comparing their Bayesian Information Criterion (BIC) values using the aicw function in R.

Phylogenetic principal components analysis

Dental measures (incisor depth, incisor width, cheekteeth length, and widest molar width) were included in phylogenetic principal components analysis (pPCA). I calculated the geometric mean of the variables and then log transformed the values over their geometric means. I then conducted the pPCA using the correlation matrix using the phyl.pca function from the package phytools in conjuction with the pruned Upham et al. 2019 rodent phylogeny.

Stochastic mapping and ancestral state estimation

Analyzing the macroevolutionary trends across discrete character states requires an estimation of how these states have evolved on the phylogeny. The fitDiscrete function from the R package geiger was used to determine for the best fit model of discrete character evolution for masseter condition on the subsetted tree of 278 sampled taxa. I assessed the fit of an equal-rates model (ER), in which the transition rates between each pair of states are equal, a symmetric model (SM), in which the rates to and from an individual state are the same but each pair of state's rates are allowed to vary, and an all-rates-different model (ARD), in which each transition

rate is allowed to be unique. The model with the lowest Akaike weight score was used in an ancestral character estimation using the ace function from the R package ape. I created a stochastic character map on this phylogeny using the make.simmap function from the R package phytools (Revell 2012) under the best fitting model.

Macroevolutionary models of trait evolution

Models of trait evolution were fitted to incisor depth, width, occlusal area of the cheekteeth, and the anterior margin of the coronoid process using the OUwie function from the OUwie package (Beaulieu and O'Meara 2012) in R. This function allows for the parameters of evolutionary models for continuous traits to vary according to underlying discrete character states (here masseter condition). I assessed the fit of these data to a Brownian motion (BM) model in which only single rate is allowed (BM1), a BM model with distinct rates for each discrete character state (BMS), and four different Ornstein Uhlenbeck (OU) models: OU1, in which there is a single alpha (alpha being a parameter describing the "constraint" on trait value evolution through time, or the propensity to regress back to the trait optimum), sigma squared (evolutionary rate of continuous character), and mean (or optimum, the value a clade's evolution is centered on) value for each character state, OUM, in which there is only one alpha and sigma despite different state mean values, OUMA, in which alpha can vary between states, OUMV, where sigma can vary between states, and OUMVA, in which both alpha and sigma vary between states. Model fit was assessed using the lowest Akaike weight scores. These models were fitted across masseter conditions to test the hypothesis that clades of differing masseter conditions evolve dental metrics under different models of evolution or at different rates and/or alpha parameters under an OU model. This would be expected if the evolution of derived masseter conditions influenced the functional evolution of these characters, initiating new

selective potentials necessitating more or less variation to accrue in the lineages for these characters through time.

Results

Allometric and dental relationships

The best fit model for covariation of incisor depth and mandible length across masseter conditions was a single slope and intercept model (BIC weight = 0.9991). Incisor depth is significantly and positively correlated with mandible length ($p<0.001$; slope = 1.205; intercept = -2.547) (Fig. 1.2A). Myomorphs are relatively symmetric across the trendline, whereas hystricomorphs lie above the trendline more than below, just as sciuromorphs lie below the trendline more than above, particularly at large mandible lengths. The best fit model for covariation of incisor width and mandible length across masseter conditions was a single slope and intercept model (BIC weight = 0.9995). Incisor width is significantly and positively correlated with mandible length ($p<0.001$; slope = 1.0164; intercept = -2.577) (Fig. 1.2B). Masseter condition is far less biased on either side of the trendline, although sciuromorphs still lie primarily below the line. The best fit model for covariation of the square root of OACT and mandible length across masseter conditions was a single slope and intercept model (BIC weight = 0.9995). Incisor width is significantly and positively correlated with mandible length ($p<0.001$; slope = 0.994; intercept = -1.830) (Fig. 1.2C). Hystricomorphs are particularly concentrated above the trendline more so than other masseter conditions, whereas some smaller bodied myomorphs lie far below the trendline.

The best fit model for covariation of incisor depth and incisor width across masseter conditions was a single slope and intercept model (BIC weight = 0.9986). Incisor depth is

significantly and positively correlated with incisor width ($p<0.001$; slope = 1.0810; intercept = 0.430) (Fig. 1.3A). A particular group of mostly sciuromorphs lie well below the trendline along a one to one line. The best fit model for covariation of incisor depth and square root of OACT across masseter conditions was a single slope and intercept model (BIC weight = 0.9992). Incisor width is significantly and positively correlated with the square root of OACT ($p<0.001$; slope = 0.847; intercept = 0.765) (Fig. 1.3B). There are far more hystricomorphs above the trendline than below, just as there are far more sciuromorphs below the trendline than above it. The best fit model for covariation of incisor width and the square root of OACT across masseter conditions was a single slope and intercept model (BIC weight = 0.9992). Incisor width is significantly and positively correlated with mandible length ($p<0.001$; slope = 0.741; intercept = 0.485) (Fig. 1.3C). Masseter conditions are less segregated here across the trendline compared to OACT over incisor depth.

Phylogenetic principal components analysis

pPCA analysis resulted in 4 PCs, with PC1 comprising 50.95% of the variance, PC2 26.82% of the variance, PC3 22.23% of the variance, and PC4<0.0001% of the variance. Incisor depth and width are positively loaded onto PC1 with cheekteeth length (CTRL) and widest molar width (WMW) loading negatively (Table 1.1). For PC2, incisor depth loads negatively (-0.697) whereas incisor width loads positively (0.759), and CTRL and WMW comprise minor loadings. For PC3, CTRL loads negatively (-0.714) whereas WMW positively (0.610), and incisor depth and width comprise minor loadings. The highest values of PC1 are inhabited by subterranean taxa with robust incisors, whereas low values of PC1 exhibit taxa with relatively small incisor width and depth are primarily grazing specialists, particularly hystricomorphs, and faunivores (Fig. 1.4, 1.5). The highest values of PC2 are exclusively inhabited by sciuromorphs and very

few myomorphs that gnaw into hard nuts, seeds, and glean bark, whereas low values of PC2 are inhabited by taxa of various masseter conditions and ecologies, primarily fossorial and grazing taxa (Fig. 1.4). High values of PC3 are inhabited by taxa with short and wide CTRs of diverse taxonomic origins and morphotypes, but are primarily fossorial or gnawing specialists (Fig. 1.5, 1.6). Low values of PC3 are almost exclusively inhabited by herbivorous myomorphs, particularly the grazing specialized arvicolines that have long, narrow CTRs.

Reconstructing Masseter Morphotype Evolution

An all rates different model, in which transition rates in and out of discrete masseter conditions are allowed to vary independently, had the highest Akaike weight score (0.9385) (Table 1.2). Thus, the all rates different model was used in estimating the ancestral masseter condition. Ancestral character estimation resulted in protrogomorphy as the primitive condition, despite only a single occurrence among extant rodents. Inspection of maximum likelihood estimates for transition rates show that this result is due to rates of almost zero for all conditions except protrogomorphy, conforming with the tree's lack of inferred evolution of derived masseter conditions from other derived masseter conditions in ancestral state estimation (Fig. 1.6). Excluding the only protrogomorph taxon, *Aplodontia rufa*, but retaining the condition protrogomorphy in the analyses yielded the same result. Excluding protrogomorphy as a condition and removing *Aplodontia* resulted in hystricomorphy as the primitive state. Using the best-fit all rates different model, I calculated the transition rate matrix for masseter conditions.

Modes of Ecomorphological Macroevolution across Masseter Conditions

For relative incisor depth, incisor width, and OACT, a multi-rate, single-alpha OU model (OUMV) was the best fit for the data (Tables 1.3-1.5). For incisor depth, the next best fit was a multi-alpha, single-rate OU model (OUMA), followed distantly by a Brownian motion model

with different parameters for morphotype rates and mean (BMS). For OACT, a close second best fit model was an OU model with both multiple rates and multiple alphas (OUMVA). For incisor width, the second best fit model was BMS.

For incisor depth, the optima under the best fit OUMV model were 0.075 (SE=0.0055) for hystricomorphs, 0.086 (SE=0.0028) for myomorphs, and 0.093 (SE=0.0058) for sciuromorphs. Rates under the OUMV model were slightly lower for myomorphs (9.18e-6) than for hystricomorphs (2.09e-5) and sciuromorphs (2.10e-5). In the second best fit OUMA model, alpha was lower for myomorphs (0.00265) than for hystricomorphs (0.00605) and sciuromorphs (0.00571).

For incisor width, the optima under the best fit OUMV model were 0.143 (SE=0.0175) for hystricomorphs, 0.128 (SE=0.00922) for myomorphs, and 0.106 (SE=0.0120) for sciuromorphs. Rates under the OUMV model were higher for hystricomorphs (9.718e-5) compared to myomorphs (3.298e-5) and sciuromorphs (4.372e-5). These correspond to similar rates and optima in the second best fit BMS model.

For OACT, OUMV was the best model fit (weight = 0.6107; AICc = -1336.457) with OUMVA a close second (weight = 0.3877; AICc = 1335.548). The optima under the best fit OUMV model were 0.165 (SE= 0.00566) for hystricomorphs, 0.151 (SE=0.00312) for myomorphs, and 0.157 (SE=0.00394) for sciuromorphs. Rates under the OUMV model were far higher for hystricomorphs (1.012e-4) than for myomorphs (8.029e-5) and sciuromorphs (4.170e-5). In the second best fit OUMVA model, alpha was lower for myomorphs (0.0591) compared to hystricomorphs (0.0782) and sciuromorphs (0.0913). Rates in the OUMVA model differed from the the OUMV model, with myomorphs having higher sigma squared values (7.879e-5) than hystricomorphs (7.505e-5) and sciuromorphs (1.470e-5).

The best fitting OU models demonstrate that masseter conditions favor particular incisor and cheekteeth dimensions, conforming to the hypothesis that masseter conditions are adaptations for either gnawing or chewing strategies. In particular, sciuromorphs demonstrate the highest optimum for incisor depth and lowest optimum for OACT, consistent with their gnawing biased ecologies, and hystricomorphs exhibit the lowest optimum for incisor depth but highest optimum for OACT, consistent with the hypothesis that hystricomorphy favors chewing ecologies over gnawing focused ecologies. The low rates and intermediate optima for myomorphs in each of these characters is further consistent with the hypothesis that myomorphy does not require extreme dental conditions given its complex anterior masseter biomechanics, allowing for more efficient utilization of similar sized dentition. Overall, these data conform to the hypothesis that masseter conditions are important for differentiating gnawing and chewing functions evolutionarily, leading to differential rates of evolution, particularly lower rates for myomorphs.

Discussion

Dental allometry in rodents across masseter condition

Each of the important functional measures of the dentition, incisor depth, width, and OACT, scale positively and linearly with mandible length without significant differences in masseter condition (Fig. 1.2-1.4). Although the regressions are best fit by a single model, the graphical visualizations of these data demonstrate that masseter condition slightly biases the relationship between each measure and mandible length. Myomorphs are generally smaller animals than both sciuromorphs and hystricomorphs and thus mostly occupy the lower portion of each graph, but notably their spread is relatively equal across either side of the PGLS regression line.

Sciuromorphs tend to have larger incisor depths per mandible length compared to other rodents across the spectrum of mandible length, whereas most hystricomorphs have incisor depths lower than the PGLS trendline across all taxa (Fig. 1.2A). At large mandible length sizes, muroids occupy space primarily above the PGLS trendline. These data would thus suggest that although rodents scale incisor depth under a single slope, individual groups show slight biases that could be related to their ecological usage. Sciuromorphs tend to specialize in diets that require proficient chisel-like gnawing behavior with the incisors, in which incisor depth would be particularly important to resisting stresses and strains. Hystricomorphs tend to specialize in herbivorous diets, either folivorous or grazing specialities, and would thus not require particularly deep incisors to crop plants of soft material properties. Myomorphs demonstrate a range of of incisor depth values on either side of the PGLS trendline, but their increased incisor depths at large mandible sizes can be explained by the fact that these large body sized muroids are almost exclusively subterranean and/or bamboo feeding specialists that require deep, robust incisors to dig and/or gnaw into woody bamboo material.

Incisor width is far less biased by masseter condition, with each morphotype demonstrating many species on either side of the PGLS trendline (Fig. 1.2B). OACT also demonstrates little bias for both myomorphs and hystricomorphs, but large hystricomorphs tend to lie above the PGLS trendline, demonstrating relatively higher OACT fitting with their mostly herbivorous dietary preferences (Fig. 1.2C). There is a notable group of taxa far below the this trendline that demonstrate particularly low relative OACT, which include the faunivorous taxa *Chrotomys mindorensis* and *Rhynchomys soricoides* and putatively faunivorous *Tylomys naudicadatus* and *Meriones rex*, as well as the subterranean taxa *Heterocephalus glaber* and *Spalax leucodon*. Outside of the durophagous mollusc and crustacean specialized faunivores

such as *Hydromys*, most rodent faunivorous demonstrate reduced relative OACT, likely due to ingestion of softer material properties from animal flesh compared to fiborous and nutty plant material.

Ecomorphology and functional morphology of rodent incisors

This study takes a simple approach to assessing ecomorphology utilizing a functional perspective of what rodents directly interact with at each stage of foraging and ingestion, and considers species by what should be their most biomechanically challenging task in this process. For most species, this would appear to be the food item itself, but for fossorial, grazing, and bark gleaning taxa, earlier actions in their foraging strategy must be considered and balanced with what is known in the literature for the animals diet and behavior.

Incisor depth and width are strongly correlated across rodents and best described by a single PGLS regression (Fig. 1.3A). Masseter condition appears particularly unbiased across this trendline with the exception of a group of mostly sciuromorphous and some myomorphous hard nut and seed feeding specialists, along with bark gleaning specialists, that follow a one to one line distinctly separated from other rodents. This deviation that so closely aligns with the one to one line implies that rodents that use their incisors to chisel require incisors that are relatively square in cross-section (incisor width is a measure of both left and right incisors), whereas the norm across rodents is to have incisors that are mediolaterally wider than labiolingually deep. These taxa with squared incisors in cross-section have notably higher relative incisor depth compared to mandible length, implying that these taxa are not necessarily reducing incisor width but instead greatly increasing incisor depth for their body size to resist the immense strains imparted on the incisors during chisel-like gnawing into hard woody substrates.

OACT over incisor depth is slightly more biased by masseter condition than over incisor width, with more hystricomorph taxa occupying space above the OACT over incisor depth trendline with few sciuromorphs, whereas both hystricomorphs and sciuromorphs occupy both sides of the OACT over incisor width trendline fairly equally (Fig. 1.3B-C). These patterns hint at the opposing dietary preferences of taxa with relatively higher incisor depth compared to higher relative OACT, with taxa that primarily gnaw into their food with deep incisors typically lacking the need for high relative OACT. On the other hand, taxa with wide incisors are not necessarily chiseling specialists, with relatively wide incisors found in highly herbivorous taxa and those that gnaw to dig into soil or feed on bamboo.

pPCA analysis demonstrates various guilds of rodent groups that span masseter conditions and sometimes exclusively include members of a single masseter condition that are revealing toward ecofunctional relationships between dental metrics and diet and foraging strategies, as well as the biases of masseter condition. Positive values of PC1 exhibit taxa with robust incisors in both depth and width and small cheekteeth in both cheektooth row length (CTRL) and widest molar width (WMW). Positive values of PC2 exhibit taxa with shallow but wide incisors, whereas positive values of PC3 exhibit taxa with short CTRL but large WMW. One can thus interpret these pPCA results to assess whether groupings of taxa in the pPCA plots also share ecofunctional strategies.

In PC2 over PC1 (Fig. 1.4), high values of both PC1 and PC2 exhibit primarily subterranean and fossorial taxa such as bathyergids, spalacids, ctenomyids, and geomyids. These taxa require generally robust but particularly wide incisors to gnaw into complex soils of various hardness as well as tough roots and tubers that they feed on. In the process these rodents' incisors must withstand substantial wear from contact with hard materials in earthy grit. Species with low

values of PC1 but high values of PC2 include a guild of ctenohystrican grazers and faunivorous rodents. This unconventional grouping is united in a general reduction in relative incisor size, with relatively low depths and widths. Faunivorous taxa lack the need for robust incisors when capturing generally small insects, soft-bodied invertebrates, and/or fish, whereas taxa that specialize on leaves do not require robust incisors to crop soft plant material. Between these guilds exist species that exhibit high values for PC2 but intermediate values for PC1, which include semi-fossorial root and tuber specialists such as *Thryonomys* and *Myocastor*, as well as bark feeders such as *Otomys, Hystrix*, and *Euyrzygomatomys*. These taxa would seem to require high incisor width to deal with the complex substrates of woody to near woody material but do not practice particularly chisel-like gnawing mechanics like hard nut and seed specialists, thus are lacking in incisor depth compared to subterranean taxa. Taxa with low values for PC2, and thus high relative incisors depths but low relative incisor widths, include hard nut and seed specialists among both sciuromorphs (both sciurids and heteromyids) and myomorphs (*Chiropodomys, Uromys*, oryzomyines, and arboreal taxa), as well as bark gleaning micro-squirrels among the sciurids. These taxa chisel into plant items with hard material properties (some of which are the hardest material properties known in the plant world, such as the fruit that *Rheithrosciurus* feeds upon [Lucas et al. 2012]), but open into nutritious cavities with softer material properties. Bark gleaning has an analogous set of material considerations, as their foraging tactics require them to gnaw off hard pieces of bark that are relatively large compared to their small body size to access softer nutritious invertebrates and plant exudates that lie beneath (Hautier et al. 2009). The subterranean and fossorial guild here contains a diverse assemblage of masseter conditions; however, the hard nut and seed/bark gleaning guild is biased toward sciuromorphs and myomorphs (with the sole hystricomorph, *Graphiurus murinus*, recently

evolved from glirid myomorphs), whereas the low incisor size guild is dominated by hystricomorph grazers (as well as faunivores of both myomorphs and sciuromorphs).

Species with high values of PC3 exhibit short CTRL and large WMW. These include most of the subterranean and fossorial taxa as well a most heteromyids (sciuromorphs) and some bark and bamboo feeders (*Otomys* and *Phloeomys*/*Cannomys*, respectively). Taxa with low PC3 values exhibit long CTRL and small WMW, and these include primarily highly derived myomorph herbivores such as grazing arvicolines (voles and lemmings), *Uromys* (murine), and *Steatomys* (nesomyid) (Fig. 5-6). These latter taxa have highly derived occlusal patterns and in some cases ever growing cheekteeth that presumably chew in highly specialized manners that allow WMW to remain small. Caviids (hystricomorphs) are superficially similar, although do not achieve the same degree of relative narrowness of the CTR, indicating that myomorphous rodents likely have particularly different chewing patterns. One of these taxa, *Uromys*, resides alone in morphospace when plotting PC3 over PC2, indicating that its condition, exhibiting deep, chiseling incisors and a long narrow cheektooth row, is rare among rodents. On the opposite corner of the morphospace, there is a tight grouping of taxa that exhibit wide incisors and short, wide cheektooth rows from a diverse set of masseter conditions and rodent families. These taxa are primarily subterranean, along with the bamboo specialist *Phloeomys*.

From these data, we can infer a model of incisor functional utilization across rodents that is both general across taxa and has specific clauses for certain clades and masseter morphotypes. High relative incisor depth is only seen in taxa that are known to gnaw into hard substrates (or in taxa that completely lack ecological dietary data). Low relative incisor depth is only seen in faunivorous and highly herbivorous taxa, excluding any taxa with fossorial habits during foraging behavior. All taxa with relatively high incisor depth and width are fossorial, with the

highest values belonging to subterranean chisel-tooth diggers, subterranean scratch digger *Bathyergus suillus,* and the large bodied root and tuber specialists *Myocastor* and *Thryonomys*. The next most robust incisors include some non-fossorial species, such as the bamboo specialist *Phloeomys* and beaver *Castor.* All of these taxa must chisel through hard, complex substrates that would impart strong loads not only through the labiolingual depth dimension but potentially in any dimension, necessitating general robusticity over the efficiently designed chiseling incisors found in taxa that gnaw primarily into regularly shaped hard nuts and seeds. Once a nut or seed wall is penetrated during chiseling, the hard outer casing will split open, revealing the nutritious starchy material inside. These rodents thus require only simple penetration in one direction to obtain their dietary needs. Feeding on hard roots, tubers, bark, and bamboo are all far more intensive materials that do not simply "open" into a concealed cavity that is easy to process and ingest. They must instead be thoroughly processed, potentially requiring unpredictable gnawing angles at any given moment. This is particularly true for chisel-tooth digging through hard soils. The presence of many grazing species in the wide incisor region, from sciuromorphic marmots to myomorphic voles, is likely due to the rough, fibrous, and grit laden nature of many grass species and their terrestrial runner shoots. Wide incisors could also aid in cropping efficiency, widening the field of each bite to maximize the amount material ingested at a time. The severe lack of incisor depth and width in the diverse assemblage of ctenohystrican grazers (caviids, chinchillids, ctenodactylids, and *Abrocoma*) is thus an interesting problem, given many of these species feed on plants close to the ground in arid and sandy habitats. The degree to which these grazers forage differently from other rodent grazers warrants further attention, but the presence of adjacent herbivores such as *Trogopterus*, a high canopy folivore, and *Dicrostonyx*, an Arctic tundra C3 grazer, suggest these animals truly lack significant loading on

their incisors during ingestion, and thus the type of foliage consumed, its environmental context, and the animals specific foraging and ingestion style truly matters for the biomechanical loads experienced and adapted to. Comparing these taxa to other herbivores with wider incisors, such as *Otomys*, *Euryzygomatomys*, and *Hystrix*, demonstrates that incisor width is selected for in herbivores with complex foraging strategies and diets that go beyond soft vegetation and include lignified material and digging.

The argument that the ctenohystrican guild feeds on softer vegetation is strengthened by the co-presence of faunivores in this portion of the graph, which do not require gnawing to capture and ingest prey, but instead simple penetration of mostly soft-tissue and thin chitinous layers. Faunivores have evolved dozens of times in rodents, and in almost all cases the incisors become reduced with respect to close generalist and herbivorous relatives. The extreme reduction seen in the exclusively vermivorous *Rhynchomys* and other rodent vemivores not included in this study are reminiscent of the kind of rostral reductions seen in insectivorous mammals generally such, such as anteaters, numbats, echidnas, and pangolins, as well as nectivorous bats among phyllostomids and pterpodids. All of these taxa lack significant loading during prey capture, ingestion, and food processing, and it is reasonable to assume that loading is progressively weakened in rodents that feed on almost exclusively insects and particularly vermivores.

The specificity of certain parts of this incisor depth and width graph to masseter condition hints at general differences in performance capabilities and adaptabilities among rodents of differing masseteric construction. Why do hystricomorphs fail to evolve thin but deep incisors to chisel into hard nuts and seeds (outside of *Graphiurus*, which is a recently evolved hystricomorph reduced from myomorphic glirid ancestors. The degree to which glirid

myomorphy and hystricomorphy are directly comparable to other taxa is an open question)? This trend is particularly striking when comparing the distributions in morphospace between hystricomorphs and myomorphs, with myomorphs harboring dozens of species with relative deep incisors below which no hystricomorphs exist. Why is it that primarily hystricomorphous ctenohystricans inhabit the extreme reduction of incisors during grazing? Why do myomorphous muroids almost exclusively lie within the center of this graph, with few outliers in incisor depth, when they encapsulate the majority of rodent diversity overall and are by far more diverse ecologically?

The evolution of cheekteeth in rodents is a far more well studied and explored topic than that of incisors. Cheekteeth in rodents follow similar ecomorphological patterns to those in other mammals, in which herbivorous taxa have generally larger cheekteeth and almost always more complex cusp patterns compared to omnivorous and carnivorous rodents (Evans et al. 2007). Most other mammal groups contain far fewer nut and seed specialists and are more likely to have soft-fruit specialists. The most comparable group to nut and seed feeding rodents would be stenodermatine phyllostomid bats and primates that specialize on crushing hard fruits. Crucially, however, the biomechanics of these animals is gearing toward crushing behavior at the most biomechanically advantageous positions at the back of the mouth with large molars, and not chiseling behavior with sharp incisors at the front of the mouth. Some comparable mammals biomechanically and ecologically to rodents would be lagomorphs and diprotodontid marsupials, although in all cases the upper incisors are more numerous than in rodents and the lower incisors lack the same strongly arched hemi-circular structure. The aye-aye is by far the most comparable mammal to rodents biomechanically, with an enormous set of ever growing incisors that looks remarkably similar to most gnawing proficient squirrels, with severely deep incisors that are

relatively thin medio-laterally (Morris Phillip et al 2019). The aya-aye is, however, a sole species with a very specific ecology coupled with set of unique adaptations. There are thus few examples to compare to rodents to biomechanically among extant mammals in terms of the amount of oral processesing that occurs through incisor gnawing vs cheekteeth chewing when the incisors are permanently ever-growing structures. One could assume that the abilities to process food through incisor gnawing prior to chewing with the cheekteeth may release the cheekteeth from certain processing requirements and duties, allowing for a reduction in cheekteeth size and complexity when certain food items are more easily processed through gnawing behavior. This is particularly true for nuts and seeds, which once gnawed through with the incisors are far more easily digested with the cheekteeth in rodents compared to other mammals that must crush these food items with powerful molars first.

In the pPCA analysis, there is no relationship between relative incisor depth and relative cheektooth size across rodents, with the data instead suggesting covariation with incisor width. The lack of a relationship between incisor depth and cheekteeth size across rodents is crucially important. It strengthens the argument that incisor gnawing and cheekteeth chewing are functionally and evolutionarily independent systems, unlike the anterior and posterior dentition in other mammals, which are necessarily functionally and evolutionarily linked. Rodents lack mutual occlusion of the incisors and cheekteeth when the mouth is closed. When the cheekteeth occlude, the lower incisor is too posterior to occlude with the upper incisor. When the mandible is thrust forward to occlude the lower incisor to the upper incisor, gape is increased, precluding the ability of the cheekteeth to occlude until the lower incisor is returned to a posterior position outside of incisor occlusion. This system implies that variations in incisor dimensions should not be expected to directly impact chewing performance, and variations in cheekteeth should not

affect incisor gnawing. One can imagine how evolutionarily these systems should be allowed to evolve more independently than functionally integrated toothrows in other mammals. Changes in relative size of the anterior dentition require compensatory changes across the tooth row to assure proper occlusion. In rodents, enlargement of the incisors does not require compensatory changes in the rest of the jaw to assure normal cheekteeth occlusion, until the incisors become large enough that the diastema region must be depressed to accommodate the increase in size. Importantly, this later compensatory change is a change in the mandible, not in the the cheekteeth themselves.

Overall, rodents follow a similar trend to other mammals in that larger relative area of the occlusal surface of the cheekteeth is tied with herbivorous behavior, and smaller cheekteeth are seen in omnivorous and carnivorous rodents. The largest relative OACT values are found in highly herbivorous species, such as the folivorous echimyids *Ollalomys* and *Kanneobateomys,* the plains vischacia *Lagostomus*, the folivorous sciurid *Trogopterus*, and the bamboo root and shoot specialist *Cannomys*, a muroid. Taxa with low relative OACT are faunivores, such as *Chrotomys, Rhynchomys, Mus triton, Dendromus, Geoxus*, although there are some interesting exceptions, such as *Spalax, Heterocephalus, Crateromys*, and *Phloeomys*. Each of these latter taxa are herbivores, but they have particularly large mandibles and relatively enormous incisors, with the former two being subterranean chisel-tooth diggers, and the latter two enigmatic cloud forest bamboo specialists. *Spalax* and *Heterocephalus* have far smaller cheekteeth than other spalacids and bathyergids, likely due to a much softer diet. *Crateromys* and *Phloeomys* require intense gnawing proficiency to process woody bamboo, and have highly derived molar cusp morphology for murines. *Tylomys* also demonstrates extremely low values of relative OACT, but it's diet is unknown (Zaragoza-Quintana et al 2016) and its close tylomyine relatives do not

share its low relative OACT values. Other taxa with low relative OACT include bark gleaning squirrels and seed eating heteromyids. The faunivorous squirrel *Rhinosciurus* is more similar to *Hydromys* in exhibiting a high relative OACT, likely implying important crushing behavior while feeding on large, chitonous arthropods.

Incisor width and cheektooth size appear far more related in the pPCA data than compared to incisor depth. This is fitting with the interpretation that wide incisors are primarily adapted for efficient cropping of vegetative matter, resistance to wear while grazing, and digging behavior (which is usually associated with large cheekteeth for processing grit-laden food). Additionally, relatively thin incisors are associated with faunivores and hard nut and seed feeders, which do not require large cheekteeth for food processing.

Modes of Ecomorphological Macroevolution across Masseter Conditions

Modeling the discrete character evolution of masseter conditions across rodents yielded the all-rates-different model as the best fit, and the ancestral character estimation found protrogomorphy as the primitive condition (Fig. 6). These data are in line with our paleontological understanding of rodent masseteric evolution. Early rodents were protrogomorphs, with diverse representation across many families found in localities across North America and Eurasia. Attempts to characterize this evolution in a phylogenetic context found the derived masseter conditions to evolve numerous times independently from various protrogomorph groups, including groups with independently derived masseter conditions that are now totally extinct (Marivaux 2004). These data, along with the backbone of molecular phylogenies of extant taxa, provide a model for masseteric evolution, in which sciuromorphy and hystricomorphy must evolve directly from protrogomorphy, while myomorphy seems to necessarily evolve from the addition of sciuromorphy onto hystricomorphy, but not vice versa. It

is possible that myomorphy could evolve from sciuromorphy through the addition of hystricomorphy, although sciuromorphs restrict their infraorbital foramen between their zygomatic plate and the rostrum, making such an addition seem less likely than would already be expected even in the primitive state. Adding sciuromorphy onto hystricomorphy appears far easier, as the zygomatic plate can form ventromedially to the already expanded infraorbital foramen without much interference to the existing bone and muscle architecture. Several losses of a derived masseter condition have been argued. One, accepted here, is that glirid myomorphs gave rise to the hystricomorphous *Graphiurus*. Although the intricacies of the glirid masseteric architechture deserve further study, *Graphiurus* is clearly a functional hystricomorph, with virtually no zygomatic plate, a condition not seen even in the far more deserve myomorph clade Muroidea (insectivorous and vermivorous taxa have severely reduced zygomatic plates, although they are still evident and are often associated with the concomitant reduction of the hystricomorphous component, fitting with a general reduction of all masticatory elements). *Heterocephalus glaber*, the naked moe rat, was recently argued as a functional protrogomorph based on iodine stained CT scanning results (Cox and Faulkes 2014). Although I agree that the infraorbital portion of the zygomaticomandibularis (ZMIO) is heavily reduced and fails to penetrate the infraorbital foramen in a functionally meaningful manner, I am hesitant to designate *Heterocephalus* as a protrogomorph, as its masseteric system is otherwise totally consistent with the highly derived ctenohystrican hystricomorphous arrangement, and aside from a small ZMIO, its orbital portion of the zygomaticomandibularis (ZMO) and other jaw muscles defers little from bathyergid masticatory systems. It is thus not clear how *Heterocephalus* differs functionally from other hystricomorphs, although it is clear that its current state is not homologous to protrogomorphy. Coding *Heterocephalus* as a protrogomorph would result in

hystricomorphy being estimated as the primitive state on the phylogeny, as it would allow for transitions from derived masseter conditions into protrogomorphy on the phylogeny (Swanson et al. 2019). Hystricomorphy would be the most parsimonius and most likely primitive state in this scenario, as it evolves the most often among the derived conditions. Accepting *Aplodontia rufa* as the only protrogomorph is thus useful until *Heterocephalus* is more well understood and a consensus can be reached as to how to approach it paradigmatically in masseteric evolution.

Each set of evolutionary models for the trait evolution of relative incisor depth, width, and OACT across masseter morphotypes were best fit by a variable rates Ornstein-Uhlenbeck model (OUMV) with a single alpha parameter. For incisor depth, optima were lower for hystricomorphs and higher for sciuromorphs compared to myomorphs (since protogomorphy is represented by a single taxon, its results cannot be reasonably interpreted), which is fitting with the generally higher incisor depth of sciuromorphs and more average dimensions found in myomorphs. Evolutionary rates estimated in the OUMV model were comparable between hystricomorphs and sciuromorphs but lower for myomorphs. This is interesting given that the second best model fit, an OU model with multiple alphas, yielded a lower alpha for myomorphs compared to hystricomorphs and sciuromorphs. This implies that although myomorphs evolve incisor depth at a lower evolutionary rate, they also appear less constrained than hystricomorphs and sciuromorphs. These results conform with a model in which myomorphs are freer to evolve their incisor dimensions but have yet to have the time to fully surpass their masseteric counterparts in achieving certain incisal specializations.

For the evolution of relative incisor width, the best fit model was also an OUMV model, although a multirate Brownian Motion model (BMS) was the next best fit in this case. The optima for hystricomorphs is higher than for myomorphs and sciuromorphs with an appreciably

higher standard error. Additionally, the evolutionary rates for relative incisor width among hystricomorphs are appreciably higher in both OUMV and BMS models, with myomorphs once again demonstrating the lowest rates. These results make sense considering the repeated evolution of thin incisors among the specialized ctenohystrican grazing guild (represented by caviids, chinchillids, ctenodactylids, and *Abrocoma*), as well as the repeated evolution wide incisors among the independently evolved subterranean and fossorially foraging specialists that exist among hystricomorphs (bathyergids+*Heterocephalus*, ctenomyids, *Myocastor*, thryonomyids, plus the enigmatic *Dinomys branickii*).

For the evolution of relative OACT, the best fit model was OUMV with the next best fit model also allowing for multiple alphas (OUMVA). Hystricomorphs have the highest optimum, followed by sciuromorphs and myomorphs with the lowest optimum. For rates under the OUMV model, sciuromorphs have half the rate of myomorphs, and myomorphs have lower rate than hystricomorphs. The optima are relatively similar in the next best fitting OUMVA model, although the rates between myomorphs and hystricomorphs are flipped, with myomorphs having slightly higher rates than hystricomorphs while sciuromorph rates are considerably lower than both.In the OUMVA model the alpha for myomorphs is lower than that of hystricomorphs and sciuromorphs, with sciuromorphs having the highest overall alpha.

These results demonstrate that masseter condition bias the trait optima of incisors and cheekteeth, as each masseter condition's trait evolution is best explained by OU models rather than Brownian motion. In particular, the direction of each trait optimum for each masseter condition fits with the predictions, in which sciuromorphs are biased toward high incisor depths and low OACT, fitting with selection for gnawing based ecologies in the line with the hypothetical preferred action of the ADM. Hystricomorphs demonstrate lower incisor depth and

higher OACT optima, fitting with the hypothesis that the ZMIO selects for more chewing intensive ecologies. Myomorphs exhibit trait optima in between sciuromorphs and hystricomorphs in each case, demonstrating that myomorphy allows for both gnawing and chewing intensive ecologies.

Finally, these results are particularly interesting in that they fit with what one would expect from the hypothesis in the rodent literature that myomorphy is a muscular system that allows for more efficient masticatory processing compared to hystricomorphy and sciuromorphy (Cox et al. 2012). If myomorphy can more efficiently impart bite forces and control chewing and gnawing strokes with its more diverse musculature, than one would expect that selection on extreme dentition would be relaxed, allowing for relatively smaller dental dimensions to accomplish similar functional goals. This would also mean lower rates of morphological evolution for myomorphs, as smaller changes in dental dimensions would impart larger functional changes *in vivo*. This hypothesis would also make sense out of the lower alphas for myomorph dentition, as the lack of relative dental diversity in myomorphs would not be due to constraint but instead lack of need to evolve such extreme morphologies. Thus, myomorphs should still be evolving their dentition more freely, while sciuromorphs and hystricomorphs might be expected to have reached the extremes of what's possible in their masticatory output. The results here support the initial hypothesis given the low rates of evolution of dental traits compared to sciuromorphs and hystricomorphs, demonstrating the myomorphs do need to evolve compensatory adaptations to their dentition as readily as sciuromorphs and hystricomorphs with their more limited masseter arrangements.

Conclusions

I have presented a model for understanding the functional evolution of rodent dentition that should be the basis for a more comprehensive and contextualized view of rodent ecomorphology. Rodents have particularly complex diets compared to other mammals in that the majority of species would be considered generalist omnivores if they belonged to any other mammalian order. Highly herbivorous and or otherwise dietarily specialized species have been recorded to regularly consume insects and meat. Even for specialized herbivores, the basic design of the rodent incisor still provides for a potent carnivorous weapon, as can be attested by the defensive means in which many rodents use their incisors under the threat of predation. This basic difference between rodents and other mammals creates a fundamental advantage in dietary exploration and opportunism. The ever growing and self-sharpening nature of rodent incisors doubles this advantage, allowing rodents to be both versatile and effective in their dietary opportunism. For example, many mammals may opportunistically exploit dietary resources that are laden in grit or otherwise contribute to higher than adapted rates of tooth wear. Because these species lack ever-growing, self sharpening dentition, they suffer sometimes severe consequences for their exploration, reducing the efficacy of these explorations and diminishing the chances that those mammals may be positively selected to continue exploiting these new resources. Rodents, on the other hand, can explore new diets more effectively, as their ever-growing and self sharpening dentition allows them to recover within their lifespan from the consequences of abnormal wear. These incisors are themselves an unique tool for rodents to exploit new resources in ways far more versatile than the incisors of carnivorans, bats, shrews, or those found in ungulates (ungulates often lack upper incisors entirely). No other mammals have incisors that could, with the same dimensions, easily and efficiently crop plants, pierce into the body cavity of prey, dig in the ground, and gnaw into lignified seeds, nuts, bark, and bamboo. The fact that

adaptability of these teeth to all of these respective specializations can be quantified through two simple dimensions, depth and width, is a testament to the elegance of rodent incisors as an evolutionary innovation. Incisor shape can be inordinately complex across even closely related and mammals that feed on similar foods, and vary stupendously across mammals as a whole, including in number and arrangement on top of individual shape. Rodents, however, can accomplish more with less, and have evolved an incisal design that does not require change in shape aside for depth and width. Here, I argue that the basic dimensions of rodent incisors are sufficient to explain much of rodent ecomorphology on their own, principally because these dimensions have direct biomechanical interpretations. Thus, incisal depth and width can provide useful proxies for studying the evolution of rodent ecofunctional diversification as well as mechanistic processes in their masticatory operation and evolution.

Overall, I argue that incisor depth is useful proxy for gnawing proficiency in rodents, as this dimension would necessarily receive the bulk of loads and stress during dorsoventral gnawing/chiseling behavior, and high relative incisor depth is closely associated with rodent species that require gnawing forces to exploit dietary resources (hard nuts and seeds, bamboo, bark) or effectively utilize in chisel-tooth digging behavior. Relative incisor depth can be coupled with relative incisor width to reveal the particularities of gnawing usage. Rodents that chisel into hard nuts and seeds have low relative incisor width, as loading forces are almost always unidirectional and simple during these behaviors. Rodents that gnaw into more complex substrates require high relative incisor width to withstand additional mediolateral and torisional forces that may be imparted during the extraction of heavy chips of wood and/or hard soil, as well as the excessive wear that may variably be present during these more complex activities. Low relative incisor depth and width is indicative of low gnawing performance and lack of

importance of gnawing in the diet. This is consistent with a diverse range of diets that can be more easily distinguished by factoring in relative OACT. Both faunivores and soft-foliage folivores and grazers have diminutive incisors, but herbivores almost always have larger OACT, with many faunivores exhibiting some of the smallest OACT values among rodents (m3 is commonly lost in extreme faunivores, with *Paucidentomys* lacking cheekteeth entirely). *Hydromys melanogaster* is among the potentially durohagous rodents that have low relative incisor dimensions but high relative OACT despite not being a herbivore. Studies of orientation patch count have robustly demonstrated that carnivory can easily be distinguished from herbivory in these large molars through cusp complexity. The cusp complexity of *Hydromys* molars are very simple compared to other murids, including close relatives. These three measures, relative incisor depth, width, and OACT, are thus sufficient to categorize rodents dietarily and functionally despite the enormous array of diets and functions rodents have adapted to.

These data also indicate potential fundamental differences in masticatory operation and evolution between rodent clades of differing masseter conditions. Hystricomorphs fail to explore the dietary space of proficient chiseling rodents that feed on hard nuts and seeds and have low relative incisor width, despite easily expanding into the tooth digging realm that usually requires intensive chewing functions. Additionally, myomorphs only moderately explore this space despite their far greater diversity generally. Hystricomorphs have repeatedly evolved diminutive incisors with high relative OACT, while sciuromorphs and hystricomorphs have only barely broached this territory. Finally, despite their enormous relative diversity, myomorphs show low relative disparity in incisal metrics and OACT, as well as evidence for lower rates of character evolution for these traits despite also exhibiting lower estimates of evolutionary constraint. All

of these data are in line with the simplistic hypothesis that hystriocmorphs are better chewers, sciuromorphs better gnawers, and that myomorphs are better at both. If myomorphs are more efficient in their ability to impart forces during both chewing and gnawing, they would potentially not need such extreme dental dimensions to adequately perform compared to sciuromorphs and hystricomorphs. Cox et al 2012 used finite element modeling to argue that myomorphy is more efficient at imparting forces at both the incisors and the cheekteeth, although there was reason to be skeptical of this categorical model given that only three taxa were studied, one from each masseter condition: *Sciurus carolinensis*, a gnawing specialized sciurid, *Cavia porcellus*, a chewing specialized hystricomorph, and *Rattus norvegicus*, a generalist myomorph. This study appeared biased toward its own conclusion given its taxon sampling. However, the study herein supports the overall conclusions of Cox et al 2012, although only in that it is consistent with a model of superior myomorph masticatory efficiency. A comparative analyses that demonstrates that the derived components of myomophy, the anterior deep masseter and ZMIO, are responsible for both chewing and gnawing adaptions would be necessary to corroborate this hypothesis.

References

Arregoitia, L.D.V., Fisher, D.O., and Schweizer, M. (2017). Morphology captures diet and locomotor types in rodents. Open Science 4, 160957.

Beaulieu, J.M., and O'Meara, B.C. (2012). OUwie: analysis of evolutionary rates in an OU framework. R package version 3.

Cano, A.R.G., Kimura, Y., Blanco, F., Menéndez, I., Álvarez-Sierra, M.A., and Fernández, M.H. (2017). Ecomorphological characterization of murines and non-arvicoline cricetids (Rodentia) from south-western Europe since the latest Middle Miocene to the Mio-Pliocene boundary (MN 7/8–MN13). PeerJ 5, e3646.

Cox, P.G. (2017). The jaw is a second-class lever in Pedetes capensis (Rodentia: Pedetidae). PeerJ 5, e3741.

Cox, P.G., and Baverstock, H. (2015). Masticatory Muscle Anatomy and Feeding Efficiency of the American Beaver, Castor canadensis (Rodentia, Castoridae). Journal of Mammalian Evolution 23, 191–200.

Cox, P.G., and Faulkes, C.G. (2014). Digital dissection of the masticatory muscles of the naked mole-rat, Heterocephalus glaber (Mammalia, Rodentia). PeerJ 2, e448.

Cox, P.G., and Jeffery, N. (2011). Reviewing the Morphology of the Jaw-Closing Musculature in Squirrels, Rats, and Guinea Pigs with Contrast-Enhanced MicroCt. The Anatomical Record: Advances in Integrative Anatomy and Evolutionary Biology 294, 915–928.

Cox, P.G., Rayfield, E.J., Fagan, M.J., Herrel, A., Pataky, T.C., and Jeffery, N. (2012). Functional Evolution of the Feeding System in Rodents. PLoS ONE 7, e36299.

Croft, D.A., Niemi, K., and Franco, A. (2011). Incisor morphology reflects diet in caviomorph rodents. Journal of Mammalogy 92, 871–879.

Dumont, E.R., Dávalos, L.M., Goldberg, A., Santana, S.E., Rex, K., and Voigt, C.C. (2012). Morphological innovation, diversification and invasion of a new adaptive zone. Proc. R. Soc. B 279, 1797–1805.

Evans, A.R., Wilson, G.P., Fortelius, M., and Jernvall, J. (2007). High-level similarity of dentitions in carnivorans and rodents. Nature 445, 78–81.

Fabre, P.-H., Hautier, L., Dimitrov, D., and Douzery, E.J.P. (2012). A glimpse on the pattern of rodent diversification: a phylogenetic approach. BMC Evolutionary Biology 12, 88.

Galetti, M., Guevara, R., Neves, C.L., Rodarte, R.R., Bovendorp, R.S., Moreira, M., Hopkins, J.B., and Yeakel, J.D. (2015). Defaunation affects the populations and diets of rodents in Neotropical rainforests. Biological Conservation 190, 2–7.

Galewski, T., Mauffrey, J.-F., Leite, Y.L.R., Patton, J.L., and Douzery, E.J.P. (2005). Ecomorphological diversification among South American spiny rats (Rodentia; Echimyidae): a phylogenetic and chronological approach. Molecular Phylogenetics and Evolution 34, 601–615.

Harmon, L.J., Weir, J.T., Brock, C.D., Glor, R.E., and Challenger, W. (2008). GEIGER: investigating evolutionary radiations. Bioinformatics 24, 129–131.

Hautier, L., Michaux, J., Marivaux, L., and Vianey-Liaud, M. (2008). Evolution of the zygomasseteric construction in Rodentia, as revealed by a geometric morphometric analysis of the mandible of Graphiurus (Rodentia, Gliridae). Zoological Journal of the Linnean Society 154, 807–821.

Hautier, L., Lebrun, R., Saksiri, S., Michaux, J., Vianey-Liaud, M., and Marivaux, L. (2011). Hystricognathy vs Sciurognathy in the Rodent Jaw: A New Morphometric Assessment of Hystricognathy Applied to the Living Fossil Laonastes (Diatomyidae). PLoS ONE 6, e18698.

Hautier, L., Lebrun, R., and Cox, P.G. (2012). Patterns of covariation in the masticatory apparatus of hystricognathous rodents: Implications for evolution and diversification. Journal of Morphology 273, 1319–1337.

Hopkins, S.S.B. (2008). Phylogeny and evolutionary history of the Aplodontoidea (Mammalia: Rodentia). Zoological Journal of the Linnean Society 153, 769–838.

Janis, C.M., and Ehrhardt, D. (1988). Correlation of relative muzzle width and relative incisor width with dietary preference in ungulates. Zoological Journal of the Linnean Society 92, 267–284.

Lucas, P.W., Gaskins, J.T., Lowrey, T.K., Harrison, M.E., Morrogh-Bernard, H.C., Cheyne, S.M., and Begley, M.R. (2012). Evolutionary optimization of material properties of a tropical seed. J. R. Soc. Interface 9, 34–42.

Men, X., Guo, X., Dong, W., and Qian, T. (2007). Population dynamics of Dremomys pernyi and Callosciurus erythraeus in protective and non-protective pine forests at different ages. Front. Biol. China 2, 242–246.

Meng, J., Hu, Y., and Li, C.-K. (2003). The osteology of Rhombomylus (Mammalia, Glires) : implications for phylogeny and evolution of Glires. Bulletin of the AMNH ; no. 275.

Paradis, E., and Schliep, K. (2018). ape 5.0: an environment for modern phylogenetics and evolutionary analyses in R. Bioinformatics 35, 526–528.

Pinheiro, J., Bates, D., DebRoy, S., Sarkar, D., and R Core Team (2019). nlme: Linear and Nonlinear Mixed Effects Models.

R Core Team (2013). R: A language and environment for statistical computing. R Foundation for Statistical Computing (Vienna, Austria).

Revell, L.J. (2010). Phylogenetic signal and linear regression on species data. Methods in Ecology and Evolution 1, 319–329.

Revell, L.J. (2012). phytools: An R package for phylogenetic comparative biology (and other things). Methods in Ecology and Evolution 3, 217–223.

Samuels, J.X. (2009). Cranial morphology and dietary habits of rodents. Zoological Journal of the Linnean Society 156, 864–888.

Santana, S.E., Dumont, E.R., and Davis, J.L. (2010). Mechanics of bite force production and its relationship to diet in bats. Functional Ecology 24, 776–784.

Slater, G.J., Dumont, E.R., and Van Valkenburgh, B. (2009). Implications of predatory specialization for cranial form and function in canids. Journal of Zoology 278, 181–188.

Swanson, M., Oliveros, C.H. and Esselstyn, J. (2019). A phylogenomic rodent tree reveals the repeated evolution of masseter architectures. Proceedings of the Royal Society B: Biological Sciences. 286, 20190672.

Upham, N.S., Esselstyn, J.A., and Jetz, W. (2019). Ecological causes of uneven diversification and richness in the mammal tree of life. BioRxiv 504803.

Zaragoza Quintana, E., Pech-Canché, J., Sosa-Escalante, J., Hernández-Betancourt, S., León-Paniagua, L., and MacSwiney, M. (2016). Small rodents in the Yucatan Peninsula: knowledge and perspectives in 114 years of research. Therya 7, 299–214.

Figures

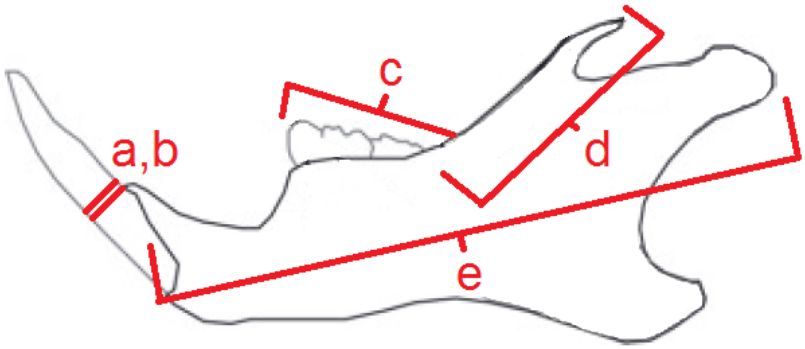

Figure 1.1. Representative rodent mandible demonstrating principal caliper measurements collected: a) incisor depth, the perpendicular line between the tangents on both lingual/mesial and labial/distal sides of the incisor, b) incisor width, here oriented in and out of the page, a meaure of medialateral width that includes both incisors measured immediatelyl distal to the incisor alveoli, c) cheektooth length, the distance from the most anterior point of p4/m1 to the most posterior point of m3 (widest molar width not shown, but is measured from the at the widest mediolateral portion of the widest molar), d) temporalis attachment/cornoid height, measured from the most dorsal portion of the coronoid to where the coronoid meets the toothrow anteriorly, measured in the plane of the coronoid process, e) mandible length, measured from the mandibular condyle to the most distal lateral margin of the incisor alveolus, measured in the plane of the dentary.

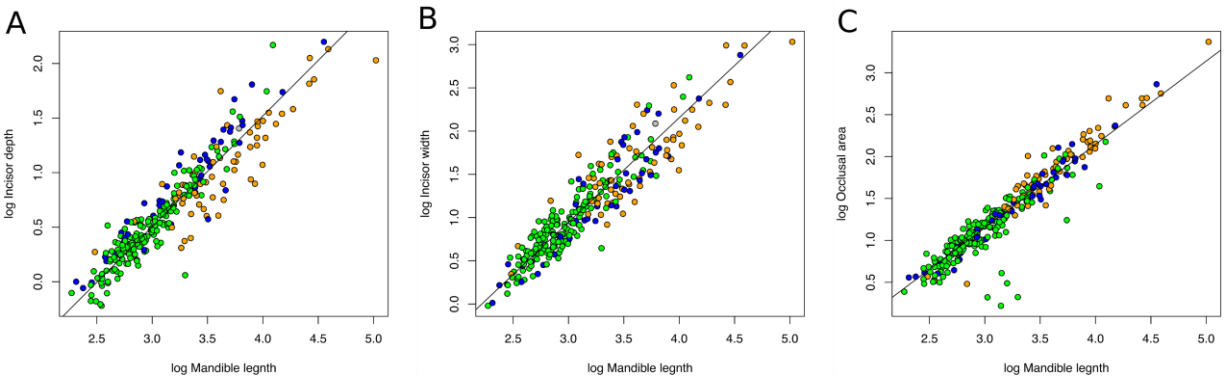

Figure 1.2. Allometric scaling of dental measures A) log incisor depth, B) log incisor width, and log of the square root of occlusal area of the cheekteeth for 278 taxa across the masseter conditions protrogomophy (gray), sciuromorphy (blue), hystricomorphy (orange), and myomorphy (green). Solid line represents a significant ($p<0.0001$) PGLS across all taxa.

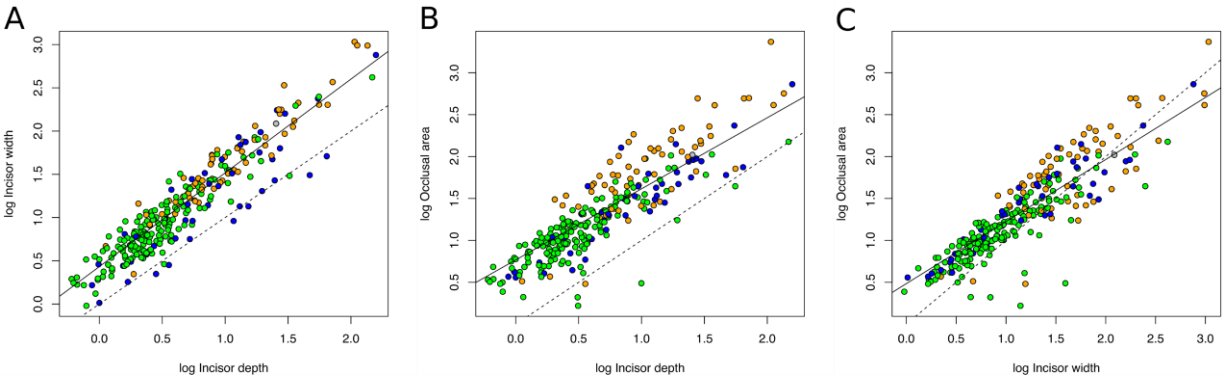

Figure 1.3. Allometric scaling of dental measures for A) log incisor width over log incisor depth, B) log sqOACT over log incisor depth, and C) log of the sqOACT over log incisor width for 278 taxa across the masseter conditions protrogomophy (gray), sciuromorphy (blue), hystricomorphy (orange), and myomorphy (green). Solid line represents a significant ($p<0.0001$) PGLS across all taxa and dotted line represent a one to one line.

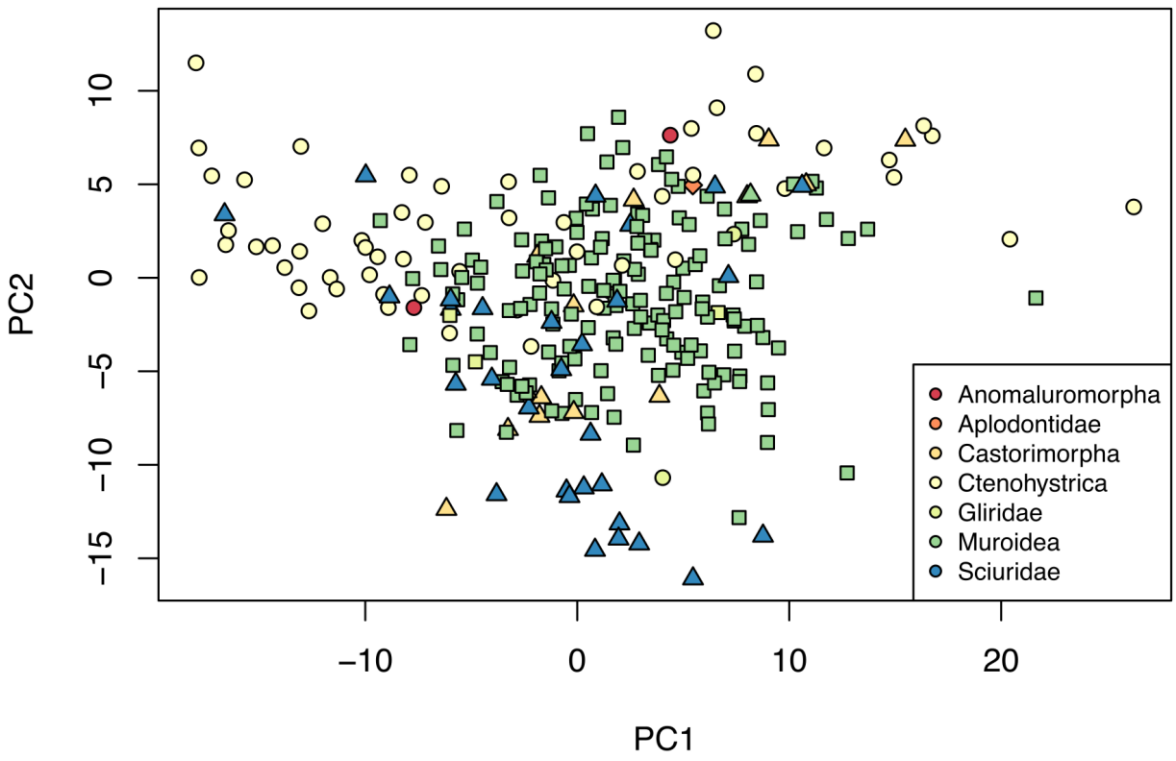

Figure 1.4. Phylogenetic principal components analysis for 276 taxa across masseter conditions protrogomophy (diamond), sciuromorphy (triangle), hystricomorphy (circle), and myomorphy (square). PC1 encompasses 50.95% of the variation, PC2 encompasses 26.82% of the variation.

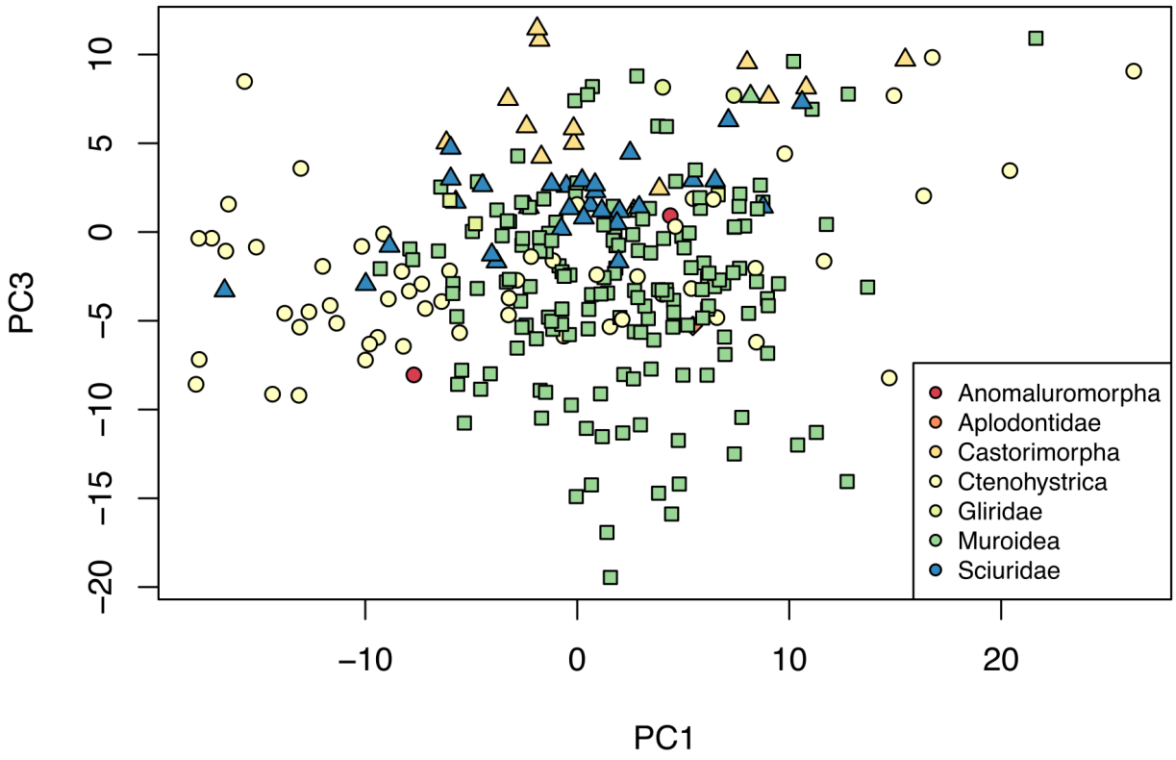

Figure 1.5. Phylogenetic principal components analysis for 276 taxa across masseter conditions protrogomophy (diamond), sciuromorphy (triangle), hystricomorphy (circle), and myomorphy (square). PC1 encompasses 50.95% of the variation, PC3 encompasses 22.23% of the variation.

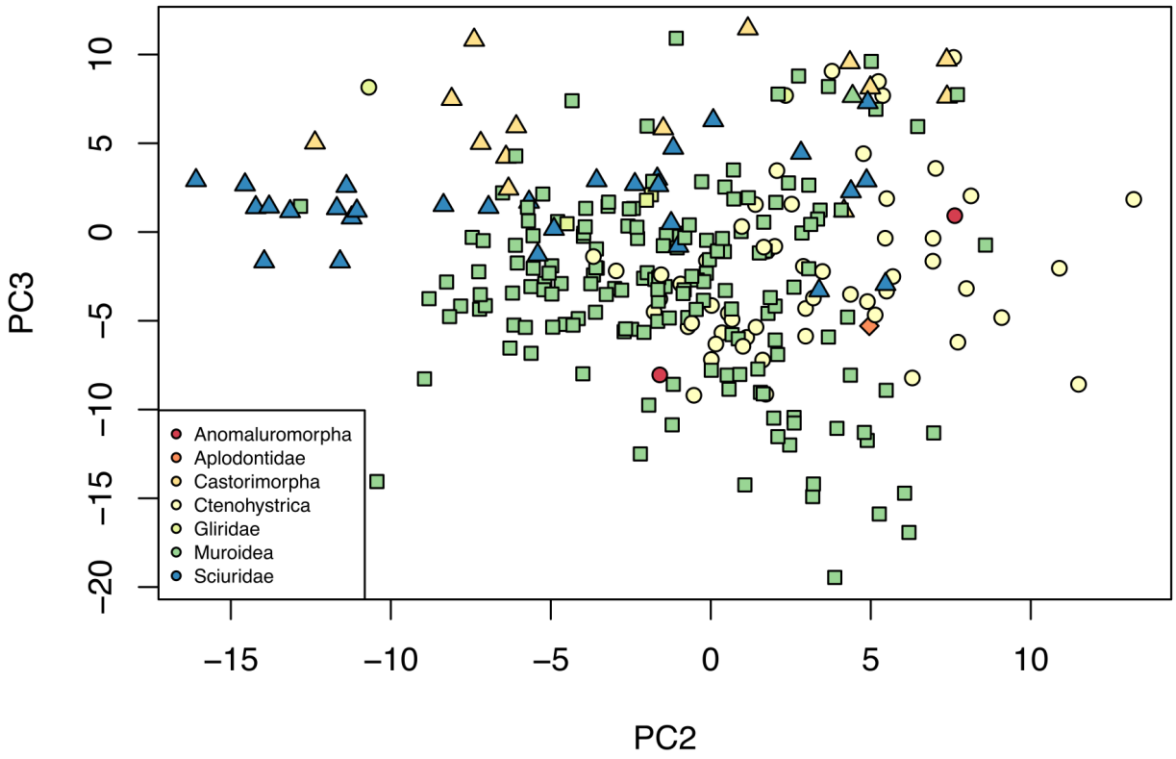

Figure 1.6. Phylogenetic principal components analysis for 276 taxa across masseter conditions protrogomophy (diamond), sciuromorphy (triangle), hystricomorphy (circle), and myomorphy (square). PC2 encompasses 26.82% of the variation, PC3 encompasses 22.23% of the variation.

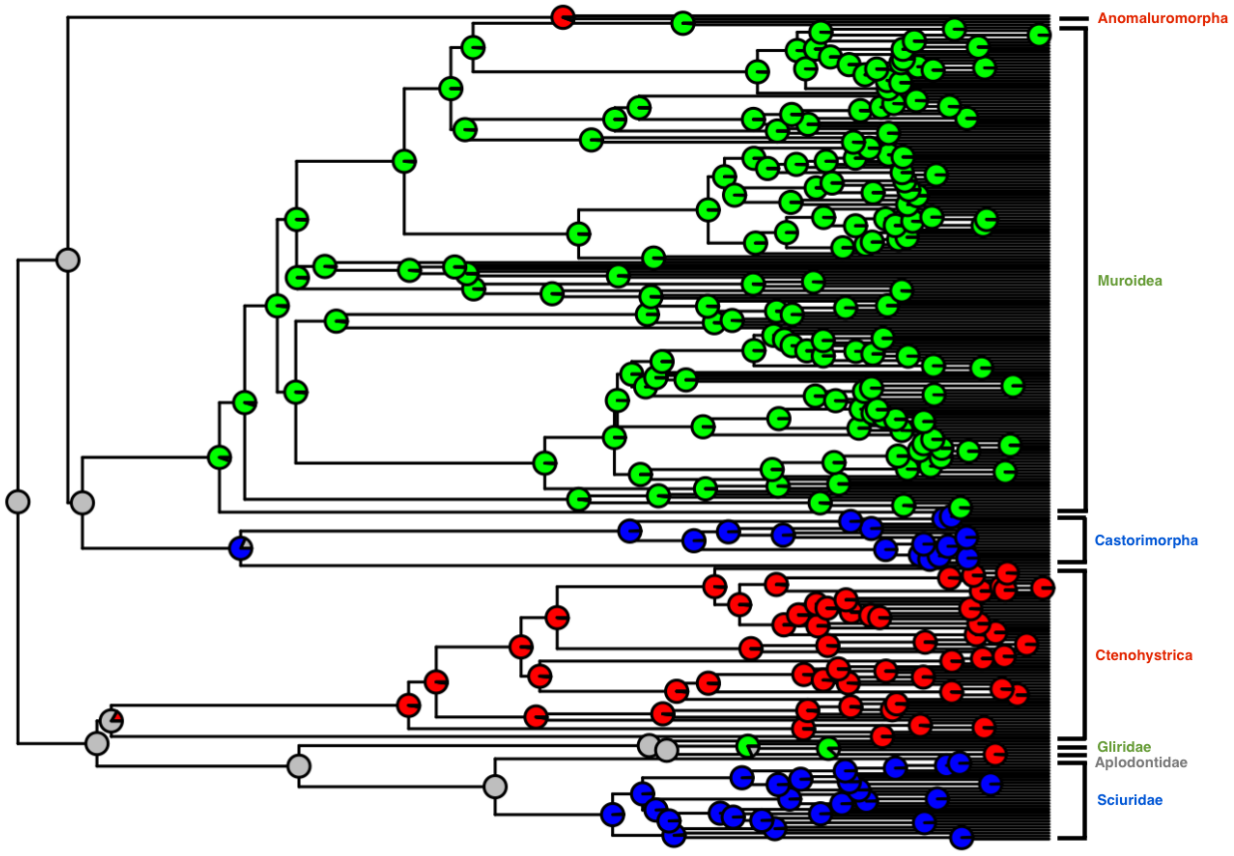

Figure 1.7. Ancestral character estimation with pie charts at nodes representing likelihood of character ancestry (gray = protrogomorphy, blue = sciuromorphy, red = hystriomorphy, green = myomoprhy), based on the best fit all-rates-different model for discrete character data.

Table 1.1. Loadings for phylogenetic PCA results. PC1 = 50.95% of variance, PC2 = 26.82%, PC3 = 22.23%, PC4 <0.0001%.

	PC1	PC2	PC3	PC4
log Incisor depth	0.7130078	-0.6973832	-0.07263941	2.516076E-08
log Incisor width	0.6482311	0.75943186	0.05531502	-2.615693E-08
log CTR length	-0.6968511	0.07098322	-0.71369455	-8.661544E-10
log WM width	-0.7897160	-0.06890720	0.60959042	-1.081256E-10

Table 1.2. Model fit for the evolution of discrete character states for masseter condition. ER = equal rates model, SYM = symmetric model, ARD = all rates different model.

	fit	delta	w
ER	70.32899	5.839388	0.05063554
SYM	73.41852	8.928920	0.01080369
ARD	64.48960	0.000000	0.93856077

Table 1.3. Transition rate matrix for the evolution of discrete character states for masseter condition, estimated using likelihood and mean root node prior probabilities.

	Hystricomorph	Myomorph	Protrogomorph	Sciuromorph
Hystricomorph	0	0	0	0
Myomorph	0	0	0	0
Protrogomorph	0.02547	0.02137	-0.061119	0.014273
Sciuromorph	0	0	0	0

Table 1.4. Fit of evolutionary models for continuous character evolution of relative incisor depth. BM1 = brownian motion, single rate; BMS = brownian motion, multi-rate; OU1, Ornstein-Ohlenbeck (OU), single optimum; OUM = OU, single alpha and sigma^2, different state means; OUMA = OU, multi-alpha, single sigma^2, different state means; OUMV = OU, single alpha, multi-sigma^2, different state means; OUMVA = OU, multi-alpha, multi-sigma^2, different state means.

	fit	delta	w
BM	-1656.631	46.7110	0.0000
BMS	-1686.965	16.3765	0.0003
OU1	-1675.357	27.9847	0.0000
OUM	-1676.924	26.4182	0.0000
OUMA	-1698.674	4.6679	0.0883
OUMV	-1703.342	0.0000	0.9997

Table 1.5. Fit of evolutionary models for continuous character evolution of relative occlusal area of the cheekteeth. BM1 = brownian motion, single rate; BMS = brownian motion, multi-rate; OU1, Ornstein-Ohlenbeck (OU), single optimum; OUM = OU, single alpha and sigma^2, different state means; OUMA = OU, multi-alpha, single sigma^2, different state means; OUMV = OU, single alpha, multi-sigma^2, different state means; OUMVA = OU, multi-alpha, multi-sigma^2, different state means.

	fit	delta	w
BM	-1278.348	58.1095	0.0000
BMS	-1294.717	41.7403	0.0000
OU1	-1321.723	14.7341	0.0004
OUM	-1322.251	14.2063	0.0005
OUMA	-1322.892	13.5648	0.0007
OUMV	-1336.457	0.0000	0.6107
OUMVA	-1335.548	0.9089	0.3877

Table 1.6. Fit of evolutionary models for continuous character evolution of relative incisor width. BM1 = brownian motion, single rate; BMS = brownian motion, multi-rate; OU1, Ornstein-Ohlenbeck (OU), single optimum; OUM = OU, single alpha and sigma^2, different state means; OUMA = OU, multi-alpha, single sigma^2, different state means; OUMV = OU, single alpha, multi-sigma^2, different state means; OUMVA = OU, multi-alpha, multi-sigma^2, different state means.

	fit	delta	w
BM	-1271.697	29.1684	0.0000
BMS	-1295.218	5.6478	0.0560
OU1	-1276.185	24.6809	0.0000
OUM	-1271.545	29.3206	0.0000
OUMV	-1300.866	0.0000	0.9439

Chapter 2: The evolutionary biomechanics of novel masseter muscles in rodents and their role in distinct gnawing and chewing functions

Abstract

The novel jaw musculature of rodents, particularly the derived anterior divisions of the masseter muscles, has long been considered important to their evolution. However, the function of these derived masseter units has remained understudied and poorly understood. Chapter 1 demonstrated that ecomorphological aspects of the dentition differ among lineages characterized by differing masseter conditions are biased toward different specialized functions and ecologies, but it is unclear whether the novel musculature has evolved specialized roles in the masticatory apparatus. Crucially, the mutually exclusive occlusion of the incisors during gnawing and the cheekteeth during chewing presents a number of theoretical challenges to individual muscle function because they require separate positions of the mandible relative to the cranium that may further differentiate the biomechanics of masseter conditions. I collected muscle lengths and mechanical advantages in both incisor gnawing and cheekteeth chewing positions from 243 species of rodents spanning all independently evolved masseter conditions. I tested the hypotheses that sciuromorphic muscles are adapted to gnawing, hystricomorph muscles are adapted to chewing, and myomorph muscles are adapted to both gnawing and chewing functions. Muscle length change data reveal that the temporalis and superficial masseter change unidirectionally across masseter conditions when moving from chewing to gnawing positions (lengthing and shortening, repsectively), whereas anterior deep masseter and the infraorbital portion of the zygomaticomandibularis change lengths in different directions depending on masseter conditions. These results imply that the temporalis and superficial masseter may not function optimally at both positions of the jaw across rodents, whereas the derived masseters

likely perform quite differently in different masseter conditions. Phylogenetic regressions of mechanical advantage against relative measures of incisor depth and cheekteeth occlusal area demonstrate that each muscle in the masticatory apparatus covaries with incisor depth more than to occlusal area of the cheekteeth, likely due to the higher bite forces necessary during gnawing. Evolutionary trait modeling of mechanical advantages reveals lower rates of mechanical advantage evolution for myomorphs compared to sciuromorphs and hystricomorphs, conforming to the hypothesis that myomoprhy is functionally flexible and does not require substantial biomechanical alterations to adapt to the many varying ecologies that myomorphs repeatedly evolve. Overall, this study demonstrates that rodent jaw muscles likely require compensatory adaptations of muscle function to accommodate separate biting positions of the mandible, but the greater demands of gnawing exert a stronger selective pressure on mechanical advantages than does chewing function. Myomorphy appears to be a more stable evolutionary condition from the perspective of mechanical advantage evolution, likely because of the high mechanical advantages of both the anterior deep masseter and infraorbital portion of the zygomaticomandibularis. Three dimensional analysis of mechanical advantages that are measured as the orthogonal distance from the muscle vector to the jaw joint would further refine our understanding of the mechanics of these systems and offers a further test to the hypothesis that myomorphy facilitates a more efficient utilization of both incisors and cheekteeth in rodent functional evolution.

Introduction

Understanding the functional roles of novel morphologies and their macroevolutionary consequences is a fundamental goal of modern evolutionary biology. Organisms are constrained by their evolutionary histories, genome architectures, developmental processes, physical

attributes, and environmental settings, all in various ways limiting the evolutionary trajectories that can be realized and explored through time. Large, saltatorial jumps in the evolution of morphology provide categorically new opportunities for organisms to utilize in evolution, potentially opening entirely new styles of ecological exploitation. Although we often observe major, novel differences in morphology through evolutionary time, demonstrating their functional significance in an organism and across macroevolution is far more challenging. Approaching these problems requires reasonable evidence for interpreting a novel structure's biomechanical utility *in vivo*, as well as a sufficient comparative perspective to determine the crucial differences between taxa over time. Here, I aim to determine the biomechanical utility of novel masseter muscles in rodents, in particular whether these muscles have evolved to specifically perform gnawing and/or chewing functions, as well as the consequences of evolving these novel muscles for rodent diversification.

Rodents have a unique masticatory apparatus among mammals, in which the incisors fail to occlude during cheekteeth occlusion (chewing) and the cheekteeth fail to occlude during incisor occlusion (gnawing) (Druzinsky 2010a). Although other mammals, such as lagomorphs, wombats, other diprotodont marsupials, and the aye-aye, are superficially similar in having a large diastema between the incisors and cheekteeth along with a loss of canine teeth, only rodents demonstrate these mutually exclusive occlusion patterns (Morris Phillip et al. 2019). Such a fundamentally unique masticatory behavior has a number of important biomechanical and evolutionary consequences for rodents. In order to gnaw at the incisors, rodents must move their entire mandible anteriorly, displacing the mandibular condyle from posterior to the zygomatic process of the squamosal into a more anterior position, either directly ventral to the zygomatic process of the squamosal or anterior to it. This marked shift in jaw position could drastically

change the biomechanics of each individual jaw muscle, with muscle lengths being variously stretched or shortened in the gnawing and chewing positions depending on the individual muscle's origin and insertion. If individual muscles have different biomechanics when in the gnawing and chewing positions, it is likely that these muscles have different performance metrics in these positions, with one position fitting more closely with that muscle's performance optimum on the length tension curve. Therefore, we might expect certain muscles to perform better or worse in each position, thus implying adaptation to perform in one position and not the other, or to have evolved trade offs that would allow adequate functioning in both positions.

Following the evolution of the gnawing/chewing functional separation at the base of rodents, the clade diversified into numerous families across the world before later evolving derived, novel masseter muscles to supplement their unique biomechanics. Today, these various masseter conditions are termed protrogomorphy (the primitive condition in which no masseter units originate anterior to the orbit on the rostrum), sciuromorphy (a derived condition in which the anterior deep masseter (ADM) is the only muscle that originates anterior to the orbit on a specialized attachment on the rostrum termed the zygomatic plate), hystricomorphy (a derived condition in which the infra-orbital portion of the zygomaticomandibularis (ZMIO) is the only muscle that attaches anterior to orbit of on the rostrum by penetrating the infra-orbital foramen and originating on the lateral surface of the rostrum), and myomorphy (a secondarily derived condition in which both the ADM and ZMIO originate anterior to the eye on the rostrum, with the ADM and zygomatic plate always positioned ventrolaterally to the ZMIO and the infra-orbital foramen). Among extant taxa, each of these three derived conditions evolves multiple times, with two origins of myomorphy (Gliridae and Muroidea), two origins of sciuromorphy (Sciuridae and Castorimorpha, four including Gliridae and Muroidea), and four origins of

hystricomorphy (Ctenohystrica, Anomaluromorpha, Dipodoidea, and Graphiurus, six including Gliridae and Muroidea). Additional independent derivations of these same masseter conditions appear to evolve multiple times in the fossil record, creating a dazzling array of repeatedly evolved, complex morphologies, each with an unknown function. Almost all of these evolutionary events occurred during the Eocene and Oligocene, with very little subsequent changes to the masseter morphotypes from the Miocene onward, with the exceptions of *Graphiurus* (an apparent reduction hystricomorphy from myomorphic glirids) (Hautier et al. 20) and *Heterocephalus* (a reduction of the hystricomorphy into a state in which the infraorbital foramen is no longer fully and consistently penetrated by the ZMIO, resembling a superficially protrogomorphous state while otherwise sharing the same muscle arrangements and dimensions as other highly derived hystricomorphous relatives) (Cox and Faulkes 2014).

With apparent functional independence of the gnawing and chewing positions of the mandible (ref: Chapter 1) and the necessarily different biomechanics for the same muscle in each position, it appears likely that muscles would evolve to specialize on particular mandible positions or evolve to accommodate both positions simultaneously. Relevant data on this question from the literature are lacking, although some authors have demonstrated differential utilization of masseter units during gnawing and chewing behavior. Druzinsky (2010a, 2010b) demonstrated that sciuromorphs (both sciurids and castorimorphs) are particularly suited to gnaw at the incisors with their ADM compared to the protrogomorphous *Aplodontia rufa*, which has an ADM-like muscle division that is heavily reduced in comparison. Similarly, Cox 2017 demonstrated in the hystricomorphous anomaluromorph springhare (*Pedetes capensis*) that the ZMIO is critical to maximizing mechanical advantage in chewing. Cox et al. 2012 used finite element modeling for three representative taxa, the sciuromorphous gray squirrel *Sciurus*

carolinensis, the hystricomorphous *Cavia porcellus*, and the myomorphous *Rattus norvegicus*, to demonstrate that each of these masseter condtion fits a stereotypical model in which sciuromorphy is efficient at gnawing, hystricomorphy is efficient at chewing, and myomorphy is efficient at both. This study was restricted to only three taxa, however, and each was biased toward their ultimate conclusion, with *Sciurus* being a genus of hard nut and seed gnawing speciailists, *Cavia* a genus of grazing herbivores, and *Rattus* a genus of adaptable generalists that have successfully invaded environments of extreme human disturbance. Although there are hints at a potential model of rodent masseteric biomechanics that have been discussed in the literature for decades, what is needed is an broad, comparative, biomechanically informed analysis (much like Druzinksy 2010a/b) across all of rodents that takes into account the discrepancy in gnawing and chewing behavior on muscle function.

My first chapter demonstrated that relative incisor depth and relative occlusal area of the cheekteeth (OACT) are important predictors of rodent ecofunctionality, primarily relating to the physical interactions that these teeth must endure as opposed to simply and directly relating to the specific nutritional uptake particular species are adapted to. The labiolingual depth of incisors is directly related to the tolerable stress and loads an incisor regularly functions under, as Freeman and Lemen 2008 found comparing these depth measures to in vivo bite force data. Furthermore, my data demonstrated that high relative incisor depth is found only in species that regularly gnaw into hard nuts, seed, wood, bamboo parts, and/or use their incisors to dig in hard soils. Low relative incisor depth was found in taxa that require minimal gnawing proficiency, such as faunivores and folivores. OACT is a measure more comparable to typical metrics used across mammalian ecomorphological studies to assess the degree of herbivory. My data demonstrated that high relative OACT is found primarily in highly herbivorous taxa (as well as

the only durophagous taxon on the dataset, *Hydromys melanogaster*) and is low in taxa with diets that require low molar processing, such as faunivores and seed eaters. Importantly, the distribution of taxa in ecofunctional morphospace differed between clades of differing masseter construction. Ctenohystrican hystricomorphs lacked any taxa with high relative incisor depth and low relative incisor width, with high relative incisor depth only found in taxa with high relative incisor width that specialize in digging. Sciuromorphs in general contained few taxa with low relative incisor depth. Evolutionary modeling results demonstrated that hystricomorphs overall had lower relative incisor depth and high relative OACT, while sciuromorphs had high relative incisor depth and low relative OACT. Myomorphs were intermediate in both scenarios, with lower estimations for evolutionary rate and alpha parameters in the best fitting Ornstein Uhlenbeck models. These data demonstrate that hystricomorphs and sciuromorphs explore the bounds of ecomorphospace at higher evolutionary rates than myomorphs, despite that myomorphs have far higher rates of taxonomic diversification and an enormous diversity of diets and ecologies. It could be that myomorphs simply have more generalists and omnivores, diluting the signal of fast evolutionary rates in traits; however, this hypothesis is not mutually exclusive to the hypothesis that myomorphs do not require the same robusticity in incisors and size in cheekteeth to accomplish the same functions given a more sophisticated masseteric system.

I hypothesize that differences in dental traits among hystricomorphs, sciuromorphs, and myomorphs are related to differences in masseteric biomechanics. Specifically, I hypothesize that the ZMIO in hystricomorphs is a muscle originally adapted to chewing behavior, the ADM of sciuromorphs originally adapted to gnawing behavior, and that the co-occurence of these muscles in myomorphs provides further opportunities for each of these muscles to operate under both gnawing and chewing positions of the jaw. Such a scenario would allow myomorphic

systems to perform at higher power per bite and higher precision per bite. To test these hypotheses, I will compare the mechanical advantages of each important adductor muscle (namely the ADM, ZMIO, superficial masseter, posterior deep masseter, and temporalis) across each masseter condition to ecofunctionally important traits related to gnawing (relative incisor depth) and chewing (relative OACT) proficiency to assess whether muscles of particular masseter conditions have co-evolved with demands of gnawing and chewing functions. Such a comparative approach to assess evolutionary functional relationships requires a sufficient number of taxa in each clade. I will thus conduct additional analyses that exclude small clades such as Gliridae, Anomaluromorpha, Dipodoidea, and Castorimorpha and focus on the traditionally recognized namesakes for each masseter condition: Ctenohystrica for hystricomorphy, Sciuridae for sciuromorphy, and Muroidea for myomorphy.

Mechanical advantages have been used in many comparative studies to understand dietary and functional evolution (Weastneat 1995, Wainwright et al. 2004, Alfaro et al. 2005, Wainwright et al. 2005, Bellwood et al. 2006, Anderson et al. 2014, Becerra et al. 2014, Curtis and Santana 2018). Mechanical advantages are a useful tool for understanding biomechanical evolution in a comparative context as they are dimensionless metrics defined as the ratio of the in-lever of a muscle (in a mandibular context the distance from the jaw joint to the muscle insertion) to its out-lever (the distance from the jaw joint to the bite point in the context of jaws). Mechanical advantage is also a fundamentally simple physical principle that applies universally across taxa, in which a higher mechanical advantage necessarily increases force amplification in a system regardless of other contextual features. Organisms can often vary substantially in many important aspects of mandibular mechanics, whether that be within an organism's lifetime, across conspecifics, or across species, such as in muscle mass, sarcomere length, typical gape

during use, etc.; however, in all of these cases a higher mechanical advantage will increase force amplification compared to a lower mechanical advantage. The basic physics that underlie mechanical advantage provide for an optimization pathway that natural selection can utilize to increase force output from muscles without evolving more powerful muscles or investing in the higher physiological demands of higher muscle mass. Although increased muscle mass may temporarily evolve during microevolutionary events, if possible a higher mechanical advantage without a higher muscle mass can provide for the same functional output without costing the organism the energy required to maintain those larger muscles. One can thus hypothesize that changes in mechanical advantage across species over time can provide a faithful signal of adaptation, whether that be toward higher mechanical advantage and higher force amplification or lower mechanical advantage and higher biting velocity. Accordingly, if changes in mechanical advantage covary evolutionarily with changes in dental dimensions, we can predict that these changes in mechanical advantage represent adaptations that these muscles have evolved to perform at those particular bite points. A failure to covary could represent a lack of functional relationship or a complexity of functional relationships that cannot be simply represented by a single correlation.

Finally, I will explore how differences in mechanical advantage have evolved for individual muscle groups across rodents with masseter conditions by fitting various Brownian Motion and Ornstein Uhlenbeck based models to the data using the most up to date phylogeny for rodents (Upham et al 2019). I predict that each masseter condition will fit an OU model, in which mechanical advantages are selected toward a trait optimum favored by that condition functionally. In particular, sciuromorphs should demonstrate high trait optima for ADM mechanical advantage compared to hystricomorphs, and hystricomorphs should demonstrate

high trait optima for ZMIO mechanical advantage compared to sciuromorphs. Myomorphs should favor high trait optima for both ADM and ZMIO mechanical advantages, although may not surpass these groups given that they harbor dual anterior masseter, relaxing selection for mechanical advantage maximization. I predict that myomorphs will demonstrate lower evolutionary rates for ADM and ZMIO mechanical advantages, fitting with previous dental data and a model in which the ADM and ZMIO have synergistic effects on one another's performance capabilities, decreasing the raw variation necessary to impact a similar range the biomechanical outputs important to food processing and other masticatory functions. Importantly, these mechanical advantage measures should not demonstrate higher alpha parameters in these OU models for myomorphs, as that would imply a limited range of possible mechanical advantages allowed for the myomorphic system to perform, which is contrary to the hypothesis that complexity of the myomorphic system allows for a variety of utilizations biomechanically.

Methods

Specimens and Data Collection

Data were collected from dry skulls in the Field Museum of Natural History (FMNH) Mammalogy collections. Species were broadly sampled across rodents to include representatives from each major clade and family, with particular focus on sampling species from each independently evolved masseter condition. Crania with associated intact mandibles were photographed with a scale bar in lateral view in both gnawing and chewing positions. Chewing positions were obtaining by placing the cranium onto the mandible such that the cheekteeth were aligned and in total occlusion. Gnawing positions were obtained by moving the mandible

forward such that the upper incisors' occlusal plain rested on the tip of the lower incisor and the mandibular condyle rested underneath the zygomatic process of the squamosal. Specimen photographs were digitized using the software ImageJ.

Each specimen was measured in 2D photographs in lateral view for two different out-levers based on gnawing and chewing bite points, in-levers for each muscle in each mandible position (superficial masseter [SM], anterior deep masseter [ADM], posterior deep masseter [PDM, zygomaticomandibularis [ZM] orbital portion [ZMOP] or infraorbital portion [ZMIO], and temporalis muscle), muscle length from origin to insertion for each muscle in each mandible position, and mandible length. Muscle lengths were measured from the middle of the insertion point on the mandible (based on recorded muscle anatomy in the literature and interpolated based on muscle scarring when available) to the middle of the origination regions most distal edge of attachment (for example, the most dorsal point of curvature on the zygomatic plate or the most posterodorsal point of the temporal ridge) for each muscle (Fig. 2.1). Muscle lengths for the ZMIO were treated as straight lines for simplicity given the difficulty in assessing the exact point of curvature within the orbit in lateral view. The gnawing out-lever was measured as the distance from the mandibular condyle to the tip of the lower incisor, and the chewing out-lever was measured from the mandibular condyle to the middle of the occlusal surface of the most anterior cheektooth (p4 for vast majority of non-muroid rodents, m1 for muroids and some ctenodactylids). In-levers were measured as the linear distance from the mandibular condyle to the middle of the insertion point on the mandible for each muscle (Fig. 2.2). Because this is a static analysis, in which each position is not in motion, in-levers can reliably be measured in the same way for each biting position relative to the mandibular condyle which moves with the rest of the jaw. Mandible length was measured as the distance from the mandibular condyle to the

most distal lateral margin of the incisor alveolus. Mechanical advantages were calculated as the in-lever of a muscle in a certain biting position divided by the out-lever of that same biting position.

These data were analyzed with associated data for dental dimensions (incisor depth, incisor width, occlusal area of the cheekteeth, and height of the coronoid process) from the same specimens collected in Chapter 1. These data were also collected for new specimens that were not included in Chapter 1 using techniques described there.

Phylogenetic framework.

As in Chapter 1, a modified version of the Upham et al 2019 total mammal phylogeny was used as the phylogenetic framework for comparative analyses. Specifically, the genetic data only subset that lacks polytomies was pruned to include only the 242 taxa under study here. See Chapter 1 for details.

Analysis of muscle length changes in gnawing and chewing positions

Muscle length data were natural logged. Length in the gnawing position was regressed over the chewing position to compare magnitude and direction of muscle length change across taxa. PGLS analyses were performed across all taxa and for each masseter morphotype using a modified gls function from the NLME package (Pinheiro et al.2019) along with the corPagel ("Pagel's lambda Correlation Structure") function from the ape package (Revell 2012) in R (R Core Team) to simultaneously estimate phylogenetic signal in the residual error term (Revell 2010). The intervals function was used to estimated 95% confidence intervals (CI) to compare each regression to a one to one line, which in this case indicates no change in muscle length during gnawing compared to chewing.

Coevolution of mechanical advantage and dental metrics

Mechanical advantages from gnawing and chewing positions of the jaw were regressed against relative incisor depth and relative OACT, respectively, using a variety of modified phylogenetic generalized least squares models: 1) a PGLS across all taxa, 2) a PGLS that tests for differences in intercept between masseter morphotypes, and 3) and PGLS that tests for differences in intercept and slope between masseter morphotypes. These analyses were conducted to assess whether the data were best explained by a single phylogenetic regression or multiple phylogenetic regressions based on morphotype. The fit of these models was assessed by comparing their Bayesian Information Criterion (BIC) values using the aicw function in R. Additional PGLS were conducted on the three major clades of independently evolved masseter conditions, Muroidea (myomorphy), Ctenohystrica (hystricomorphy), and Sciuridae (sciuromorphy) to assess whether these clades demonstrate significant regressions when other independent evolutions of those same morphotypes are not included.

Stochastic mapping and ancestral state estimation

Analyzing the macroevolutionary trends across discrete character states requires an estimation of how these states have evolved on the phylogeny. The fitDiscrete function from the R package geiger was used to determine the best fit model of discrete character evolution for masseter condition on the subsetted tree of 242 sampled taxa. I assessed the fit of an equal-rates model (ER), in which the transition rates between each pair of states are equal, a symmetric model (SM), in which the rates to and from an individual state are the same but each pair of state's rates are allowed to vary, and an all-rates-different model (ARD), in which each transition rate is allowed to be unique. The model with the lowest Akaike weight score was used in an ancestral character estimation using the ace function from the R package ape. I created a

stochastic character map on this phylogeny using the make.simmap function from the R package phytools (Revell 2012) under the best fitting model.

Macroevolutionary models of trait evolution

Models of trait evolution were fitted to ADM and ZM mechanical advantages in both gnawing and chewing postions using the OUwie function from the OUwie package (Beaulieu and O'Meara 2012) in R. This function allows for the parameters of evolutionary models for continuous traits to vary according to underlying discrete character states (here masseter conditon). I assessed the fit of these data to a Brownian motion (BM) model in which only a single rate is allowed (BM1), a BM model with distinct rates for each discrete character state (BMS), and four different Ornstein-Uhlenbeck (OU) models: OU1, in which there is a single value for alpha (alpha being a parameter describing the "constraint" on trait value evolution through time, or the propensity to regress back to the trait optimum), sigma squared (evolutionary rate of continuous character), and mean (or optimum, the value a clade's evolution is centered on) value for each character state, OUM, in which there is only one alpha and sigma despite different state mean values, OUMA, in which alpha can vary between states, OUMV, where sigma can vary between states, and OUMVA, in which both alpha and sigma vary between states. Model fit was assessed using the lowest Akaike weight scores. I predict that masseter condition will bias the trait optima for each mechanical advantage measure, thus favoring OU models over Brownian Motion models. In particular, I predict sciuromorphs and myomorphs will demonstrate higher trait optima for ADM mechanical advantages compared to hystricomorphs and that hystricomorphs and myomorphs will demonstrate higher ZMIO mechanical advantages compared to sciuromorphs. Finally, myomorphs should demonstrate lower rates of evolution and lower alpha parameters, as their synergistic relationship between

ADM and ZMIO should relax selection on extreme biomechanics for each individual muscle, which should make each muscle less constrained in its evolutionary potential to vary, as this complex system should be more robust to potential changes in mechanical advantages of both the ADM and ZMIO away from the optima.

Results

Reconstructing Masseter Morphotype Evolution

An all rates different model, in which transition rates in and out of discrete masseter conditions are allowed to vary independently, had the highest Akaike weight score (0.939). Thus, the all rates different model was used in estimating the ancestral masseter condition. Ancestral character estimation resulted in protrogomorphy and myomorphy as the primitive conditions with equal likelihood. Inspection of maximum likelihood estimates for transition rates show that this result is due to rates of almost zero for all conditions except protrogomorphy, conforming with the tree's lack of inferred evolution of derived masseter conditions from other derived masseter conditions in ancestral state estimation.

Muscle length changes from gnawing to chewing

PGLS regression lines for the ZM muscle lengths during gnawing and chewing fail to differentiate from a 1 to 1 line, as the confidence intervals (CI) for the intercept contain 0 (-0.0423 to 0.108) and for the slope contain 1 (0.964 to 1.007) (Fig. 2.3B). Although the PGLS regression for ZM muscle length change across all species fails to differentiate from a one to one line, myomorphs (intercept 95% CI: 0.0923 to 0.279, slope 95% CI: 0.906 to 0.964) and sciuromorphs (intercept 95% CI: -0.263 to -0.135, slope 95% CI: 1.0212 to 1.0735) do significantly differentiate from a one to one line, although in different directions, while the hystricomorph (intercept 95% CI: 0.0165 to 0.164, slope 95% CI: 0.959 to 1.00365) slope

includes the one to one line. The ADM significantly differs from a one to one line with both its intercept failing to contain zero (0.0513 to 0.192) and its slope failing to contain 1 (0.941 to 0.987) (Fig. 2.3A). PGLS for myomorph ADM length changes also significantly differ from a one to one line (intercept 95% CI: 0.0917 to 0.267, slope 95% CI: 0.913 to 0.971); however, the ADM length changes in sciuromorphs (intercept 95% CI: -0.0970 to 0.0695, slope 95% CI: 0.984 to 1.0383) and hystricomorphs (intercept 95% CI: -0.0834 to 0.326, slope 95% CI: 0.895 to 1.0370) do not significantly differ from the one to one line on their own.

The temporalis demonstrates increased muscle length during gnawing for almost every species sampled (Fig. 2.3C). However this is because the the intercept of the PGLS regression lines for the temporalis across all taxa fails to contain zero (0.0893 to 0.226). The slope does not differ from the one to one line (0.964 to 1.010). Individual PGLS analyses of myomorphs, sciuromorphs, and hystricomorphs also contain 1 in their 95% CI for the slope. The SM muscle length PGLS fails to fully distinguish from the one to one line as its intercept contains zero with its 95% confidence interval (-0.0450 to 0.0642) although its slope fails to contain 1 (0.963 to 0.996) (Fig. 2.3D). Despite this result, the SM demonstrates decreased muscle lengths during gnawing for almost every species sampled. Myomorphs do distinguish from a one to one line (intercept 95% CI: 0.0349 to 0.176, slope 95% CI: 0.919 to 0.967) in an individual PGLS analyses, though sciuromorphs (intercept 95% CI: -0.258 to -0.0397, slope 95% CI: 0.995 to 1.0551) and hystricomorphs (intercept 95% CI: -0.0798 to 0.0612, slope 95% CI: 0.971 to 1.0121) still contain a one to one line in their 95% CI.

Evolutionary covariance of mechanical advantage and dentition

The best fit model for the evolution of ADM mechanical advantages and relative incisor depth was a single regression across all taxa (w = 0.9960), with significant positive PGLS results

for muroids (p=0.039) and nearly significant for sciurids (p=0.053; trendline shown) (Fig. 2.4A). The best fit model for the evolution of ADM mechanical advantages and relative OACT was a single regression across all taxa (w = 0.8914), although a PGLS across all taxa was not significant (0.0769) (Fig. 2.4B). Sciurids demonstrated a significant negative PGLS (p=0.039). The best fit model for the evolution of ZM mechanical advantages and relative incisor depth was a model in which intercepts differ across masseter morphotype (w = 0.8955), with a nearly positive PGLS result for muroids (p=0.0616). The best fit model for the evolution of ZM mechanical advantages and relative OACT was a model in which intercepts differ across masseter morphotype (w = 0.9585), with a significant negative PGLS result for ctenohystricans (p=0.0165). The best fit model for the evolution of temporalis mechanical advantages and relative incisor depth was a single regression across all taxa (w = 0.9999), with a significant positive PGLS results for muroids (p<0.001), sciurids (p<0.001), and all taxa (p<0.001). The best fit model for the evolution of temporalis mechanical advantages and relative OACT was a single regression across all taxa (w = 0.9997), with a significant negative PGLS results for muroids (p=0.0175), ctenohystricans (p=0.01), sciurids(p<0.001), and all taxa (p<0.001). The best fit model for the evolution of SM mechanical advantages and relative incisor depth was a model in which intercepts differ across masseter morphotype (w = 0.8955), with a significant positive PGLS across all taxa (p=0.0039). The best fit model for the evolution of SM mechanical advantages and relative OACT was a single regression across all taxa (w = 0.9999), with no significant PGLS results. The best fit model for the evolution of PDM mechanical advantages and relative incisor depth was a single regression across all taxa (w = 0.9999), with a significant positive PGLS results for muroids (p=0.0078) and all taxa (p=0.0035). The best fit model for the

evolution of PDM mechanical advantages and relative OACT was a single regression across all taxa (w = 0.9994), with no significant PGLS results.

Modes of Mechanical Advantage Macroevolution across Masseter Conditions

The best fit model for ADM mechanical advantage during gnawing is a multirate OU model (OUMV) (w=0.9150) followed by a multirate and multialpha OU model (OUMVA) (w=0.0755). The optimum for hystricomorphs in the OUMV model is the lowest (0.515; SE=0.0237) and higher for myomorphs (0.635; SE=0.0101) and sciuromorphs (0.663; SE=0.0183). The rates in this OUMV model are higher for hystricomorphs (0.000620) than for sciuromorphs (0.000329) and myomorphs (0.000267). The optima and rates are relatively similar in the OUMVA model, however the alphas are lower for myomorphs (0.0415) and sciuromorphs (0.0427) than for hystricomorphs (0.0573).

The best fit model for ADM mechanical advantage during chewing is OUMV (w=0.9983) followed by the OUMVA model (w=0.0014). The optimum for hystricomorphs in the OUMV model is the lowest (0.843; SE=0.0404) and higher for myomorphs (1.112; SE=0.0179) and sciuromorphs (1.114; SE=0.0311). The rates in this OUMV model are higher for hystricomorphs (0.000973) than for sciuromorphs (0.000552) and myomorphs (0.000415). The optima and rates are relatively similar in the OUMVA model, however the alphas are higher for myomorphs (0.0343) than for sciuromorphs (0.0282) and hystricomorphs (0.0227).

The best fit model for ZM mechanical advantage during gnawing is OUMV (w=0.9995) followed by the OUMA model (w=0.0004). The optimum for hystricomorphs in the OUMV model is the highest (0.599; SE=0.0237) followed by myomorphs (0.550; SE=0.0190) and much lower for sciuromorphs (0.308; SE=0.0235). The rates in this OUMV model are highest for hystricomorphs (0.000469) and lowest for sciuromorphs (0.000151) with myomorphs (0.000273)

in the middle. The optima are relatively similar in the OUMA model, however the alphas are highest for hystricomorphs (0.0793) followed by myomorphs (0.0592) and sciuromorphs (0.0295).

The best fit model for ZM mechanical advantage during chewing is OUMVA (w=0.9499) followed by the OUMV model (w=0.0496). The optimum for hystricomorphs in the OUMVA model is the highest (0.979; SE=0.0172) followed by myomorphs (0.947; SE=0.0462) and much lower for sciuromorphs (0.542; SE=0.0324). The rates in this OUMVA model are highest for hystricomorphs (0.00115) followed by sciuromorphs (0.00113) and myomorphs (0.00104). The alphas are highest for hystricomorphs (0.0888) followed by sciuromorphs (0.0642) and myomorphs (0.0363). The optima were relatively similar in the second best fit OUMV model, although the rates were lower for sciuromorphs (0.000855) and myomorphs (0.000713) while relatively similar in hystricomorphs (0.00116).

Hystricomorphs and myomorphs exhibit higher optima for ZM mechanical advantage and sciuromorphs and myomorphs demonstrate higher optima for ADM mechanical advantage. Importantly, mymorphs generally exhibit lower rates of mechanical advantage evolution, conforming to the hypothesis that their basic condition is more generalizable and more widely capable of various outputs without as much of a substantial change in mechanical advantage.

Discussion

Muscle length changes between gnawing and chewing positions

Changes in muscle length affect its placement on the length-tension curve, a graphical description of a muscle's length during stretching and contracting and its ability to impart force in when contracting at that length (Gordon et al. 1966, Zajac 1989). Muscles have an optimum placement along this length tension curve in which they can impart force, which one could

predict would be the adapted functional position of the muscle for its important, regular activities. Length tension curves often have a large region of length that is close to optimum force contraction, but regular behaviors should be as close to this optimum as possible to conserve energy and maximize outputs. Feeding is a type of regular, necessary behavior that requires rhythmic muscle contractions and can use a substantial portion of an animal's daily energy expenditure.

The separate mandibular positions for gnawing and chewing in rodents is unique among mammals and provides an interesting problem for optimizing position along a length tension curve when regular, rhythmic behaviors occur at multiple muscle lengths. The larger the difference in these muscle lengths the more difficult it should be for any given rodent species to optimize its jaw muscle utilization. The data presented here demonstrate that these muscle length changes are indeed substantial across rodents, with the ADM, SM, and temporalis muscles all exhibiting a distribution of muscle lengths in gnawing and chewing positions that are significantly different from a one to one line. Importantly, these data demonstrate that muscle length changes are a consistent problem across rodents that would require further modifications to the mandibular and muscular design to circumvent. Alternatively, muscles could be adapted to impart optimal function in accordance with their respective length tension curve for only one position and become relegated to an secondary role in masticatory functions in the alternate biting position.

The temporalis and SM demonstrate the greatest degree of muscle length change and in the most consistent direction, which makes sense given that the movement of the jaw to accommodate incisor gnawing from a cheekteeth chewing position mostly occurs by shifting the jaw anteriorly (with some degree of rotation through gape increase) and these muscles' lengths

primarily occur in the anteroposterior axis. The temporalis is lengthened in almost every species sampled and the SM is shortened in almost every species, as would be expected given their respective posterior and anterior originations. The ADM and ZM are more dorsoventrally oriented muscles, however, the changes in gape and mandible position are large enough that the ADM still has significant differences across taxa compared to a null expectation. Interestingly, these data demonstrate that even the non-derived masticatory muscles in the rodent feeding system may have difficulty performing at both positions of the jaw, requiring muscles such as the temporalis and SM to become adapted to gnawing or chewing more particularly while acting in a secondary role in the alternate bite position. Additionally, at least the ADM is also substantially different enough from a null expectation that it is unlikely to perform as optimally in each biting position, increasing the chances that it may be a muscle more specialized for one biting position over another, as has been alluded to by previous authors (Druzinsky 2010a,b, Cox et al. 2012).

Interestingly, these patterns of muscle length change differ between the distinct masseter conditions. Across all taxa the ZM muscle length changes fail to distinguish from a one to one line, but individual PGLS regressions for myomorphs and sciuromorphs differ significantly from a one to one line. Additionally, only myomorphs have a significant difference for muscle length changes in their ADM and SM, whereas sciuromorphs and hystricomorphs fail to differ from a one to one line. These results could be a function of taxon sample size, in which myomorphs represent the majority of the dataset (and living rodent species). It could also be that myomorphs demonstrate the greatest change in relative jaw movements between gnawing and chewing positions. Unfortunately, muscle lengths between muscles that are pinnate and non-pinnate are not mechanically equivalent, thus precluding direct comparisons between the ADM and temporalis here. However, comparing pinnate ADMs to other pinnate ADMS should be

reasonable as long as the type and degree of pinnation is similar, although little data exists on the details of pinnation across these muscles across rodents.

Evolutionary covariance of jaw muscle mechanical advantage and ecofunctional proxies of the dentition

Natural selection can be expected to optimize mechanical advantage of jaw muscles such that total muscle mass can be minimized to conserve energy while still providing sufficient bite force. We thus should expect a relationship between mechanical advantage of a particular muscle and the important biomechanical and ecofunctionally relevant metrics of the dentition if that muscle is adapted to regularly perform at that bite point and in that biting position. For example, if the ADM is an important muscle for high powered gnawing behavior, then its mechanical advantage should be maximized in taxa that are adapted to gnawing into harder material properties compared to taxa that do not regularly perform high powered gnawing behaviors and rely more on molar processing of food items (e.g. many herbivores). Conversely, if the ADM is a gnawing adapted muscle and is not capable of substantially contributing to chewing behavior, then one could expect no relationship between mechanical advantage of that muscle and taxa that have prominent chewing adaptations, or even potentially a negative relationship. Measures of relative incisor depth and relative OACT are useful proxies of gnawing and chewing investment based on the analyses conducted in chapter 1. For the most part, these measures evolve independently of one another (with the exception of sciurids), thus allowing comparisons to other variables without the results being necessarily confounded by the correlations that already exist between these measures (with the exception of sciurids).

The data presented here demonstrate that mechanical advantage for jaw muscles is likely evolving with important dental dimensions in biomechanically relevant ways, although the noise

in the data is high. Mechanical advantages for the temporalis muscle are negatively correlated with relative OACT across all rodent taxa and within each major clade of independently evolved masseter condition. Conversely, mechanical advantages for the temporalis muscle are positively correlated with relative incisor depth across all rodent taxa and within myomorphic Muroidea and sciuromorphic Sciuridae. These data strongly suggest that the temporalis is adapted to gnawing mechanics but not necessarily chewing mechanics in rodents. Such a result is not entirely surprising given the general consensus that the temporalis is less important in derived herbivorous mammals compared to the function of the masseters, with the majority of mammalian herbivores demonstrating larger relative masseter mass compared to temporalis mass compared to non-herbivorous mammals (Crompton and Hiiemae 1969). The preference for masseter function over temporalis function in herbivory and other chewing intensive diets can be explained quite simply by the fact that the masseter's origin and insertion sites allow for mechanical advantages greater than 1 during molar bites, while this is generally impractical for the temporalis given its insertion on the coronoid process within the constrained space of the temporal fenestra and orbital region. This inherent disadvantage of the temporalis compared to the masseter muscles in amplifying force to the molars likely biased the temporalis to evolve into a primarily gnawing adapted muscle in rodents after the establishment of the gnawing/chewing functional dichotomy evolved. The temporalis for the most part runs in the same axis as the anteroposterior shifting of the jaw when moving between chewing and gnawing positions, thus making the temporalis far less likely to be capable of performing at near optimal bite forces in both positions compared to more dosroventrally oriented muscles. This dilemma would have further contributed to the need of the temporalis to specialize into a more gnawing focused muscle.

The mechanical advantages of the ADM demonstrate significant positive relationships with relative incisor depth across all rodents and within Muroidea and Sciuridae. The only significant PGLS between ADM mechanical advantages and relative OACT is a negative relationship within Sciuridae. This negative correlation between ADM mechanical advantage and relative OACT in sciurids is likely due to the negative correlation between relative incisor depth and relative OACT found in Chapter 1, the only clade in which these variables fail to evolve independently from one another. In total, these patterns conform to the hypothesis that the ADM is a gnawing adapted muscle, with a lack of relationship within ctenohystricans fitting given their lack of an anatomical division of the ADM. Interestingly, castorimorphs, the second largest independently evolved extant clade of sciuromorphs, do not show similar trends to sciurids for the ADM, which has traditionally been recognized as a functionally similar muscle. This could be due to the smaller sample of species for castorimorphs and/or the general differences in castorimorph ecology compared to sciurids. Castorimorphs are composed of subterranean chisel-tooth and scratch diggers, a large wood eating specialist, and a semi-diverse group of generalized granivores. Sciurids, on the other hand, contain numerous folivores, grazers, a strict faunivore, bark gleaners, and hard nut and seed specialists. Castorimorphs not only differ simply in trends, however, but also demonstrate a higher mechanical advantage of the ADM in each bite position compared to sciurids. It is thus an open question as to how and why castorimorphs differ and whether there a fundamental differences in these groups' sciuromorphic construction, as a recent description of the beaver *Castor*'s jaw muscle anatomy would suggest (Cox and Baverstock 2015).

Regressions models failed to support a single relationship between ZM mechanical advantage and relative incisor depth or relative OACT, instead supporting a model of

significantly different intercepts. This result is likely due to the large differences in ZM mechanical advantage between non-hystricomorphous species (sciuromorphs and the protrogomorph), in which the ZM orbital portion inserts more posteriorly on the mandible, and species that contain a hystricomorphous component (hystricomorphs and myomorphs), in which the ZM infraoribital portion inserts more anteriorly on the mandible. A PGLS for muroids was nearly significant for ZM mechanical advantage over relative incisor depth, demonstrating a potential positive relationship linking ZM function to gnawing. Interestingly, ctenohysticans demonstrated a significant negative relationship between ZM mechanical advantage and relative OACT, which runs contrary to the hypothesis that the ZM infraorbital portion serves as a chewing adapted muscle in ctenohystricans (Cox et al. 2012, Cox 2017). The general lack of significant results for the ZM suggests a number of possibilities: 1) the ZM functions in more than one manner across taxa, disguising true biomechanical signals in the data as they are analyzed only by discrete masseter conditions and clade, 2) the ZM is indeed a gnawing adapted muscle, or 3) that the ZM mechanical advantage is best modeled in three dimensions as opposed to two, which could be particularly likely if the ZM is a chewing adapted muscle. The idea that the ZM functions differentially across taxa is plausible given the large morphological disparity present in hystricomorph rodents, particularly given the discrete character traits that sometimes co-occur in certain hystricomorph clades, such as the relatively large, ventrally extended parocciptal processes (the origin for the digastric and associated hyoid musculature) found in taxa that also demonstrate mediolateral constriction of the glenoid fossa. Additionally, the co-presence of the ZMIO and ADM in myomorphs could fundamentally change the biomechanics of these muscles, allowing each to perform in ways that they could not do alone. Thus the potential relationship between ZM mechanical advantage and relative incisor depth in muroids

could truly reflect the role of the ZM in gnawing behavior in muroids, despite the potential fact that the ZM does not primarily function to gnaw in hystricomorphs.

SM mechanical advantage was significantly positively correlated with relative incisor depth across rodents, although not in any particular major clade. There was no relationship between SM mechanical advantages and relative OACT. SM mechanical advantage likely suffers the most from a 2D lateral view perspective, as the angular process in rodents is notoriously variable in its mediolateral position, leading early rodent workers to distinguish rodents as sciurognaths or hystricognaths based on how the angular process falls in line with the plane of the mandible as a whole (Wood 1958, Wood 1965, Hautier et al. 2011). Crucial variation in true SM mechanical advantage is thus likely lost in this current approach, making the data here difficult to interpret; however, the data here would suggest that the SM is important for gnawing. A recent 3D biomechanical comparative analyses of the angular process in mammals found that jaw yaw is primarily contributed to by the action of muscles pulling mediolaterally on the angular process, namely the SM and pterygoideus musculature, with jaw yaw being a crucial feature of plesiomorphic mammalian chewing patterns (Grossnickle 2017). There is thus good reason to suspect that a 3D analysis of SM mechanical advantages among rodents would result in more robust relationships between SM function and ecofunctionally important metrics of the dentition, likely with relative OACT in particular.

PDM mechanical advantages over relative incisor depth were significantly and positively correlated across rodents and within muroids. No relationships between PDM mechanical advantage and relative OACT were detected. The PDM resembles the plesiomorphic masseter condition of mammals most closely and is the least morphologically specialized. The data here suggest that the PDM is more likely to have increased mechanical advantage when gnawing is an

important functional feature, although it may still have an active component in regular chewing functions as in other mammals.

There are numerous limitations to this study's approach that make direct biomechanical interpretations difficult. Firstly, although relative incisor depth and relative OACT evolve independently across all rodents as a whole and within most major clades, the lack of independent evolution of these metrics in sciurids, the most diverse group of sciuromorph rodents, violates the basic assumption in comparing evolutionary trends between these variables. It is, however, interesting that sciurids lack taxa with small incisors and small cheekteeth as well as taxa with large incisors and large cheekteeth. This fact alone is suggestive of a bias in sciurid evolution, in which incisors and cheekteeth are difficult to invest in simultaneously (the lack of both small incisors and cheekteeth can be understood by *Rhinosciurus*' need to crush hard bodied arthropods effectively, although one could imagine a more derived faunivorous squirrel would mirror the small cheekteeth found in the many muroid vermivores). Ultimately, because of the necessarily correlated evolution of incisors and cheekteeth in sciurids, it is difficult to interpret the biomechanical importance of their results for mechanical advantage evolution with high confidence.

Secondly, because incisors are more distal from the jaw joint than molars, the mechanical advantage for muscles acting during incisor bites is necessarily lower compared to the mechanical advantages of the same muscles acting during molar bites. This discrepancy is an issue because bite forces at the incisors will often need to be higher than those at the cheekteeth in any given species that gnaws into hard material, meaning that the jaw muscles that become adapted to amplifying enough force into incisor bites will become over-adapted for molar bites. We should thus expect a biased signal toward detecting trends between relative incisor depth and

mechanical advantages compared to relative OACT. This is confounded by the third issue, which is that chewing is a far more complicated procedure than gnawing, and can occur in numerous directions of jaw movement and with an enormous variety of occlusal surface topologies. Relative OACT is a clearly inferior predictive measure compared to relative incisor depth in this sense, as incisors are simple and require high power to accomplish their functional outputs, whereas cheekteeth require precision and rhythmicity using very particular occlusal patterns interacting in very particular ways at sufficient bite forces that they may already be over-adapted to perform. We might thus expect reduced signal in comparisons of mechanical advantage and relative OACT, particularly if the muscles important for chewing function are also important in gnawing functions. Despite the fact that rodents may be biased to specialize jaw muscle functions across bite points, this may not necessarily occur if the muscle length changes between bite positions do not substantially hinder basic muscle function and force output. However, as long as relative incisor depth and relative OACT are independent evolutionarily, we should still expect signal detection for their particular relationships to mechanical advantage to be possible, despite the general reduction in signal.

Fourthly, this study was conducted by collecting mechanical advantage measurements in a two dimensional lateral view plane, thus excluding any important variation that might occur in the mediolateral dimension. This dimension is clearly important for the SM and may be important for other potential chewing muscles such the ZM. Furthermore, this particular two dimensional approach will necessarily bias results to detect gnawing functions over chewing functions, as gnawing bites for the most part would occur in a two dimensional framework *in vivo* compared to typical chewing strokes, which in most rodent species occur transversely in the mediolateral direction (Charles et al. 2007). Finally, the fifth issue is the lack of in-lever

measures that are orthogonal to lines from the muscle vector to the jaw joint. Here, in-levers are measured as the muscle moment from the jaw joint to its mandibular insertion, which critically lacks information about the muscle's dimensions from insertion to origin and its angle compared to force on the jaw joint. These features would greatly enhance the predictive value of these mechanical advantage measures and potentially help reveal signal in the current data.

Each of these four issues make conclusive interpretations of muscle function based on the proceeding analysis difficult. However, the fact that a number of relationships were detected repeatedly across individual clades and for rodents in general provides evidence for some patterns in muscle function between gnawing and chewing positions that are worth investigating further. The temporalis demonstrates the clearest difference between gnawing and chewing positions which is supported by muscle length change data that suggest that the temporalis is far better suited to perform under gnawing than chewing. This is further expected given that most mammalian herbivores invest in masseter muscle mass for high powered chewing given the necessarily higher mechanical advantages achievable with a masseter. The data here for the ADM conform to previous work that has argued that the this muscle is particularly suited to perform during gnawing (Druzinsky 2010a, Cox et al. 2012). This result makes a great deal of sense given that the insertion point of the ADM anterior to all of jaw muscles on the mandible maximizes the possible mechanical advantage, as would be important for rodents gnawing into some of the hardest material properties in the plant world (Lucas et al. 2012).

Results for the ZM are interesting, as they suggest that muroids utilize the ZM for gnawing, which could be argued as a reasonable possibility for similar reasons as the ADM given its anterior insertion point. The negative relationship of the ZM mechanical advantages over relative occlusal area among ctenohystricans is particularly striking, however, as it is

contrary to past hypotheses and is the only significant PGLS result for ctenohystricans across relative occlusal area aside for the temporalis (which is in agreement with other rodent clades and rodents as a whole). Additionally, there is no evidence to support a positive relationship between ZM mechanical advantage and relative incisor depth within ctenohystricans, thus the negative relationship here can not be taken as strict evidence that the ZM is a particularly gnawing adapted muscle as opposed to a muscle that has reduced mechanical advantage when relative OACT is high. It is possible that the ZM in ctenohystricans reduce mechanical advantage to increase the speed of chewing in more herbivorous taxa, but it is unclear why the velocity of the chewing stroke would be more important than the bite force when the material properties of food are highly fibrous.

This study provides a number of predictions for future work to test using *in vivo* biomechanical approaches that assess muscle action during feeding and other functional behaviors. If the ADM is indeed a gnawing adapted muscle, its electromyography (EMG) readings should be most prominent during the closing phase of the gnawing stroke. Similarly, if the ZMIO actually does function primarily in chewing, contrary to the results in the this study, its EMG activity should be highest during the closing phase of the chewing stroke.

Modes of mechanical advantage macroevolution across masseter conditions

Evolutionary trait modeling results demonstrate that mechanical advantage evolution for the ADM and ZM occur under an OU process, in particular an OUMV model with multiple rates, with the exception of ZM mechanical advantage during chewing which is best fit by an OUMVA model, in which alpha can also vary. This fits the hypothesis that masseter condition affects mechanical advantage evolution in specific ways. In particular, taxa within each masseter condition conform to the predicted trait optima, with myomorphs and sciuromorphs

demonstrating higher mechanical advantage optima for the ADM, whereas hystricomorphs and myomorphs exhibit higher optima for ZMIO mechanical advantages. These data, along with the from Chapter 1, thus support the hypothesis that the ADM is important for the feeding mechanics of sciuromorphs and myomorphs in maximizing mechanical advantage to produce higher bite forces at the incisor. Similarly, these data show that hystricomorphs and myomorphs maximize ZMIO mechanical advantage, which data from Chapter 1 would argue is used to increase bite force at the check teeth, although data in this chapter on mechanical advantage co-evolution with OACT remains equivocal.

Myomorphs tend to have lower rates of mechanical advantage evolution in gnawing and chewing positions for the ADM and ZM as well as usually lower alphas when estimated in secondary best fit models. Hystricomorphs demonstrate the opposite pattern, usually exhibiting the highest rates for mechanical advantage evolution and higher alphas when estimated. These results are interesting given that muroids (the vast majority of myomorph species) have higher rates of species diversification particularly compared to ctenohystricans (the majority of hystricomorph species). These results are also interesting given that hystricomorphs are far less diverse dietarily compared to myomorphs, with the majority of hystricomorphs being some kind of arboreal, terrestrial, or subterranean herbivore (Hautier et al. 2012), while mymorphs contain the entire range of rodent dietary specializations. It could be that myomorphs demonstrate such low rates of mechanical advantage evolution due to the majority of species retaining a particularly generalist habit, with relatively fewer species demonstrating the extreme specializations that muroids repeatedly evolve. This would make more sense than hypothesizing the myomorphs are more constrained, as myomorph alphas are generally lower, suggesting that clades that evolve more extreme morphologies are not so strongly pulled back to the mean

compared to hystricomorphs and sciuromorphs. These modeling data would thus suggest that myomorphs are freer to evolve more divergent biomechanics but have mostly retained the successful form of the plesiomorphic generalist habit. This analysis would thus support the original hypothesis in the literature (Wood 1965; Cox et al. 2012) that myomorph provides a more ideal, flexible feeding system that can more efficiently use its masseters to gnaw and chew.

Conclusions

This study sought to demonstrate how key differences in the biomechanics of rodent jaw muscles, in particular the highly derived and novel masseter muscles, are related to ecofunctionally relevant aspects of those rodents' biology as an explanation for the evolution of these muscles and/or how these muscle function in extant taxa. Many families of early rodents survived for tens of millions of years without evolving derived units of the deep masseter or zygomaticomandibularis; however, all of these families eventually went extinct millions of years prior to human interference with the exception of one family represented by a single species, Aplodontidae. Furthermore, the combinatorial condition that includes both derived masseters, myomorphy, is by far the most diverse group of rodents, representing over half of currently described species. It would thus appear that these derived, novel jaw muscles serve as some sort of innovation in mammalian feeding. The complexity of the rodent masticatory system has thus far precluded mammalogists from simply applying our more detailed understandings of mammalian feeding biomechanics to rodents to elucidate the key to their masticatory successes. Here I have utilized the novel masticatory mechanics that allow rodents to gnaw and chew independently and at a distance from one another to further understand the potential adaptive basis of each major muscle in the rodent jaw. I have shown that the changes in muscle length from shifting the mandible from the a chewing position to a gnawing position are significantly

different from a null expectation for the ZM and ADM muscles, and that the temporalis and SM change muscle lengths in a nearly unidirectional manner that biases their utilization potential between bite points. I have shown that the mechanical advantages of sciuromorph ZMOPs and hystricomorph "ADM"s (modeled as the anteriormost potential functional subdivision despite the absence of anatomical subdivisions) do not compare to the mechanical advantages of their derived counterparts among hystricomorphs (ZMIO), sciuromorphs (ADM), and myomorphs (both). Furthermore, the temporalis, fitting with muscle length change data, has the most biased evolutionary trends in mechanical advantage relative to ecofunctional dental metrics, implying that one of the most important muscles in the mammalian feeding system likely functions in fundamentally different ways in rodents. I provided further evidence that the ADM is a gnawing adapted muscle, both in sciuromorphs and myomorphs. Additionally, I documented for the first time that castorimorph sciuromorphs may be different from sciurid sciuromorphs in notable ways, and that our relative ignorance of detailed castorimorph anatomy has hindered the recognition of what may be a more complicated story of rodent masticatory evolution.

The data here suggest that the ZMIO can help perform gnawing functions in myomorphs, despite a lack of evidence that it can do so in hystricomorphs or that the ZMOP could do so in sciuromorphs. If true, these results would suggest that myomorphs can utilize their masseter muscles in more complex ways than hystricomorphs and sciuromorphs can with single derived masseter units alone. Dual anteriorly inserted derived masseter muscles could allow myomorphs to gnaw with more precision and more power, potentially releasing some of the mechanical demands of the incisor during high powered gnawing. Such a scenario could explain why myomorphs rarely evolve incisors as deep as many sciuromorphs have, despite the far greater diversity of myomorphs and high diversification rates. If the myomorph system is more versatile

biomechanically, as these data would suggest, then it would explain why myomorphs exhibit both lower rates and lower alphas for ADM and ZM mechanical advantage evolution in the parameters of their the best fit OU models compared to sciuromorphs and hystricomorphs. Rates for these traits' evolution would remain low as myomorphy acts as an innovation providing enough functional flexibility to adapt to most demands, allowing for many species to successfully continue with the original myomorphic masseter organization, while also allowing for intense specialization along the phylogeny when opportunities present themselves without a strong "pull" back to the mean.

Due to the limitations of this study and the high noise in the comparative mechanical advantage data, the results here must be interpreted carefully until further data can corroborate these findings. Three dimensional analyses of biomechanics would improve confidence in mechanical advantage measures for the ZM and SM in particular. Measuring muscle lever arms would allow for estimations of mechanical advantage that incorporate information from cranial originations of the muscles that sometimes vary tremendously, and would also allow for calculations of raw bite force produced assuming stable sarcomere lengths across species. These further approaches would improve upon this current study's power to detect real differences in biomechanics and would pave the way for the inclusion of relevant *in vivo* data to test these results.

Despite these confounding factors, this study represents the first attempt to utilize the novel gnawing/chewing functional dichotomy in rodents to reveal crucial biases in masseteric function that have been unknown since the derived masseters were first described 164 years ago (Brandt 1855). Based on these results, I have provided explicit hypotheses to be tested concerning rodent masticatory function and evolution, namely that the temporalis is biased

toward gnawing performance and is potentially functionally redundant in myomorphs (which have dual derived anterior masseter units that can effectively perform during incisor bites). I have outlined how these results and those of the evolutionary trait modeling can be interpreted, with derived masseter units potentially serving as both evolutionary innovations and constraints. Each has seemingly allowed for functional possibilities inaccessible to other mammals without derived masseter muscles, although both sciuromorphy and hystricomorphy could be considered as more limited in their biomechanical potential compared to myomorphs. These hypotheses of evolutionary impacts of derived masseter evolution can be tested with broadly sampled comparative *in vivo* data on rodent mastication to show that myomorphic taxa amplify force from masseter muscles more effectively, efficiently, and/or precisely. It could be that myomorphs are particularly limited by their complex masseteric design, which allows sciuromorphs and hystricomorphs to more effectively occupy their particular niches (presumably gnawing focused and chewing focused niches, respectively). Ultimately the large, saltatorial evolutionary jumps made in constructing the derived rodent masseteric conditions requires some sort evolutionary explanation, both in origin and in consequences. Given the general uniqueness of so many aspects of the rodent masticatory system, from derived ever-growing incisors, the gnawing/chewing functional dichotomy, and the multitude of novel derived masseter muscles, it appears as though rodents have deviated dramatically from the mammalian bauplan and achieved massive success in doing so. The findings here suggest that this success can be underlined by the crucial biomechancial changes made to the rodent feeding system, and that any attempt to explain rodent evolutionary diversification must consider the effects of these large-scale biomechanical and developmental changes for rodent ecology and macroevolution.

References

Alfaro, M.E., Bolnick, D.I., and Wainwright, P.C. (2005). Evolutionary Consequences of Many-to-One Mapping of Jaw Morphology to Mechanics in Labrid Fishes. The American Naturalist 165, 140–154.

Anderson, P.S.L., Claverie, T., and Patek, S.N. (2014). Levers and Linkages: Mechanical Trade-Offs in a Power-Amplified System. Evolution 68, 1919-1933.

Beaulieu, J.M., and O'Meara, B.C. (2012). OUwie: analysis of evolutionary rates in an OU framework. R package version 3.

Becerra, F., Echeverría, A.I., Casinos, A., and Vassallo, A.I. (2014). Another one bites the dust: Bite force and ecology in three caviomorph rodents (Rodentia, Hystricognathi). Journal of Experimental Zoology Part A: Ecological Genetics and Physiology 321, 220-232.

Bellwood, D.R., Wainwright, P.C., Fulton, C.J., and Hoey, A.S. (2006). Functional versatility supports coral reef biodiversity. Proceedings of the Royal Society B 273, 101–107.

Brandt, J.F. (1855). Beitraege zur nähern Kenntniss der Säugethiere Russlands (Buchdruckerei der Kaiserlichen Akad. der Wissenschaften).

Charles, C., Jaeger, J.-J., Michaux, J., and Viriot, L. (2007). Dental microwear in relation to changes in the direction of mastication during the evolution of Myodonta (Rodentia, Mammalia). Naturwissenschaften 94, 71–75.

Cox, P.G. (2017). The jaw is a second-class lever in *Pedetes capensis* (Rodentia: Pedetidae). PeerJ 5, e3741.

Cox, P.G., and Baverstock, H. (2015). Masticatory Muscle Anatomy and Feeding Efficiency of the American Beaver, *Castor canadensis* (Rodentia, Castoridae). Journal of Mammalian Evolution 23, 191–200.

Cox, P.G., and Faulkes, C.G. (2014). Digital dissection of the masticatory muscles of the naked mole-rat, *Heterocephalus glaber* (Mammalia, Rodentia). PeerJ 2, e448.

Cox, P.G., Rayfield, E.J., Fagan, M.J., Herrel, A., Pataky, T.C., and Jeffery, N. (2012). Functional Evolution of the Feeding System in Rodents. PLoS ONE 7, e36299.

Crompton, A.W., and Hiiemäe, K.M. (1969). How Mammalian Molar Teeth Work. Discovery 5, 23–34.

Curtis, A.A., and Santana, S.E. (2018). Jaw-Dropping: Functional Variation in the Digastric Muscle in Bats. The Anatomical Record 301, 279–290.

Druzinsky, R.E. (2010a). Functional Anatomy of Incisal Biting in *Aplodontia rufa* and Sciuromorph Rodents - Part 1: Masticatory Muscles, Skull Shape and Digging. Cells Tissues Organs 191, 510–522.

Druzinsky, R.E. (2010b). Functional Anatomy of Incisal Biting in *Aplodontia rufa* and Sciuromorph Rodents – Part 2: Sciuromorphy Is Efficacious for Production of Force at the Incisors. Cells Tissues Organs 192, 50–63.

Freeman, P.W., and Lemen, C.A. (2008). A simple morphological predictor of bite force in rodents. Journal of Zoology 275, 418–422.

Gordon, A.M., Huxley, A.F., and Julian, F.J. (1966). The variation in isometric tension with sarcomere length in vertebrate muscle fibres. The Journal of Physiology (Lond.) 184, 170–192.

Grossnickle, D.M. (2017). The evolutionary origin of jaw yaw in mammals. Scientific Reports 7, 45094.

Hautier, L., Michaux, J., Marivaux, L., and Vianey-Liaud, M. (2008). Evolution of the zygomasseteric construction in Rodentia, as revealed by a geometric morphometric analysis of

the mandible of *Graphiurus* (Rodentia, Gliridae). Zoological Journal of the Linnean Society 154, 807–821.

Hautier, L., Lebrun, R., Saksiri, S., Michaux, J., Vianey-Liaud, M., and Marivaux, L. (2011). Hystricognathy vs Sciurognathy in the Rodent Jaw: A New Morphometric Assessment of Hystricognathy Applied to the Living Fossil *Laonastes* (Diatomyidae). PLoS ONE 6, e18698.

Hautier, L., Lebrun, R., and Cox, P.G. (2012). Patterns of covariation in the masticatory apparatus of hystricognathous rodents: Implications for evolution and diversification. Journal of Morphology 273, 1319–1337.

Lucas, P.W., Gaskins, J.T., Lowrey, T.K., Harrison, M.E., Morrogh-Bernard, H.C., Cheyne, S.M., and Begley, M.R. (2012). Evolutionary optimization of material properties of a tropical seed. Journal of the Royal Society Interface 9, 34–42.

Morris Philip J. R., Cox Philip G., and Cobb Samuel N. Mechanical significance of morphological variation in diprotodont incisors. Royal Society Open Science 6, 181317.

Paradis, E., and Schliep, K. (2018). ape 5.0: an environment for modern phylogenetics and evolutionary analyses in R. Bioinformatics 35, 526–528.

Pinheiro, J., Bates, D., DebRoy, S., Sarkar, D., and R Core Team (2019). nlme: Linear and Nonlinear Mixed Effects Models.

R Core Team (2013). R: A language and environment for statistical computing. R Foundation for Statistical Computing (Vienna, Austria).

Revell, L.J. (2010). Phylogenetic signal and linear regression on species data. Methods in Ecology and Evolution 1, 319–329.

Revell, L.J. (2012). phytools: An R package for phylogenetic comparative biology (and other things). Methods in Ecology and Evolution 3, 217–223.

Upham, N.S., Esselstyn, J.A., and Jetz, W. (2019). Ecological causes of uneven diversification and richness in the mammal tree of life. BioRxiv 504803.

Wainwright, P.C., Bellwood, D.R., Westneat, M.W., Grubich, J.R., and Hoey, A.S. (2004). A functional morphospace for the skull of labrid fishes: patterns of diversity in a complex biomechanical system. Biological Journal of the Linnean Society 82, 1–25.

Westneat, M.W. (1995). Feeding, Function, and Phylogeny: Analysis of Historical Biomechanics in Labrid Fishes Using Comparative Methods. Systematic Biology 44, 361–383.

Westneat, M.W. (2004). Evolution of Levers and Linkages in the Feeding Mechanisms of Fishes. Integrative and Comparative Biology 44, 378–389.

Wood, A.E. (1958). Are There Rodent Suborders? Systematic Biology 7, 169–173.

Wood, A.E. (1965). Grades and Clades Among Rodents. Evolution 19, 115–130.

Zajac, F.E. (1989). Muscle and tendon: properties, models, scaling, and application to biomechanics and motor control. Critical Reviews in Biomedical Engineering 17, 359–411.

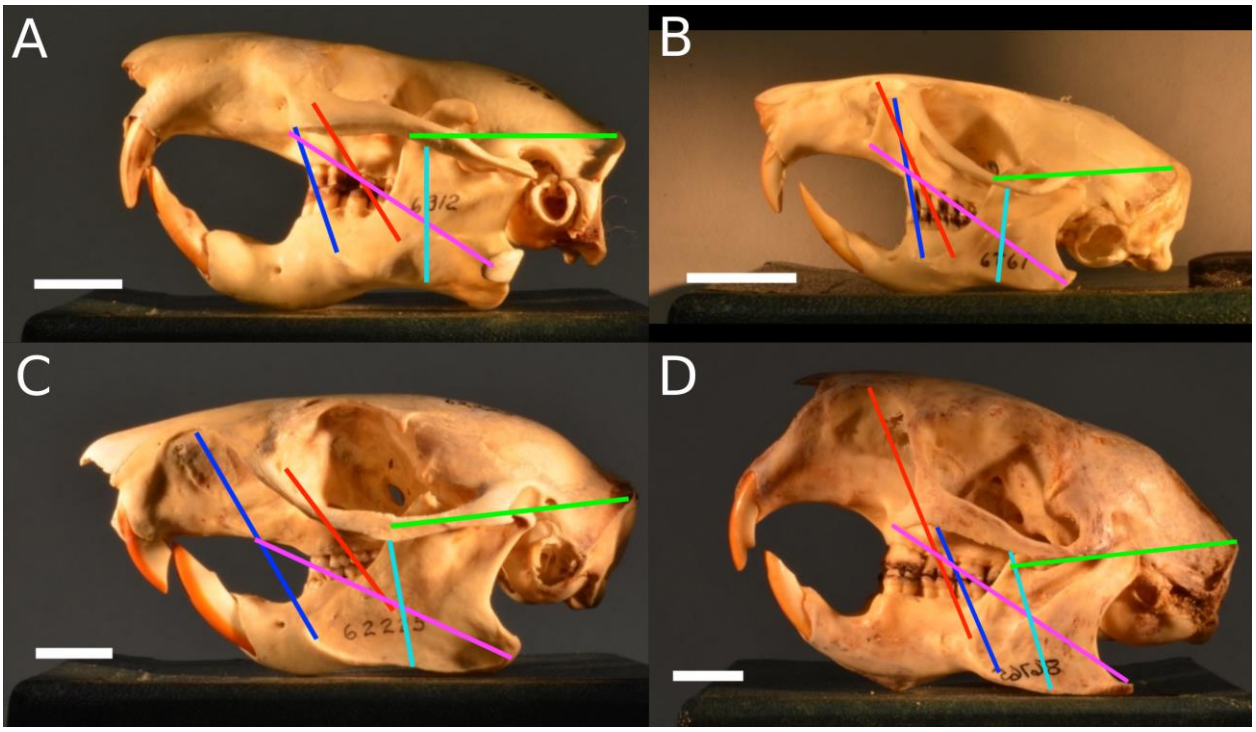

Figure 2.1. Representative depictions of muscle length measures collected for A) protrogomorphs (demonstrated on *Aplodontia rufa*) B) myomorphs (*Neotoma floridana*), C) sciuromorphs (*Epixerus ebii*), and D) hystricomorphs (*Echinoprocta rufescens*). Green line = temporalis, dark blue = ADM, light blue = PDM, red = ZMIO/OP, magenta = SM. Scale bar = 10 mm.

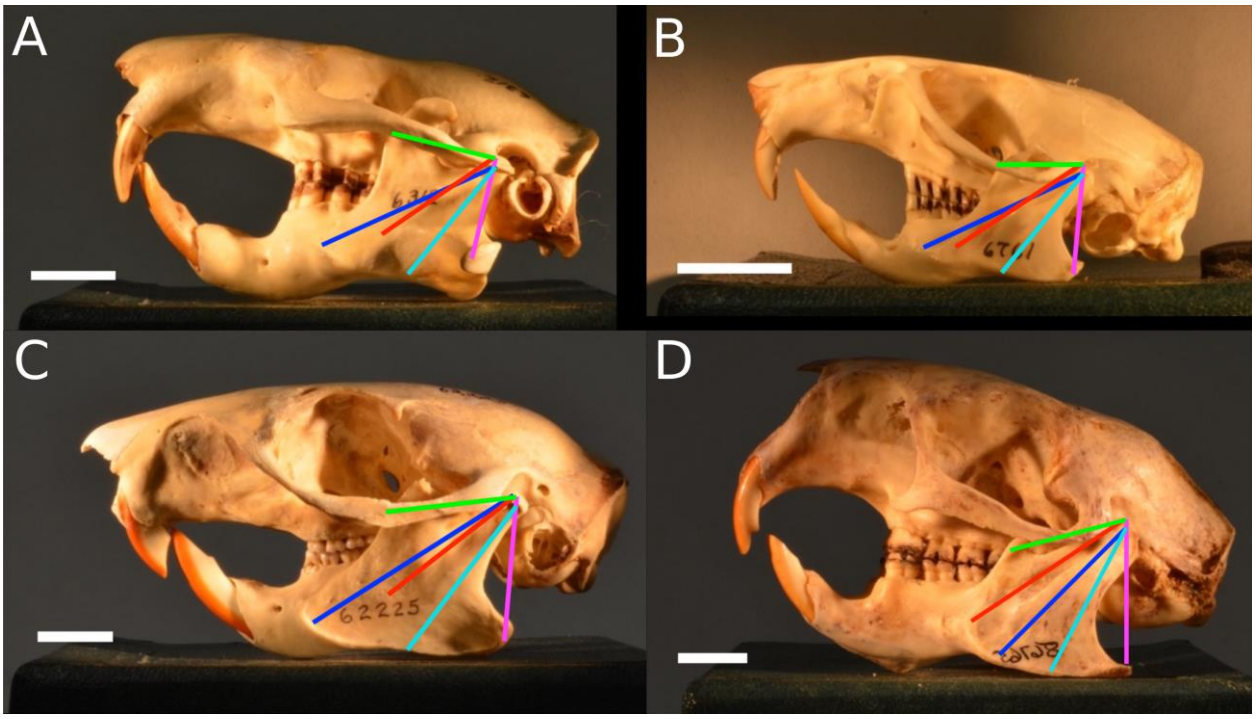

Figure 2.2. Representative depictions of mechanical advantage in-lever measures collected for A) protrogomorphs (demonstrated on *Aplodontia rufa*) B) myomorphs (*Neotoma floridana*), C) sciuromorphs (*Epixerus ebii*), and D) hystricomorphs (*Echinoprocta rufescens*). Green line = temporalis, dark blue = ADM, light blue = PDM, red = ZMIO/OP, magenta = SM. Scale bar = 10 mm.

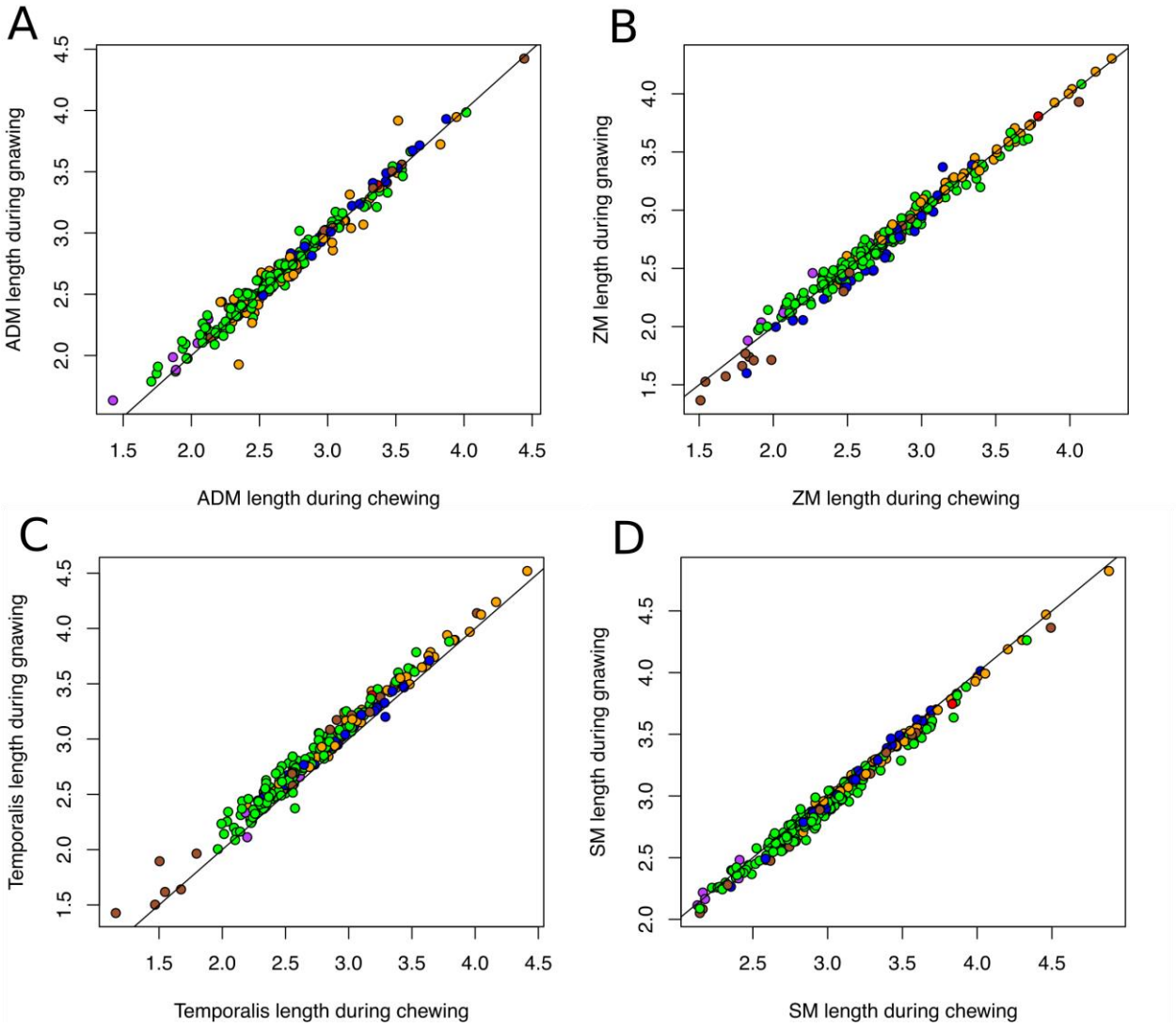

Figure 2.3. Bivariate regression of muscle lengths during gnawing over muscle lengths during chewing. Lines are one-to-one relationships. Dot color: green = muroid myomorphs; orange = ctenohystrican hystricomorphs; blue = sciurid sciuromorphs, gray = aplodontid protrogomorph, brown = castorimorph sciuromorphs, red = anomaluromorph hystricomorphs, purple = glirid myomorphs).

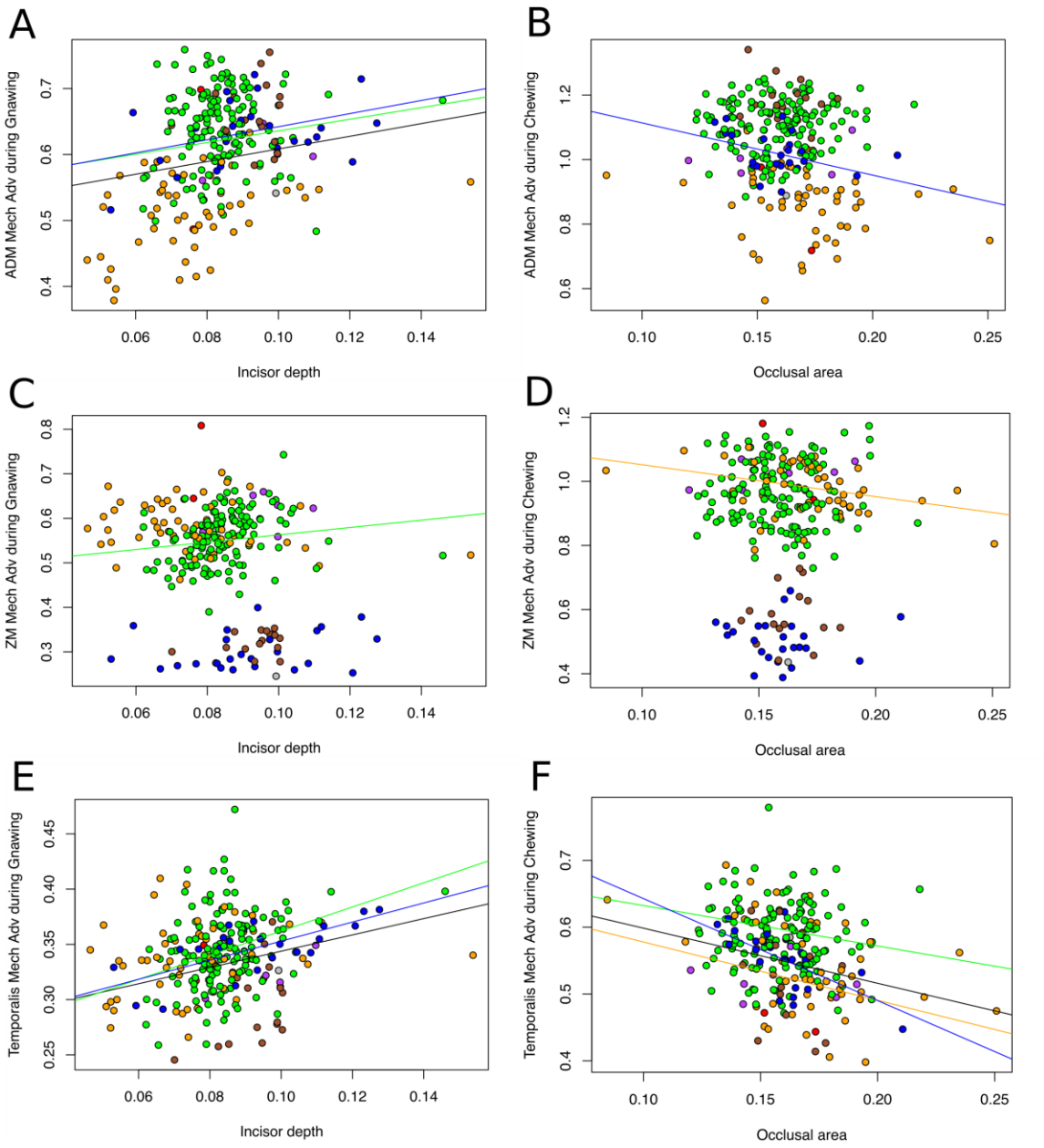

Figure 2.4. Bivariate plots of mechanical advantage of the ADM (A-B), ZM (C-D), and Temporalis (E-F) in gnawing and chewing positions over relative incisor depth and relative OACT. Solid black lines are significant PGLS across all taxa, colored lines are significant* PGLS regressions for respective independently evolved masseter conditions (green = muroid myomorphs; orange = ctenohystrican hystricomorphs; blue = sciurid sciuromorphs). *Except for ZM mechanical advantage over relative incisor depth for muroids (p=0.0616).

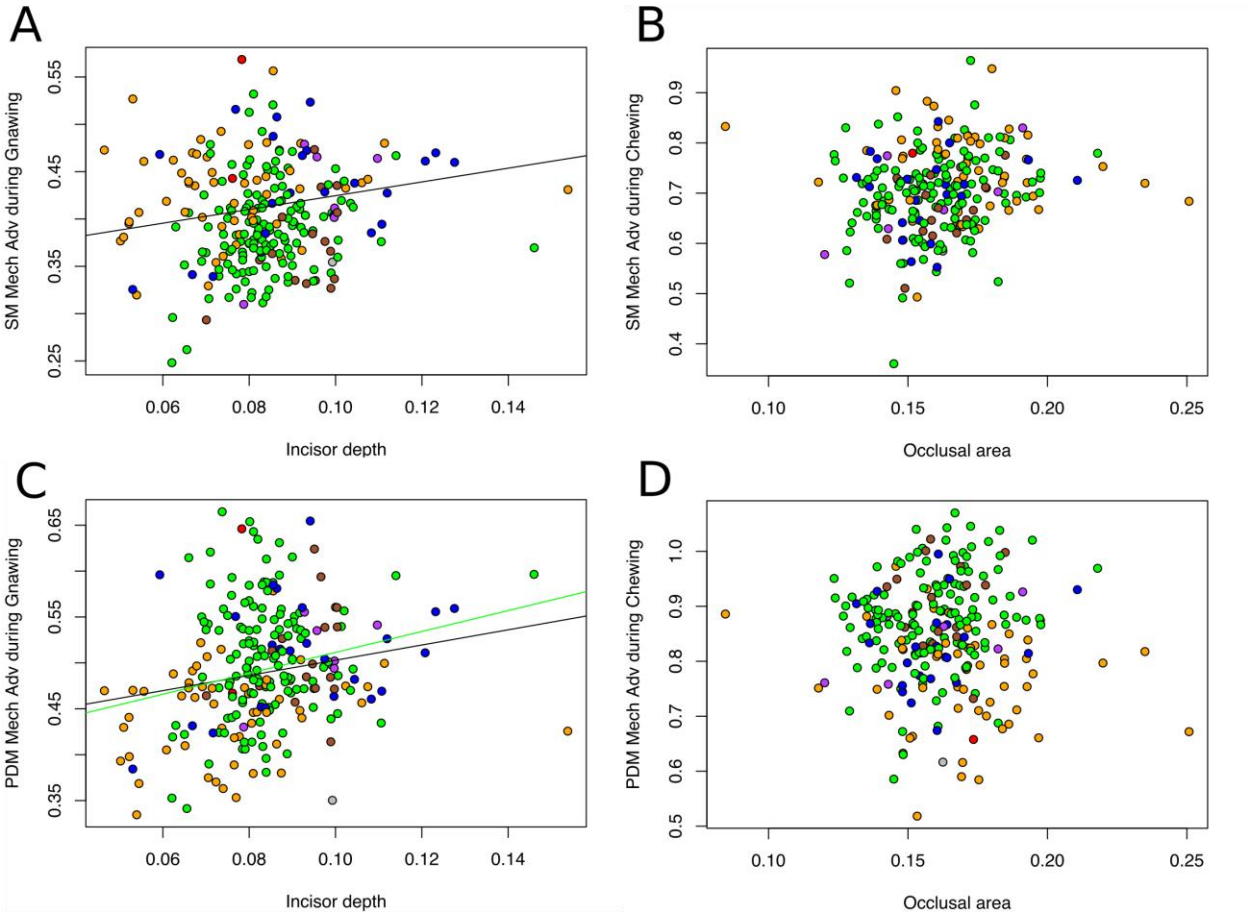

Figure 2.5. Bivariate plots of mechanical advantage of the SM (A-B) and PDM (C-D) in gnawing and chewing positions over relative incisor depth and relative OACT. Solid black lines are significant PGLS across all taxa, colored line are significant PGLS for respective independently evolved masseter conditions (green = muroid myomorphs; orange = ctenohystrican hystricomorphs; blue = sciurid sciuromorphs).

Table 2.1. Macroevolutionary modeling results for ADM mechanical advantage during chewing across masseter conditions reporting model fit (AICc), deltas, and weight (w) for Brownian motion for a single rate (BM), Brownian motion with multiple rates, OU model with single optima (OU1), OU model with multiple optima (OUM), OU model with multiple optima and alphas (OUMA), OU model with multiple optima and rates (OUMV), and an OU model with multiple optima, rates, and alphas (OUMVA).

	fit	delta	w
BM	-533.5268	42.8675	0.0000
BMS	-557.1444	19.2500	0.0001
OU1	-535.4180	40.9764	0.0000
OUM	-559.3575	17.0368	0.0002
OUMA	-555.9239	20.4704	0.0000
OUMV	-576.3943	0.0000	0.9983
OUMVA	-563.2676	13.1267	0.0014

Table 2.2. Macroevolutionary modeling results for ADM mechanical advantage during gnawing across masseter conditions reporting model fit (AICc), deltas, and weight (w) for Brownian motion for a single rate (BM), Brownian motion with multiple rates, OU model with single optima (OU1), OU model with multiple optima (OUM), OU model with multiple optima and alphas (OUMA), OU model with multiple optima and rates (OUMV), and an OU model with multiple optima, rates, and alphas (OUMVA).

	fit	delta	w
BM	-664.0688	62.3992	0.0000
BMS	-699.8956	26.5724	0.0000
OU1	-686.3182	40.1498	0.0000
OUM	-708.4141	18.0539	0.0001
OUMA	-717.3065	9.1615	0.0094
OUMV	-726.4680	0.0000	0.9150
OUMVA	-721.4793	4.9887	0.0755

Table 2.3. Macroevolutionary modeling results for ZM mechanical advantage during chewing across masseter conditions reporting model fit (AICc), deltas, and weight (w) for Brownian motion for a single rate (BM), Brownian motion with multiple rates, OU model with single optima (OU1), OU model with multiple optima (OUM), OU model with multiple optima and alphas (OUMA), OU model with multiple optima and rates (OUMV), and an OU model with multiple optima, rates, and alphas (OUMVA).

	fit	delta	w
BM	-444.1381	64.2801	0.0000
BMS	-471.5847	36.8335	0.0000
OU1	-444.8663	63.5519	0.0000
OUM	-487.3469	21.0713	0.0000
OUMA	-492.9250	15.4932	0.0004
OUMV	-502.5145	5.9037	0.0496
OUMVA	-508.4182	0.0000	0.9499

Table 2.4. Macroevolutionary modeling results for ZM mechanical advantage during gnawing across masseter conditions reporting model fit (AICc), deltas, and weight (w) for Brownian motion for a single rate (BM), Brownian motion with multiple rates, OU model with single optima (OU1), OU model with multiple optima (OUM), OU model with multiple optima and alphas (OUMA), OU model with multiple optima and rates (OUMV), and an OU model with multiple optima, rates, and alphas (OUMVA).

	fit	delta	w
BM	-689.2812	51.7592	0.0000
BMS	-721.1285	19.9119	0.0000
OU1	-687.3923	53.6481	0.0000
OUM	-713.5292	27.5112	0.0000
OUMA	-725.5447	15.4957	0.0004
OUMV	-741.0404	0.0000	0.9995

Chapter 3: DICE-μCT data reveal repeated compensatory evolution of masseteric anatomy associated with the reduction of the temporalis muscle in desert rodents with large auditory bullae

Abstract

The distinctive anatomical evolution of novel masseter muscles was traditionally used to classify rodents phylogenetically, but we now know that these seemingly novel muscles are homoplastic. Recent investigations of masseter anatomy in rodents using modern diffusible iodine contrast enhanced (DICE) CT scanning has revealed numerous surprising features of these anatomical systems, warranting a further description of the basic anatomy of jaw muscles across rodents. Rodent masseter anatomy typically is portrayed as static since the Eocene, with the exception of dormice, but the extreme reduction of the temporalis muscles in arid adapted rodents with large auditory bullae would seem to require substantial compensatory changes to the structure of the feeding system. Here I used DICE-CT to test whether the masseter anatomy of arid adapted rodents, in particular heteromyid rodents, including kangaroo rats and their pocket mice relatives, and the jerboa *Jaculus jaculus* among dipodoids, fit their respective traditional designations as sciuromorph and hystricomorph anatomies, despite their extreme reduction of space for temporalis attachment on the skull. DICE-CT results reveal that *Jaculus* exhibits extreme reduction of the temporalis muscle in overall muscle size and length, but has particularly large units of the infra-orbital and orbital portions of the zygomaticomandibularis, as well as enlarged portions of the deep masseter and superficial masseter inserting on an enlarged, laterally and medially inflected angular process. Comparisons to the skulls of dipodoids with progressively smaller auditory bullae reveals that the large orbital attachments of the zygomaticomandibularis only occur in taxa with the largest auditory bullae, whereas

modifications to the angular process evolve progressively as auditory bullae size increases. Heteromyids demonstrate a similar trend, progressively decreasing size and length of the temporalis muscle with enlargement of the auditory bullae, along with enlargement of the orbital portions of the zygomaticomandibularis and elaboration of attachments of the superficial masseter and posterior masseter to the angular process. Interestingly, heteromyids exhibit the same novel dual origination sites of the superficial masseter as was recently described for the beaver, implying that this condition is ancestral among castorimorphs and not a recent adaptation to the extreme biomechanics of beaver mastication. Finally, comparisons of osteological correlates among myomorph gerbilline rodents with repeatedly evolved large auditory bullae demonstrates that reduction of the temporalis is not accompanied by compensatory adaptions to the masseters along with the reduction of space for temporalis attachment, implying that myomorphs may not require novel biomechanics with the loss of major temporalis function. This result conforms to the hypothesis that myomorphy is biomechanically more flexible the anterior masseters can perform in ways that the more simple sciuromorph and hystricomorph conditions cannot in the absence of a large temporalis. Overall, the extreme evolution of auditory bullae and concomitant reduction of the temporalis is a driver of masseteric diversification in non-myomorph rodents that hints at crucial biomechanical differences in these groups and their evolutionary potential.

Introduction

Desert ecosystems are some of the most extreme environments on the planet and the organisms that live within them must adapt in extreme ways to survive. These selective pressures often force organisms to the morphological and physiological limits of their basic biology and are thus often illuminating to underlying developmental and functional rules that are otherwise

not so obvious compared to even close relatives living in more temperate environments. For example, the anatomy of cacti depends on coordination of stem and leaf-base tissues that otherwise are simple, nondescript features in other dicots (Boke 1980), and opuntioid cacti harbor novel, specialized leaves that are small, sometimes microscopic weapons that irritate the skin of any would-be herbivore (Boke 1944). On the other hand, succulent euphorbes as well as some other dicots exhibit robust stipular spines that produce an armor out of structures, stipules, that are otherwise restricted in function to protecting the developing leaf buds (Bell 1991). Jerboas provide an example of one of the few mammals outside of comparatively large ungulates that exhibit bilateral digit reduction (Cooper et al. 2014), apart of a suite of characters that support the functional specializations of these bipedal open-habit rodents with highly maneuverable jumping abilities (Brown et al. 1988, Kotler 1984, Moore et al. 2017). Extreme anatomical adaptations such as these might only be found in species inhabiting desert environments, but these adaptations do not appear to be directly in response to the extreme heat and dryness characterized by other more well discussed physiological desert specializations. Instead, these morphological reorganizations appear to be indirect desert adaptations due to the ecological consequences of highly open habitat structure that leads to exceptionally high predation and herbivory pressure. Desert plants must be either well armed or highly toxic to avoid the herbivory of plant-eating generalists and must commit to an arms race with their herbivorous specialists, and animals must either have strong defenses to predation or exceptional evasive tactics. The degree to which these pressures differ from even semi-open tall grass prairie and scrub forests is demonstrated by the extremes to which resident desert organisms modify otherwise immutable aspects of their basic bodyplan.

Rodents, a group that has repeatedly invaded diverse habitat types and ecological settings, have become desert specialists numerous times with examples across various large clades. Although there are many desert rodents that remain quadrupedal and mainly forage under the cover of what little vegetation is available, many desert rodents have evolved into bold, open-habitat foraging specialists that often share a radical suite of characters: bipedal stance, elongated digitigrade hindlegs with enlarged toe pads and/or thick ventral toe hair, relatively small forelegs with large claws and substantial digging capabilities, coat with locally adapted sandy/rocky coloration and pattern, a long thin tail with fluffy distal tip, large pinna, substantially enlarged auditory bullae chambers that can comprise more than 30% of total cranial volume, among other characters (Shenbrot et al. 1999). Most of these characters can be found in representatives of kangaroo rats (*Dipodomys* and *Microdipodops*, heteromyids from the clade Castorimorpha), jerboas (dipodoids from Myodonta), springhares (pedetids from the Anomaluromorpha), gerbils (gerbilline muroids from Myodonta), Australian jumping mice (genus *Notomys*, murine muroids from Myodonta), and chinchillas and viscachas (chinchillid caviomorhs from the Ctenohystrica)(notably not obligately bipedal). These shared features are clearly related to predator evasion, from basic camouflage, distraction of predator attention with distal tail flag, maneuverable and quick escape through hopping, and predator detection through hearing. Predator detection is facilitated in these open-habitat foragers by their enlarged auditory bullae that serve as resonance chambers for the low-frequency sounds produced by larger animals (either a running or ambushing mammal or wing flapping raptor) (Webster 1962, Plassman and Kadel 1991, Webster and Plassman 1992, Webster and Webster 1980) that is also found in arid adapted mammals outside of rodents (Huang et al. 2002). Mammals are restricted in their hearing by the basic physics of how sound waves are received and amplified in the passage of the outer

and middle ear, with the external pinna responsible for gathering sounds of particular frequencies and the auditory canal and bullae responsible for amplifying sounds of frequencies that depend on the total size of these structures (Webster 1962). Small mammals without large auditory bullae or elongated auditory canals cannot sufficiently hear sounds with long wavelengths/lower frequencies, and thus enlarge one or both of these structures to accommodate for crucial low frequency environment noise necessary for their survival. Although some mid to large sized rodents, such as mountain beavers (*Aplodontia rufa*), have elongated auditory canals, most small rodents under heightened predation pressure enlarge the auditory bullae, allowing for efficiently packaged volume necessary to amplify sounds a small rodent would otherwise be incapable of hearing.

The size of auditory bullae in these desert rodents has been recognized as a potential physical, functional, and/or developmental constraint, particularly given that it removes a large area on the dorsolateral side of the braincase for temporalis muscle attachment, a muscle usually responsible for much of the power in biting behavior (Nikolai and Bramble 1983). Bullae are not well fused to the skull, and often have rather thin bony walls, making any muscle attachments for jaw closing muscles untenable and highly unlikely from a biomechanical standpoint. Furthermore, the internal mechanics of these bullae in amplifying sounds would likely be perturbed during muscle contractions if muscles were to attach upon them. So far, the extent to which massive auditory bullae have led to important structural and functional changes has not been examined, but could be particularly interesting given the unique jaw movements and function of the rodent masticatory apparatus and jaw muscle diversity. Rodents have separate and distinct biting positions, with a cheekteeth chewing position in which the mandibular condyle resides in a soft tissue pocket posterior to the “glenoid” articulation of the squamosal,

and an incisor gnawing position in which the anterior mandible is brought forward anteriorly and the mandibular condyle abuts the glenoid articulation of the squamosal. The cheekteeth do not occlude during incisor biting and the incisors do not occlude during cheekteeth chewing. This style of mandibular behavior is unique among extant mammals. Furthermore, the masseter muscles of rodents are unique among mammals in that they have repeatedly and convergently evolved a number of different specialized origination sites anterior to the eye on the lateral side of the rostrum. These include sciuromorphy, which exhibits an enlarged anterior deep masseter on a anteroventrally facing zygomatic plate, hystricomorphy, which exhibits an enlarged orbital portion of the zygomaticomandibularis that penetrates through an enlarged infraorbital foramen and attaches to a laterally facing fossa, and myomorphy, in which both of these conditions exist in tandem, with the infraorbital portion of the zygomaticomandibularis and in the infraorbital foramen always residing dorsomedially to the zygomatic plate and the attached anterior deep masseter. Although these novel muscles provide ample opportunity for functional redundancies with other preexisting muscles, whether this phenomenon occurs in rodent oral biomechanics has hitherto been unexplored. The potential severe reduction of temporalis attachment space in desert hopping rodents with enlarged auditory bullae provides a series of independently evolved test cases over various masseter muscle conditions for whether any biomechanical redundancies exist among these a highly derived and numerous jaw muscles or whether interesting compensatory adaptations are necessary to accommodate for the lack of the temporalis and/or other muscles that enlarged auditory bullae exclude from usual cranial attachment space.

In this study, I describe the jaw musculature of jerboas (*Jaculus jaculus*), kangaroo rats (*Dipodomys merriami*), and pocket mice (*Chaetodipus* and *Heteromys*) using DICE-μCT scanning, and use these findings to better understand the osteological correlates of jaw muscle

attachments in these respective rodent families (Dipodidae and Hetermyidae) in comparison with more well described myomorphic rodents such as gerbils (Gerbillinae; Muridae). I aim to test whether the loss of available cranial attachment space for the temporalis muscle in these open-habitat rodents is associated with significant changes to jaw muscle morphology, attachment zones, and general biomechanical features of the feeding system and whether these changes differ by original masseter muscle configuration.

Methods

Specimens

Heteromyid specimens were loaned from the Field Museum of Natural History (FMNH) from the Mammalogy wet collections. These included two *Dipodomys merriami* (FMNH 123311 and 123315, both male collected Esmeralda, Nevada US by P.W. Freer in 1981), one *Chaetopdipus formosus* (FMNH 191149, male, collected in Washoe County, Nevada US by R.C. Terry in 2006), and one *Heteromys desmarestianus* (FMNH 128440, female, collected in Heredia, Costa Rica by M. Timm in 1986). These specimens were previous fixed in formalin and stored long term in ethanol. Jerboa (*Jaculus jaculus*) specimens were loaned from the lab of Dr. Kim Cooper (UCSD) frozen. Jerboa specimens were thawed and fixed in formalin before being stored in 90% ethanol until staining.

DICE staining and µCT scanning

Ethanol soaked specimens were gradually introduced into an aqueous solution through serial dilutions. Specimens were then soaked in a solution of 5% I_2KI weight/volume between 30 and 40 days. Specimens were repeatedly tested in the CT scanner using five minute scans to assure full penetration and diffusion of stain. Specimens were wrapped in a wet paper towel and packaged in two layers of zipped plastic bags, then placed into a plexiglass tube with a mounting

adapter and packed in with styrofoam and until the specimen was secured in place. Specimens were mounted into in a GE µCT scanner and scanned with a 240 kV directional microfocus tube with a 0.5 mm copper filter. Scan parameters were set manually for each specimen to optimize contrast and resolution. Voltage was usually set between 140 kV and 180 kV and current usually between 135 µA and 190 µA. Exposure timing were set at either 300 ms or 500 ms, projection averaging at 3, and slice skips at 1. Each scan was conducted to produce 2000 slices with typical resolution between 15 and 30 microns depending on specimen size.

Specimen Reconstruction and Muscle Segmentation

Initial scan TIFF files were uploaded into the Datos software to check for specimen movement during the scan and calculated 3D model that was then uploaded into VG Studio Max 2.2. Here basic contrast and thresholding were conducted to optimize visibility of stained muscle morphology. Coronal TIFF image stacks were then exported to upload into Mimics 3.0 for muscle segmentation. Each muscle was given a separate mask and the outlines of the muscle were outlined and filled with a pen tool in individual coronal slices before interpolating between slices (between 2 and 20 slices depending on complexity of morphological change per slice). Three dimensional objects were then calculated for each mask and smoothened to reduce noise between interpolated slices.

Comparisons to museum specimens

FMNH dry skull specimens among heteromyids, dipodoids, and gerbillines were photographed using a Nikon D5200 DSLR with AF-S DX NIKKOR 18-55mm f/3.5-5.6G VR lens mounted on a tripod. Specimens were steadied in fine grained beads to assure a consistent lateral, dorsal, and ventral view poses toward the camera lens with mandibles in and out of place

in relation to the cranium and in molar and incisor occlusion. Mandible were also photographed separately in dorsal, ventral, and lateral views.

Results

Description of Heteromys desmarestianus skull and iodine-stained muscle morphology

The skull of *Heteromys* is relatively robust compared to the other heteromyids (Fig 3.1A). The auditory bullae are not particularly large or inflated and do not detract from cranial surface area for temporalis muscle attachment. The lateral margin of the zygomatic plate is relatively thin and does not contain a large fossa within the orbit. The jaw rests in a gnawing position with the lower molars displaced anteriorly compared to the upper molars. The accessory process of the angular is small compared to *Chaetodipus* and *Dipodomys*. It is not a flattened plate-like structure but instead a robust, dorsolaterally curved process that lacks perforations.

The superficial masseter originates on a tendonous attachment at a point anterior to the anterior deep masseter on the ventrolateral side of the rostrum. This tendon continues posteriorly until it begins to wrap laterally around the anterior deep masseter and becomes the muscle belly. From here the superficial masseter begins to fan out ventroposteriorly in a trinagular shape. The ventral margin of the muscle wraps underneath the ventral margin of the mandible to insert medially along the angular process ventral to the pterygoideous musculature (Fig. 3.2A, Fig. 3.3A,D). The dorsal margin continues posteriorly until half way underneath the zygomatic arch, in which a portion of the superficial masseter ascends to meet and originate on the zygomatic arch at a point-like attachment. This ascending process of the superficial is anteroposteriorly narrow and ascends in a anterodorsal direction from main body of the superficial muscle just between the descending portion of the anterior deep masseter and the ascending portion of the

posterior masseter. It meets the rest of the muscle at it's posterior most margin as it wraps around the distal tip of the angular process.

The anterior deep masseter is the largest muscle in the head. It closely resembles a typical sciuromorphous morphology, with a large origination attachment site along the dorsolateral margin of the rostrum and onto the anterolaterally facing zygomatic plate that begins to droop ventroposteriorly. The muscle near the origination is mediolaterally thick and thins progressively into a sheet ventrally until the insertion on the mandible, which begins anteriorly midway on the lateral face of the mandible directly ventral to the p4 and continues posteriorly until the angular process. The internal structure of the anterior deep masseter is pinnately fibered with fibers directed toward the origination site (Fig 3.5. A, B).

The posterior masseter is relatively massive and mediolaterally thick, particularly where it wraps around the posterior portion of the zygomatic arch. It originates along the dorsolateral sides of the zygomatic arch just ventral to the eye anteriorly and along to the posterior portion of the arch near the jaw joint. It inserts along a lateral flaring of the angular process that does not contain attachment zones for the superficial masseter or pterygoideus musculature. The posterior masseter wraps around this accessary angular process dorsolaterally and onto the ventral side of the process until it meets the attachment area of the superficial masseter. The poserior masseter is triangular in shape from a lateral view.

The orbital portion of the zygomaticomandibularis is small and anteroposteriorly flattened. It originates at the dorsal margin of the anterior wall of the orbit and meets the anterior deep masseter as it runs ventrally (Fig. 3.5B). The rest of the muscle was not distinguishable and was thus segmented along with the anterior deep masseter, although in other heteromyids segmented in this study this muscle is distinct from dorsal to ventral attachments.

The posterior portion of the zygomaticomandibularis is relatively small. It originates on the dorsal side of the squamosal process of the zygomatic arch and inserts on the lateral face of the coronoid process. It is dorsoventrally thinner than it is mediolaterally.

The temporalis is the next largest muscle after the anterior deep masseter. The morphology in this specimen is perturbed due to a severe "injury" to the cranium, in which a mediolateral line a few millimeters thick anteroposteriorly has been caved into the brain case near the frontoparietal junction (Fig. 3.1A, Fig. 3.5C). This feature depressed the temporalis ventrally in this particular location, although the portions of the muscle ventral and posterior to this alteration appear relatively normal on both sides of the skull. The temporalis originates along the temporal/nuchal ridge on the posterolateral margin of the cranium. The muscle continues anteriorly before expanding and entering the orbit, where it's origination attachment continues anterior to the brain case within the orbit. The muscle then runs ventrolaterally where it inserts broadly onto the medial surface and anterior margin of the coronoid process.

Description of Chaetodipus formosus skull and iodine-stained muscle morphology

The skull of *Chaetodipus* is smaller than *Heteromys* and less robust (Fig. 3.1B). The auditory bullae are large and high inflated, encompassing a large portion of the posterolateral and some of the posterodorsal area of the cranium. The area for temporalis attachment is relegated anteriorly on the anterior face of the braincase, and this attachment surface is approximately half the size of zygomatic plate. The lateral margin of the zygomatic plate is relatively thick compared to *Heteromys* and contains a fossa within the orbit. The jaw rests in a gnawing position although the incisors do not occlude. The jaw joint is dislocated such that the dorsal surface of the mandibular condyle resides slightly dorsal to the glenoid fossa of the squamosal within the temporal fenestra. The accessory process of the angular is larger than in *Heteromys* but small

than in *Dipodomys*. It twists out laterally at a 45 degree angle pointing dorsolaterally. Each side contains an irregularly shaped but singular perforation at its ventroposterior margin.

The masseter muscles of *Chaetodipus* are relatively similar to *Heteromys* although differ in proportions and muscle separation. The superficial masseter originates on a tendon (not segmented) that attaches anterior to the anterior deep masseter, with the muscle belly beginning where the tendon wraps around the ADM. Here the superficial is particularly thin mediolaterally. It expands dorsoventrally in a triangular shape as it moves posteriorly, with the ventral margin of the muscle wrapping underneath the ventral margin of the mandible, inserting medially along the anuglar process (Fig. 3.2B, Fig. 3.3B,E). The ascending process of the superficial is larger than in *Heteromys*, both being anteropoteriorly and medilaterally thicker. The muscle belly of the ascending process also rises higher dorsally to originate on the zygomatic arch at point-like attachment, meeting the originations of both the posterior and anterior deep masseters.

The anterior deep masseter is the largest muscle in the head. It is similar to *Heteromys* in origination and insertion morphologies, as well as being pinnately fibered (Fig. 3.6).

The posterior masseter is larger than *Heteromys* and has a larger area of insertion on the acessory angular process of the mandible. As in *Heteromys*, the origination begins just posterior to the origination sites of the anterior deep masseter and ascending process of the superficial masseter on the zygomatic arch. It continues posteriorly until the posterior edge of the squamosal process of the zygomatic arch, and then descends ventrally to wrap around the accessory process of the mandible. Here the insertion is mainly attached to the ventrolateral face of the process with some wrapping around the posterior edge (Fig. 3.6D).

The orbital portion of the zygomaticomandibularis is fully separated from the anterior deep masseter. It originates at the most dorsal extent of the anterior wall of the orbit inside an

anteriorly directed fossa (Fig. 3.6A,B). The belly of the muscle is anteroposteriorly flattened between the eye and the anterior orbital wall, and relatively thick mediolaterally. The ventral portion of the muscle below the orbit twists to flatten against the anterior deep masseter's medial face until inserting on the dorsolateral side of the mandible below the cheekteeth.

The posterior portion of the zygomaticomandibularis is similar to that in Heteromys in most ways, originating on the dorsal surface of the zygomatic process of the squamosal and inserting on the lateral face of the mandibular ramus near the coronoid process. The muscle is generally round in cross-section.

The temporalis is smaller in *Chaetodipus* compared to *Heteromys*, although for the most part differing in the lack of a posterior lobe that reaches back to originate on the nuchal crest. Instead, the auditory bullae restricts the temporalis to an attachment zone on the anterior face of the braincase within the temporal fenestra/orbital region (Fig. 3.6C). The insertion attaches to the medial face and anterior margin of the small coronoid process and descends along the medial portion of the mandibular ramus until half way down compared to the height of the masseter muscles.

Description of Dipodomys merriami skull and iodine-stained muscle morphology

The skull of *Dipodomys* is large, with a relatively large orbit compared to *Chaetodipus* and *Heteromys* and far larger relative auditory bulla compared to even *Chaetodipus* (Fig. 3.1C). The auditory bullae cover almost the entiretly of the posterolateral, posterodorsal, and posteroventral surface of the cranium, and have relegated the temporalis attachment area to small region anterior to the braincase. The dorsolateral margin of the zygomatic plate is highly thickened externally, creating a bony wall that encloses a large fossa within the orbit. The jaw rests in a gnawing position with the molars out of occlusion. The jaw joint is dislocated such that

the mandibular condyle resides dorsally within the temporal fenestra. The accessory process of the angular is larger than either *Chaetodipus* or *Heteromys*. It is dorsoventrally flattened with a traingular shape pointing out laterally and is perforated by numerous irregular holes just anterior to the posterior edge of the bone.

The superficial masseter is sheet-like and surrounds the outer ventro-lateral portion of the masseter complex. The superficial masseter has dual origination sites on the cranium, one stretched around the anterior deep masseter by a tendon onto a point-like surface anterior to the zygomatic plate. This portion of the muscle widens posteriorly in a triangular fashion until it meets the main body of the muscle. The second origination site on the cranium reaches dorsally in a triangular shape up to the ventrolateral side of the thin zygomatic arch. The superficial masseter meets the mandible below the cheekteeth and wraps under the ventral surface of the dentary at a dorsally arched portion just anterior to the angular process, contorting into the medially directed fossa and inserting ventral to the insertions of the pterygoideus musculature (Fig. 3.2C, Fig. 3.3C,F). A posterior portion of the superficial masseter inserts on the angular process but fails to fully envelope the angular process. The angular process flares outward laterally extensively at a nearly 90 degree angle from the anteroposterior axis on the dentary and out laterally by up to 30% of the mandibles anteroposterior length. It has a nearly triangular shape with a rounded distal tip and is dorsoventrally flattened.

The anterior deep masseter is similar to *Heteromys* and *Chaetodipus*. The anterior deep masseter is massive, with the anterior margin of it origination site on the cranium beginning at the upper incisor's root in the premaxilla where it meets the nasal bones and continues dorsally and posteriorly along the prominent bony ridge of the zygomatic plate, which flares out laterally well anterior to the orbit. This leaves a large bony area from both dorsal and lateral views

between the anterior edge of the zygomatic plate and the anterior edge of the orbit composed primarily by the maxilla. The anterior deep masseter's origination continues along the lateral edge of the zygomatic plate. The thick bony area anterior to the eye quickly narrows into the small rod-like zygomatic arch, with the anterior deep masseter's origination continuing virtually seemlessly into the origination of the rest of the deep masseter, which extends further posteriorly along the zygomatic arch on its ventral margin onto the squamosal, but ending prematurely before the squamosal verges medially into the cranium, in line with the coronoid and anterior margin of the temporalis. The insertion on the mandible of the deep masseter resembles the typical condition in rodents, inserting anteriorly below p4, continuing posteriorly on the lateral surface of the mandible until the beginning on the angular process. The muscle length between the deep masseter's posterior mandible insertion and the posterior cranial origination is very short. This distance gradually expands anteriorly until the beginning of the zygomatic plate in the which the anterior deep masseter's muscle length covers a great distance from the bottom of the mandible to the dorsal margin of the skull, nearly 40% of the total skull length. The anterior deep masseter overlaps the infraoribtial foramen, in heteromyids represented by a large circular lateral perforation of the rostrum.

The accessory process of the angular is the exclusive insertion area for the posterior masseter. The posterior masseter envelopes distal portion of the angular process with extensive muscle material wrapped around both dorsal and ventral sides of the process, leaving only the posterior margin of the angular processes' edge exposed. the main body of the posterior masseter continues anterodorsally toward its origination site on the posterior portion of the zygomatic arch, which is thin, cynlindrical, and nearly straight. The posterior masseter's origination envelopes the entire posterior portion of the zygomatic. The muscle's anterior margin of its

origination ends in a triangular point from lateral view, making the entire muscle in lateral view triangular in shape aside from the dorsal swelling of the muscle above the plane of the zygomatic arch.

The zygomaticomandibularis is similar to *Chaetodipus* but far larger and split anteriorly into two ascending units. The medial unit is both anteroposteriorly and mediolaterally thickened. It originates on the dorsal wall of the anteriorly directed orbital fossa. It quickly narrows ventral to the orbit before inserting on the dorsolateral face of the mandible ventral to the cheekteeth.

Description of Jaculus jaculus skull and iodine-stained muscle morphology

The skull of *Jaculus* is robust, with large bony walls surrounding the infraorbital foramen (Fig. 3.4A, Fig. 3.12A). The auditory bullae are voluminous, composing the majority of the posterolateral surfaces of the cranium. The temporalis attachment is restricted to the anterior surface of the braincase within the temporal fenstrae. The maxillary and jugal walls lateral to the infraorbital foramen are massive, with large laterally flaring components with posteromedial fossa for muscle attachments within the orbit. As in heteromyids, the lacrimal is also enlarged and prominently poses dorsally over the orbit with orbital muscle attachment scars. The zygomatic arch is small and thin just posterior to the infraorbital foramen but thickens posteriorly at the zygomatic process of the squamosal, with a posterolaterally directed angle of bone that makes an acute angle to turn back medially into the cranium. The jaw rests in a nearly gnawing position, with the incisors failing to occlude and the lower cheekteeth displaced slightly anterior to the upper cheekteeth. The angular process is large and twists such that the medial side faces dorsally and the distal tip points laterally. A single, large, roundly margined perforation exists in the middle of the angle.

The superficial masseter originates at a point like source anterior to the deep masseter on the ventral side of the zygomatic process of the maxilla that buttresses the lower portion of the infraorbital foramen. The superficial fans out ventroposteriorly until it meets the ventral portion of the mandible, where it wraps around from the lateral side to insert medially along the angular process. The superficial does not envelope the entirety of the angular process.

The deep masseter originates along the ventrolateral margin of the zygomatic arch from just posteroventral to the infraorbital foramen to the posterior portion of the zygomatic process of the squamosal. It is visible in lateral view above the superifical masseter. It inserts along the lateral side of the mandible near the ventral margin, starting anteriorly below m1 continuing posteriorly to the angular process, where it continues dorsolaterally along the angular process. The most distal aspect of the angular is exclusively enveloped by the deep masseter.

The zygomaticomandibularis orbital and infraorbital portions are large, with the ZMIO inserting on the lateral aspect of the mandible at a point like source via a tendon. The ZMIO widens toward its origination, beginning dorsally before turning anteriorly at almost a right degree angle where it originates along the dorsal margins of the lateral side of the rostrum anterior to the infraorbital foramen. The ZMOP inserts laterally adjacent to the ZMIO, although with an anteroposteriorly wide surface that continues into a tendon upon attachment to the mandible. The ZMOP widens dorsally and twists such that the posterior edge of the muscle attaches to the most lateral portion of the bony jugal lateral flaring of the lateral edge of the infraorbital foramen. This bony region supports the lateral component of the ZMOP origination site, with the anteromedial portion of the ZMOP continuing anterodorsally along the ventral margin of the dorsal bony bar of the infraorbital foramen.

The temporalis is dramatically reduced, originating just slightly posterior to the jaw joint on the anterior face of the enormously enlarged auditory bulla. The temporalis is dorsoventrally flattened and inserts along the medial and anterior margin of the small coronoid process of the mandible. The internal and external pterygoideus muscles (not figured) insert onto the medial wall of the angular process and originate in a dorsomedial direction onto the basicranium.

Comparison to other heteromyid taxa

Liomys, the sister genus to *Heteromys* (Fig. 3.7), is similar to *Heteromys* in most basic aspects of the skull (Fig. 8). *Liomys* has a large zygomatic plate for the origination of the anterior deep masseter but little to no orbital structures to support large muscle attachments. The temporal ridge is extensive as in *Heteromys,* and similarly limited to halfway dorsally along the lateral side of the braincase, but reaches posteriorly to the nuchal crest. The mandible is mediolaterally flat with a small accessory process of the angular that only slightly points out dorsolaterally from the plane of the mandible. The auditory bullae is similarly small and does not envelope posterolateral cranial surfaces dorsal to the auditory meatus.

Just as *Liomys* is generally similar to *Heteromys*, *Perognathus*, the sister genus the *Chaetodipus* (Fig. 3.7), closes resembles *Chaetodipus* in cranial and mandibular morphology (Fig. 3.9). The zygomatic plate is large and the anterior wall is more well developed than in *Liomys* and *Heteromys,* demonstrating robustness in lateral view posterior to the zygomatic plate. The auditory bullae is massive and composes most of the posterolateral surface of the braincase region of the cranium except for a region just anterior to the bullae where the temporalis still contains a broad insertion, wrapping around the anterior margins of the bullae dorsally and ventrally. The mandible has a large plate-like accessory process of the angle that twists dorsolaterally at a 45 degree angle from the plane of the mandible.

Other species of *Dipodomys* contain even larger accessory processes of the angle than that found in *D. merriami*, such as *D. ingens* (Fig. 3.10). As in *D. merriami*, other *Dipodomys* species have extensively laterally flared angulars with broadly rounded distal tips. Medially these processes contain a flattened platform that resembles those found in some herbivorous sciurids and aplodontids. The orbital region posterior to the zygomatic plate is large and highly robust, with deep anteriorly directed fossa for muscle attachments and a prominently dorsally roof lacrimal process. In almost all *Dipodomys* species, the auditory bullae are highly voluminous and comprise the vast majority of posterolateral and posterodorsal cranial surfaces. The region for temporalis attachment is highly reduced and relegated just anterior to the auditory bullae. The coronoid process is also highly reduced compared to *Liomys* and *Heteromys* and even further reduced than in *Perognathus* and *Chaetodipus*.

Comparison to other dipodoid taxa

Sicista, an outgroup to other dipodoids (Fig. 3.7), exhibits a small, narrow rostrum with a relatively small infraorbital foramen that does not comprise the entire dorsoventral height of the rostrum (Fig. 3.11A). The margins of the infraorbital foramen are contained by gracile bone that lack prominent orbital fossa. The auditory bullae are small and do not envelope cranial space dorsal to the auditory meatus. Instead, the temporalis attaches broadly across the available braincase and reaches the nuchal crest posteriorly. The coronoid process is proportionally sized for a typical rodent and the mandible is contained within a single flat plane with a small angular process that flares laterally only marginally. *Zapus* and *Napaeozapus*, which are more closely related to *Jaculus* than to *Sicista* (Fig. 3.7), are generally similar to *Sicista*, although both exhibit slightly larger relative infraorbital foramina, a more robust jugal with orbital muscle attachment area, and a larger angular process with an increased degree of lateral twisting (Fig. 3.11B,C).

Dipodine taxa are far more similar to *Jaculus jaculus* in skull morphology, although they can be lumped into two categories based on degree of bullae size and muscle attachment morphology. *Allactaga* and *Pygeretmus* have relatively small bullae compared to *Jaculus jaculus* but much more voluminous than among non-dipodine dipodoids (Fig. 3.12). Most of this volume of the bullae is ventral to the auditory meatus and does not envelope the braincase as in *Jaculus jaculus*. The orbital regions in *Allactaga* and *Pygeretmus* are massive compared to *Zapus*, *Napaeozapus*, and *Sicista*, as are the infraorbital foramina. Despite their large size, the infraorbital foramina are not surrounded by robust bony walls laterally and dorsally but instead thin, narrow bony struts. The region for temporalis attachment exists dorsal to the auditory meatus and reaches posteriorly to the nuchal crest but does not rise further than halfway up dorsally across the lateral face of the braincase, and the anteroposterior distance from the orbit to nuchal crest is small compared to that in *Sicista*, *Zapus*, and *Napaeozapus*. The coronoid process is smaller and the angular process has a slight lateral flare with a point-like distal tip. This angular process also contains a large, rounded perforation that comprises a majority of its area.

These latter dipodines differ from more derived dipodines like *Jaculus jaculus*, *Jaculus orientalis*, and *Stylodipus telum*, with the latter species being far more robustly built overall and containing enormous auditory bullae (Fig. 3.13). Both *Jaculus* and *Stylodipus* exhibit auditory bullae that comprise the vast majority of the posterolateral cranial surface, enveloping the braincase dorsal to the auditory meatus. These bullae relegate the temporalis attachment region to a small surface on the anterior face of the braincase that fails to reach the nuchal crest posteriorly. The orbit and infraorbital foramen are both large as in *Allactaga* and *Pygeretmus*, although the infraorbital foramen is robustly surrounded by thick walls of jugal, maxilla, and lacrimal bone. The jugal in particular exhibits a posterolateral flare of bone at the midlevel

dorsoventrally in orbital height, and the lacrimal process dorsally incases the orbit. The coronoid process is small, but the angular process is highly enlarged and dorsoventrally flattened, containing both laterally and medially directed platforms for muscle attachment. Like *Allactaga* and *Pygeretmus, Jaculus* and *Stylodipus* contain large, rounded perforation within this angular process.

Comparisons to Gerbillinae

Gerbillines vary tremendously across species in auditory bullae size and available space for the temporalis attachment, although they do not vary similarly in masseter muscle attachment zones of the skull (Fig. 3.14). Gerbillines are typified by a mid-sized zygomatic plate that constrains a mediolaterally flattened infraorbital foramen against the rostrum, with the infraorbital foramen visible dorsally and anteriorly but not laterally. The angular process is prominent, falling in line with the plane of the mandible but highly recurved posterodorsally to a point-like distal tip. Many species contain small to mid-sized auditory bullae to fail to envelope cranial space dorsal to the auditory meatus, such as *Rhombomys opimus, Psammomys obesus, Tatera indica*, and *Gerbillus dasyurus*. *Rhombomys* is the most robust of these, with a temporalis attachment region to encompasses the entire lateral and dorsal surface of the braincase and a relatively large mandible compared to cranial size for gerbillines, including a large, flat angular process. *Psammomys, Tatera*, and *Gerbillus* demonstrate more similar dimensions of the mandible and gracility of the cranium to other gerbillines, and each lack derivations of the anterior orbital wall and lateral jugal posterior to the zygomatic plate. *Pachyuromys duprasi, Desmodillus auricularis, Meriones crassus* and *Meriones libycus* exhibit some of the largest relative auditory bullae sizes that also envelope most of the posterolateral surface of the braincase dorsal to the auditory meatus. In *Meriones* and *Desmodillus*, this relegates the

temporalis attachment anterodorsally on the braincase and fails to reach the nuchal crest posteriorly. The area for temporalis attachment is thus reduced by nearly half of that in other large auditory bullae species such as *Sekeetamys, Gerbilliscus*, and *Taterillus*. The angular process does not substantially differ in any recognizable form between species with large and small auditory bullae. The angular process is somewhat more acutely angled in *Psammomys obsesus* and *Meriones crassus*, but these species are at the opposite ends of the auditory bulla size spectrum (small to large respectively). The zygomatic plate and infraorbital foramen also retain their proportional sizes in essentially all species examined. *Tatera indica*, *Gerbilliscus phillipsi*, and *Meriones libyicus* each demonstrate a slight swelling of bone on the lateral margin of the orbit just posterior to the zygomatic plate that could potentially harbor orbital muscle attachments for the zygomaticomandibularis; however, these species also span the auditory bulla size spectrum (small to large respectively), and these swelling are not present in most other gerbilline taxa, including those with the largest auditory bulla sizes such as *Pachyuromys duprasi, Desmodillus auricularis*, and even *Meriones crassus*.

Discussion

Comparative myology of the superficial and posterior masseters in Castorimorpha

The myology of castorimorph rodents, the group that includes beavers (Castoridae), pocket gophers (Geomyidae), and pocket mice and kangaroo rats (Heteromyidae) has been little studied compared to rodents generally, despite the commonness of these taxa in North American and Eurasian ecosystems. *Castor* was apart of the initial descriptions of rodent masseter muscles by Brandt (1855), but since had received almost no anatomical attention until the thorough description provided by Cox and Baverstock (2015). These authors found *Castor* to be unique among mammals in demonstrating a superficial masseter with dual origination sites on the skull

that straddle the anterior deep masseter anteroposteriorly, with the anterior attachment resembling the typical rodent condition of a point-like attachment of a tendon on a raised bony boss of the maxilla, but the posterior attachment more closely resembling the sheet-like attachments of the deep masseter along the length of the zygomatic arch. Cox and Baverstock argued that the superficial masseter was particularly important for the gnawing mechanics of *Castor*, as the anterior deep masseter was relatively small for a sciuromorph while the superficial masseter was particularly large, and surprisingly removing the superfical masseter from their analysis reduced the bite force output estimated at the incisor by 40%. Considering *Castor* alone, one could attribute this highly derived superficial masseter to an apomorphy related to *Castor*'s extreme diet and foraging strategies falling trees through incisor gnawing, or the evolutionary history Castoridae which was dominated by fossorial taxa until recently (Samuels and Van Valkenburgh 2009). However, the current study reveals that this unique superficial masseter morphology is present in each of the representative heteromyid taxa examined, providing for the possibility that a superficial masseter with dual cranial originations is a castorimorph plesiomorphy and not a recent adaptation to extreme ecological conditions.

The superficial masseter is generally similar in each of the heteromyid taxa examined here, although is notably smaller in *Heteromys* in overall size as well as exhibiting a particularly small ascending process. These heteromyids also differ from *Castor* in that their zygomatic origination attaches at a point instead of a broad sheet-like attachment along the anteroposterior axis of the zygomatic arch. Interestingly, these heteromyids do have a similar muscle that inserts across the accessory process of the angular and originates along the posterior half of the zygomatic arch just posterior to the ascending process of the superficial. This muscle has been termed the posterior masseter here due to the ambiguity of its homology and that this is what the

muscle was termed in the most recent description of heteromyid masseter musculature (Howell 1932). The posterior masseter is however a poorly studied entity that has been various named in many different rodent groups that may or may not be homologous. It is possible that the posterior masseter described here for heteromyids is a division of the superficial masseter that originally resembled the condition currently seen in *Castor*, in which the origination runs along the entire length of the zygomatic process before bifurcating into the primitive condition attachment anterior to the anterior deep masseter on the rostrum. This is potentially further evidenced by the condition seen in *Heteromys*, in which the ascending process of the superficial is difficult to ditinguish morphologically at insertion site along the mandible from the rest of the superificial masseter anteriorly and the posterior masseter posteriorly. The posterior masseter in heteromyids is thus either a unique enlargement of the posterior masseter into a massive feeding muscle or a novel division of the superficial masseter thus far unknown among rodents. Cox and Baverstock described a "posterior masseter" for *Castor*, although their posterior masseter is a medial muscle that is posteriorly adjacent to the orbital portion of the zygomaticomandibularis and resembles the same posterior portion of the zygomaticomandibularis described for heteromyids in this study. Terming the large muscle that inserts along the accessory process of the angular in heteromyids the posterior masseter is consistent with Howell's (1932) description of *Dipodomys* as well as with Woods and Howland's (1979) description of the posterior masseter in caviomorph rodents, in which the posterior masseter is a lateral muscle that originates laterally on the zygomatic arch and inserts posteriorly onto the posterior margin of the mandible dorsal to the angular process. The posterior masseter described for heteromyids here could reasonably be homologized with these posterior masseters in caviomorphs given their similar positions and orientation, while Cox and Baverstock's posterior masseter is more consistent with posterior

units of the zygomaticomandibularis that have been described in the literature before (Cox and Jeffery 2011).

Heteromyidae is the sister group to Geomyidae within the Castorimorpha, greatly increasing the likelihood that if the dual originations of the superficial masseter between heteromyids and *Castor* is a homologous condition that such a feature would also be present in geomyids. Interestingly, geomyids also demonstrate an accessory angular process dorsal to the presumed angular process. This accessory process in geomyids sticks out prominently laterally and recurves dorsally, although it is far smaller than the condition seen in heteromyids. If the superficial and posterior masseters are originally derived from a larger, single superficial masseter like that seen in *Castor*, it is thus quite possible that heteromyids and geomyids have both inherited a split superficial with an independent posterior masseter, the insertions of which have diverged in each clade, with a broad plate like bony attachment in heteromyids and small, recurved bony attachment in geomyids.

Comparative myology of the anterior deep masseters and ZMOP in Castorimorpha

Cox and Baverstock noted that the muscle mass of anterior deep masseter is relatively small in *Castor* compared to other described sciuromorphs, with the superifical masseter seemingly compensating for this discrepancy. These authors also described how the ZMOP is particular large in Castor compared to other sciuromorphs. The anterior deep masseter is by far the largest muscle in each of the heteromyid taxa sampled here, contrasting with *Castor*, although the ZMOP is relatively similar to that described by Cox and Baverstock. This is particularly true for *Chaetodipus* and *Dipodomys*, in which the ZMOP is massive and thick within the orbit, originating within an anteriorly concave fossa in front of the eye. In *Dipodomys*, this muscle appears to be so large that it is divided into two separate anatomical units

mediolaterally. In *Heteromys* this conditions become more difficult to interpret. An analogous (although far smaller and flatter) muscle originates within the same anteriorly directed fossa within the orbit, but becomes indistinguishable from the anterior deep masseter toward its insertion, thus was not separated into a differently colored mask in this reconstruction. This issue could be a result of specimen quality, in which long term storage in ethanol can shrink muscles and make distinguishing adjacent muscle layers particularly difficult. On the other hand, this orbital muscle could potentially be a division of the anterior deep masseter and not the ZMOP, as naive assessment of *Heteromys* would indicate. However, such a condition has never been described before in rodents and is contrary to the typical interpretation in other sciuromorphs (Ball and Roth 1995, Thorington and Darrow 1996) and the condition in both *Chaetodipus* and *Dipodomys* is far less ambiguous. If the orbital muscle is indeed a deep masseter division, it could be that this is also the case in *Chaetodipus* and that the lateral orbital muscle separately described here for *Dipodomys* is the only true ZMOP. This interpretation would require a far more thorough comparative myological analysis to confirm, and thus presently I accept both anterior orbital muscles of *Dipodomys* to be division of the ZMOP, with the condition of *Heteromys* left to resolve with further analysis of more specimens and the inclusion of *Liomys*.

The evolution of auditory bullae and the masticatory apparatus in Heteromyidae

Heteromyids vary greatly in auditory bullae size, with *Heteromys* resembling a typical rodent condition in which the bullae reside ventrally on the basicranium to *Dipodomys* exhibiting cranial restructuring to accommodate a set of bullae so voluminous that they envelope the braincase in every dimension except anteriorly. This latter enlargement presents clear problems to the maintenance of a large temporalis muscle, which normally originates on the dorsal and posterior margins of the skull roof. In *Chaetodipus* the temporalis remains a mid-sized muscle

relative to other feeding muscles but has had its total muscle length substantially decreased as it has been relegated to a more anterior position relative to the encroaching bullae. In *Dipodomys*, the bullae is so large that the temporalis can no longer broadly attach to the surface of the cranium, instead originating along a small surface just dorsal to the jaw joint. Although originally described by Howell (1932), this study is the first time this extreme reduction of the temporalis has been described using modern 3D methods for studying anatomy, and demonstrates the radical departure from the norms of mammalian masticatory anatomy that these arid-adapted rodent have evolved. As the temporalis is usually the most prominent muscle in the feeding system of most mammals and even most rodents, as it is for *Heteromys* described here, it would be expected that such a radical reduction of the temporalis would have profound consequences for the biomechanics of the heteromyid feeding apparatus, which has previously been hypothesized by others (Nikolai and Bramble 1983).

Potential compensatory adaptations to the loss of the temporalis can be hypothesized based on the increase in muscle size described here in *Chaetodipus* and *Dipodomys*. Interestingly, the anterior deep masseter does not appear to enlarge with a reduction of the temporalis, as it is already massive in *Heteromys*. Instead, the superficial masseter, the ZMOP, and the posterior masseter increase the most in size in *Chaetodipus* and *Dipodomys*. The superficial is particularly small in *Heteromys*, as is its ascending process, but becomes quite large in *Chaetodipus* and *Dipodomys*, particularly with a more well developed ascending process. The ZMOP is clearly distinct from the anterior deep masseter in both *Chaetodipus* and *Dipodomys*. This muscle is clearly thicker anteroposteriorly in *Chaetodipus* and becomes greatly enlarged in *Dipodomys* with potentially two separate divisions within the orbit. Finally, the posterior masseter remains relatively large in both *Chaetodipus* and *Dipodomys*, but gains a more

elaborate insertion site morphology as the temporalis size decreases, with the lateral position of the posterior masseter in *Dipodomys* resembling the distance from distal tip to jaw joint that the temporalis would have if it could reach back posteriorly to the nuchal crest in the absence of the auditory bullae. This latter observation is particularly suggestive of compensatory adaptations to the loss of the temporalis. Indeed, the potentially homologous superficial masseter of *Castor* described by Cox and Baverstock was argued to contribute substantially to bite force at the incisor, which would be important for seed gnawing specialists such as *Chaetodipus* and *Dipodomys*.

Comparing heteromyid and dipodoid masticatory and auditory bullae evolution

Howell (1932) also described the morphology of *Jaculus* along with *Dipodomys*, noticing the similarities due to the massive enlargement of the auditory bullae. Just as with *Dipodomys*, however, the descriptions by Howell were too superficial and illustrative to say much for certain about the details of muscle morphology at each layer of the masseters for *Jaculus*. Thus, I present here the first description of the masticatory morphology and myology of *Jaculus* since 1932. Comparing these iodine staining CT scanning data to skeletal specimens of other dipodoid species, we can infer numerous trends in dipodoid evolution that are analogous to that seen in heteromyids. ZMIO and ZMOP of *Jaculus* are greatly enlarged, with clearly separate divisions for the infraorbital and orbital portions. The infraorbital portion penetrates the enormous infraorbital foramen to attach to its origination, and inserts via a tendon to the mandible. The infraorbital foramen is far smaller in *Sicista*, *Zapus*, and *Napaeozapus*. Additionally, the ZMOP originates along the robust lateral bony wall of the infraorbital foramen within the orbit in *Jaculus*. This attachment region does not exist in dipodines like *Allactaga* and *Pygeretmus* that exhibit much smaller auditory bullae, although these taxa do retain highly enlarged auditory

bullae (Fig. 3.11). *Zapus* and *Napaeozapus* demonstrate some thickening anteroposeriorly and dorsoventrally on the lateral bony wall of the infraorbital foramen, suggesting they may have a prominent ZMOP despite also having a small set of auditory bullae (Fig. 3.10). *Sicista* lacks this morphology. Additionally, the angular process becomes more derived the larger the auditory bullae become, characterized by perforations and mediolateral flaring. Here attaches what I presume to be the posterior portion of the deep masseter, a strange feature given that the angular process is usually contained by the superficial masseter laterally alone. This muscle appears continuous in *Jaculus jaculus* from posterior attachment at the angular to anterior attachments posterodorsally to the superficial masseter along the zygomatic arch. A more in depth study of *Jaculus* specimens, including an ontogenic series and comparison to other dipodoid species would be required to ascertain if this unit is indeed the deep masseter.

The derived nature of the angular process in *Jaculus* and *Stylodipus* (Fig. 3.12), the taxa with largest auditory bullae and smallest regions for temporalis attachment, suggest that, like heteromyids, the muscle attaching to the angular process could be compensating for the reduction of the temporalis. Similarly, both the ZMIO and ZMOP demonstrate enlargement with auditory bullae enlargement, particularly the ZMOP. Although the ZMIO penetrates the infraorbital foramen in the these hystricomorphous taxa, the general proportions and anatomical relations of the ZMIO and ZMOP between *Jaculus* and heteromyids are surprisingly similar, further suggesting biomechanical convergence to solve similar problems in these groups.

Comparison to trends in the evolution of Gerbillinae

Gerbillines are diverse myomorphous muroid rodents closely related to murines and deomyines (Fabre et al 2012). They are diagnosable compared to other muroids by the tight constriction of the ZMIO against the rostrum by a prominent zygomatic plate, which, based on

my results from Chapter 2, may be an adaptation to seed feeding specializations as these muscles are important for gnawing in myomorphs. Although gerbillines do not evolve obligatory ricochetal behavior as in heteromyids and dipodoids, they are remarkably similar ecologically and morphologically otherwise, particularly in their repeated enlargement of auditory bullae (Alhajeri et al. 2015). Interestingly, gerbillines do not exhibit similar patterns in masticatory compensation as reported here for heteromyids and dipodoids. Instead, the variation in angular process size and shape and orbital attachments for a potential ZMOP, as well as the general size and shape of both the anterior deep masseter and ZMIO, appear unrelated to increased size of the auditory bullae. Indeed, the angular process remains relatively small and within the plane of the mandible as auditory bullae size increases, and the bony enlargements for potential ZMOP attachment are found in species with both large, mid-sized, and small auditory bullae (Fig. 3.13). The temporalis attachment area clearly decreases in size as the auditory bullae size increase, with species such as *Rhombomys opimus* demonstrating a large attachment area across the entire dorsolateral surface of the braincase for the temporalis, while *Pachyuromys duprasi* and *Meriones crassus* have very limited area for temporalis attachment.

Although this comparison to gerbillines might call into question the need for compensatory adaptation to the loss of a temporalis, I instead argue based on results from Chapter 2 that gerbillines can be interpreted as already containing muscles that compensate for temporalis action, making a reduction of the temporalis a loss of a redundant feature of the masticatory system. Both the anterior deep masseter and the ZMIO appear well suited based on mechanical advantage to greater amplify bite force at the incisor, while even a large temporalis would have a substantially lower mechanical advantage at the incisor due to a necessarily short in-lever given the restrictions of the temporal fenestra. Working in tandem, the anterior deep

masseter and ZMIO likely do most of the work in muroid gnawing performance compared to the temporalis even in species with normal temporalis sizes. However, the temporalis is still closely related to the evolution of relative incisor depth, as described in Chapter 2, thus for taxa that have simple masseter conditions such as heteromyids (sciuromorphs) and dipodoids (hystricomorphs), the temporalis likely plays a more a critical role working alongside either the anterior deep masseter or the ZMIO alone. One could expect the loss of the temporalis to be a more severe problem for non-myomorphous rodents without a way to continue to balance forces across the mandible. The posterior masseter in heteromyids and the posterior portion of the deep masseter in dipodoids appear to accomplish this task, as their posterior orientations would potentially allow for balancing forces at the jaw joint similarly to what the temporalis would have previously been capable of conducting. The emphasis of the ZMOP would also make both sciuromorphous and hystricomorphous taxa more closely resemble myomorphs, as they would gain a further enlarged anterior masseter unit with a vertical orientation and an anterior insertion point. This would appear to be a redundant feature in myomorphs if it were to evolve, potentially explaining why gerbillines fail to appreciably gain morphological adaptations within the orbit along with temporalis reduction.

Conclusions

Here, I have shown the temporalis muscle becomes greatly reduced in taxa with adaptations to arid environment, open habitat foraging strategies that necessitate proportionally larger auditory bullae to sufficiently detect and amplify low frequency sounds from predators. This trade-off requires compensatory changes to the biomechanics of sciuromorph and hystricomorph feeding systems that are here described as features that either mimic temporalis function (such as the posterior masseter in heteromyids and the posterior portion of the deep

masseter in dipodoids) or mimic myomorphous construction (ZMOP enlargement in both heteromyids and dipodoids). This is in contrast to what happens when myomorphs reduce the temporalis with auditory bullae expansion, as myomorphs already have a more sophisticated masticatory apparatus with both anterior deep masseter and ZMIO attachments anteriorly.

The results presented here are the first attempt to describe masseter muscles in heteromyids and dipodoids in nearly 100 years, and open numerous questions about the homology of various masseter units among them and their close relatives. As with other recent attempts to describe the masticatory anatomy of what would seem to be well known species (Cox and Baverstock 2015, Cox and Faulkes 2014, Baverstock et al. 2013, Hautier et al. 2009, Hautier 2010), this study also reveals how little we know and understand about basic anatomical issues in key taxa. I argue that studying organisms that are adapted to extreme environments and physiologies often provide useful cases for understanding the bounds of morphological evolution in both developmental and biomechanical contexts. Thus, studying arid-adapted, large auditory bullae rodents in far more detail anatomically, ontogenetically, and comparatively than is presented here could further test our understandings of masseter homology and biomechanics in rodents beyond what is readily discernible in most rodent taxa.

References

Alhajeri, B.H., Hunt, O.J., and Steppan, S.J. (2015). Molecular systematics of gerbils and deomyines (Rodentia: Gerbillinae, Deomyinae) and a test of desert adaptation in the tympanic bulla. Journal of Zoological Systematics and Evolutionary Research 53, 312–330.

Baverstock, H., Jeffery, N.S., and Cobb, S.N. (2013). The morphology of the mouse masticatory musculature. Journal of Anatomy 223, 46–60.

Bell, A. (1991). Plant Form: An Illustrated Guide to Flowering Plant Morphology (200 Madison Ave., New York, NY 10016: Oxford University Press).

Boke, N.H. (1944). Histogenesis of the leaf and areole in Opuntia cylindrica. American Journal of Botany 31, 299–316.

Boke, N.H. (1980). Developmental Morphology and Anatomy in Cactaceae. BioScience 30, 605–610.

Brandt, J.F. (1855). Beitraege zur nähern Kenntniss der Säugethiere Russlands (Buchdruckerei der Kaiserlichen Akad. der Wissenschaften).

Brown, J.S., Kotler, B.P., Smith, R.J., and Wirtz, W.O. (1988). The effects of owl predation on the foraging behavior of heteromyid rodents. Oecologia 76, 408–415.

Cox, P.G., and Baverstock, H. (2015). Masticatory Muscle Anatomy and Feeding Efficiency of the American Beaver, *Castor canadensis* (Rodentia, Castoridae). Journal of Mammalian Evolution 23, 191–200.

Cox, P.G., and Faulkes, C.G. (2014). Digital dissection of the masticatory muscles of the naked mole-rat, *Heterocephalus glaber* (Mammalia, Rodentia). PeerJ 2, e448.

Cox, P.G., and Jeffery, N. (2011). Reviewing the Morphology of the Jaw-Closing Musculature in Squirrels, Rats, and Guinea Pigs with Contrast-Enhanced MicroCt. The Anatomical Record: Advances in Integrative Anatomy and Evolutionary Biology 294, 915–928.

Fabre, P.-H., Hautier, L., Dimitrov, D., and Douzery, E.J.P. (2012). A glimpse on the pattern of rodent diversification: a phylogenetic approach. BMC Evolutionary Biology 12, 88.

Hautier, L. (2010). Masticatory muscle architecture in the gundi *Ctenodactylus vali* (Mammalia, Rodentia). Mammalia 74, 153–162.

Hautier, L., Fabre, P.-H., and Michaux, J. (2009). Mandible shape and dwarfism in squirrels (Mammalia, Rodentia): interaction of allometry and adaptation. Naturwissenschaften 96, 725–730.

Howell, A.B. (1932). The Saltatorial Rodent Dipodomys: The Functional and Comparative Anatomy of Its Muscular and Osseous Systems. Proceedings of the American Academy of Arts and Sciences 67, 377–536.

Huang G., Rosowski, J., Ravicz, M., Peake, W. (2002). Mammalian ear specializations in arid habitats: structural and functional evidence from sand cat (*Felis margarita*). Journal of Comparative Physiology A. 188, 663-681.

Kotler, B.P. (1984). Risk of Predation and the Structure of Desert Rodent Communities. Ecology 65, 689–701.

Moore, T.Y., Cooper, K.L., Biewener, A.A., and Vasudevan, R. (2017). Unpredictability of escape trajectory explains predator evasion ability and microhabitat preference of desert rodents. Nature Communications 8, 440.

Nikolai, J.C., and Bramble, D.M. (1983). Morphological structure and function in desert heteromyid rodents. Great Basin Naturalist Memoirs 44–64.

Plassmann, W., and Kadel, M. (1991). Low-Frequency Sensitivity in a Gerbilline Rodent, *Pachyuromys duprasi*. Brain, Behavior, and Evolution 38, 115–126.

Samuels, J.X., and Valkenburgh, B.V. (2009). Craniodental adaptations for digging in extinct burrowing beavers. Journal of Vertebrate Paleontology 29, 254–268.

Shenbrot, G.I., Krasnov, B.R., and Rogovin, K.A. (1999). Life Forms of Desert Rodents and Convergent Evolution Among the Species of Different Faunas. In Spatial Ecology of Desert Rodent Communities, (Springer, Berlin, Heidelberg), pp. 125–150.

Webster, D.B. (1962). A Function of the Enlarged Middle-Ear Cavities of the Kangaroo Rat, *Dipodomys*. Physiological Zoology 35, 248–255.

Webster, D.B., and Plassmann, W. (1992). Parallel Evolution of Low-Frequency Sensitivity in Old World and New World Desert Rodents. In The Evolutionary Biology of Hearing, D.B. Webster, A.N. Popper, and R.R. Fay, eds. (New York, NY: Springer New York), pp. 633–636.

Webster, D.B., and Webster, M. (1971). Adaptive Value of Hearing and Vision in Kangaroo Rat Predator Avoidance. Brain, Behavior, and Evolution 4, 310–322.

Webster, D.B., and Webster, M. (1980). Morphological Adaptations of the Ear in the Rodent Family Heteromyidae. American Zoologist. 20, 247–254.

Woods, C.A., and Howland, E.B. (1979). Adaptive Radiation of Capromyid Rodents: Anatomy of the Masticatory Apparatus. Journal of Mammalogy 60, 95–116.

Figures

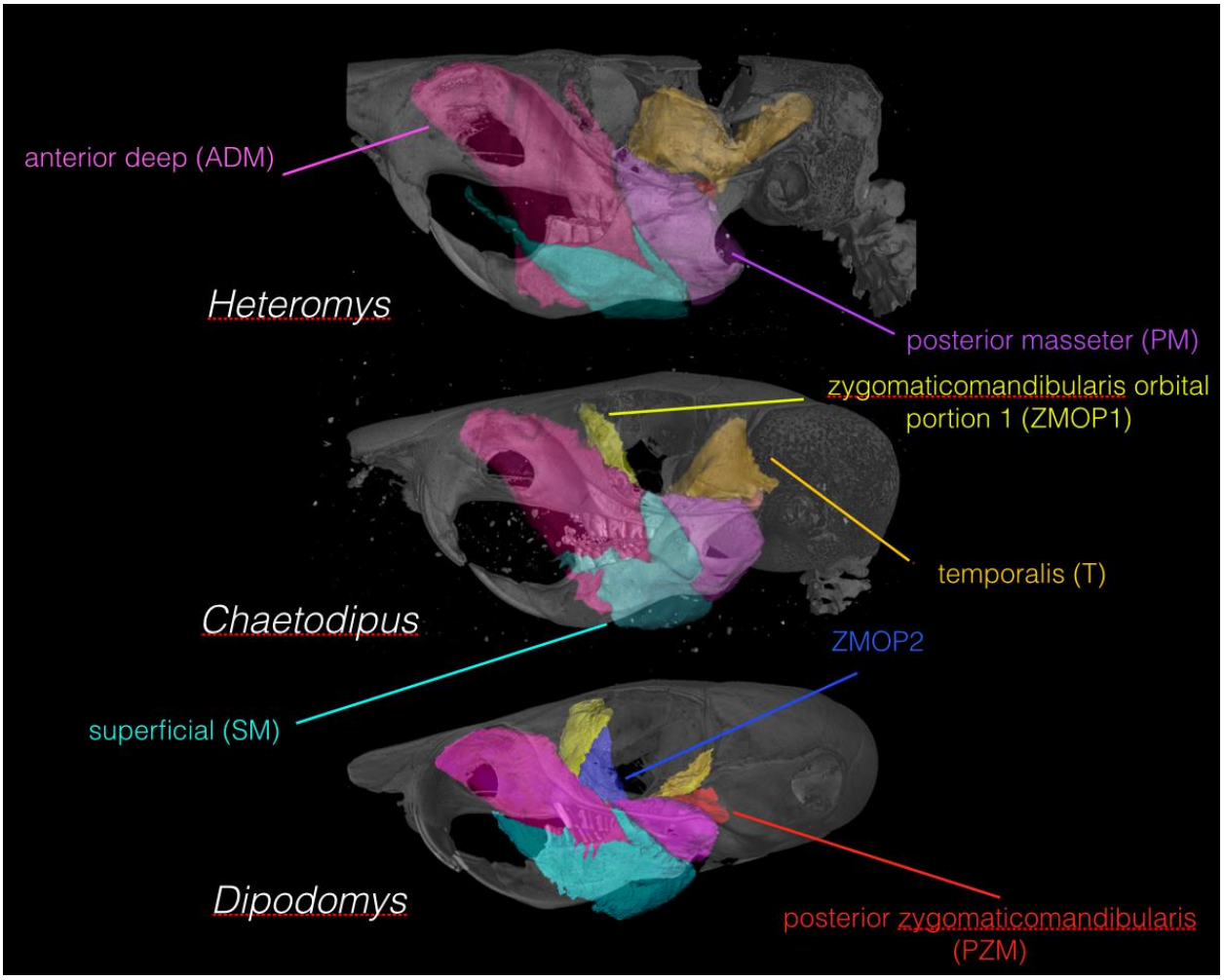

Figure 3.1. Adductor muscle reconstructions from iodine stained CT scans in lateral view for A) *Heteromys desmarestianus*, B) *Chaetodipus formosus*, C) *Dipodomys merriami*. Magenta = anterior deep masseter, light blue = superficial masseter, purple = posterior masseter, yellow = ZMOP, dark blue = ZMOP lateral, orange = temporalis, red = posterior portion of the zygomaticomandibularis. Anterior is to the left, dorsal is up.

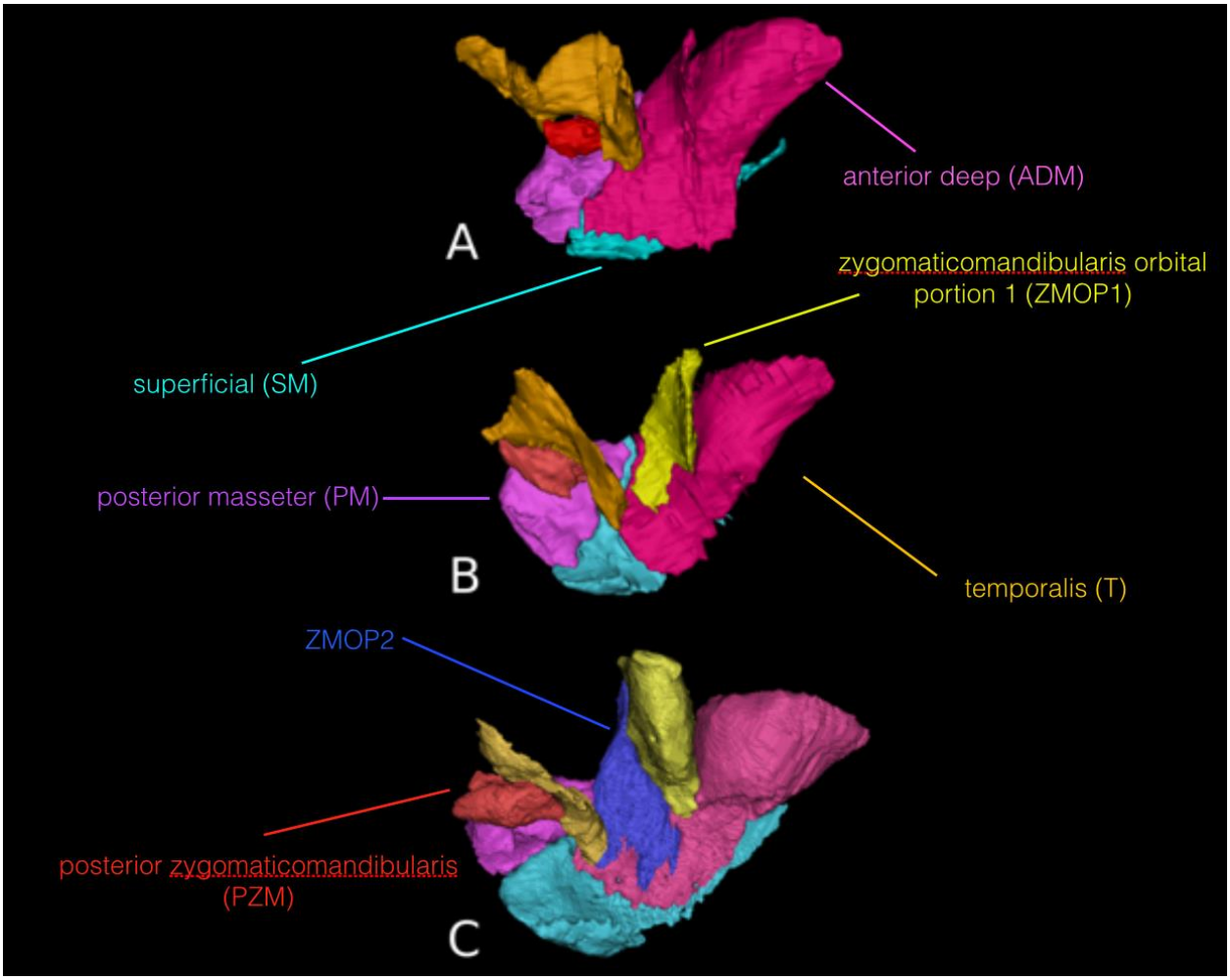

Figure 3.2. Adductor muscle reconstructions from iodine stained CT scans in medial view for A) *Heteromys desmarestianus*, B) *Chaetodipus formosus*, C) *Dipodomys merriami*. Magenta = anterior deep masseter, light blue = superficial masseter, purple = posterior masseter, yellow = ZMOP, dark blue = ZMOP lateral, orange = temporalis, red = posterior portion of the zygomaticomandibularis. Anterior is to the right, dorsal is up.

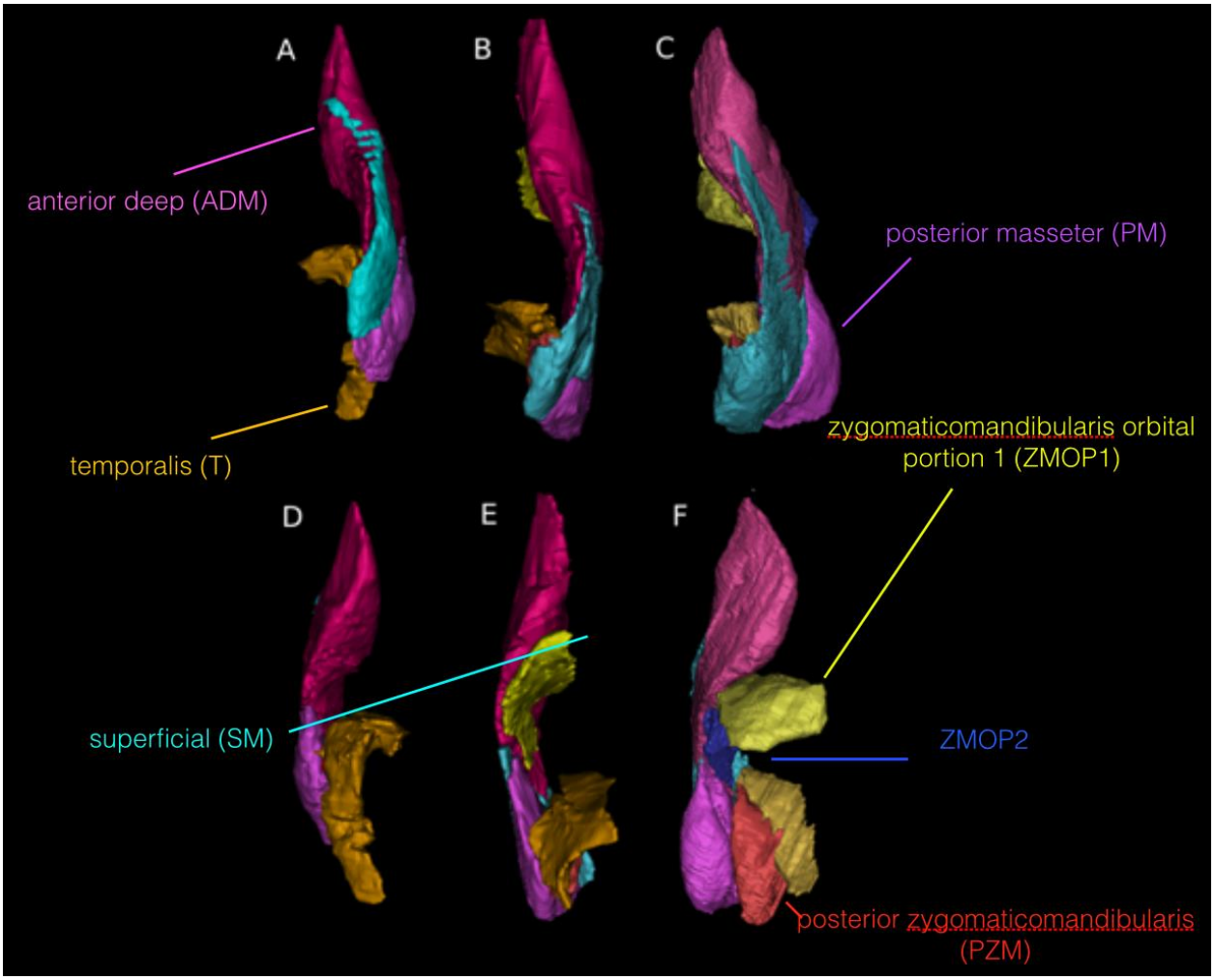

Figure 3.3. Adductor muscle reconstructions from iodine stained CT scans in ventral view for A) *Heteromys desmarestianus*, B) *Chaetodipus formosus*, C) *Dipodomys merriami*. Magenta = anterior deep masseter, light blue = superficial masseter, purple = posterior masseter, yellow = ZMOP, dark blue = ZMOP lateral, orange = temporalis, red = posterior portion of the zygomaticomandibularis. Anterior is up.

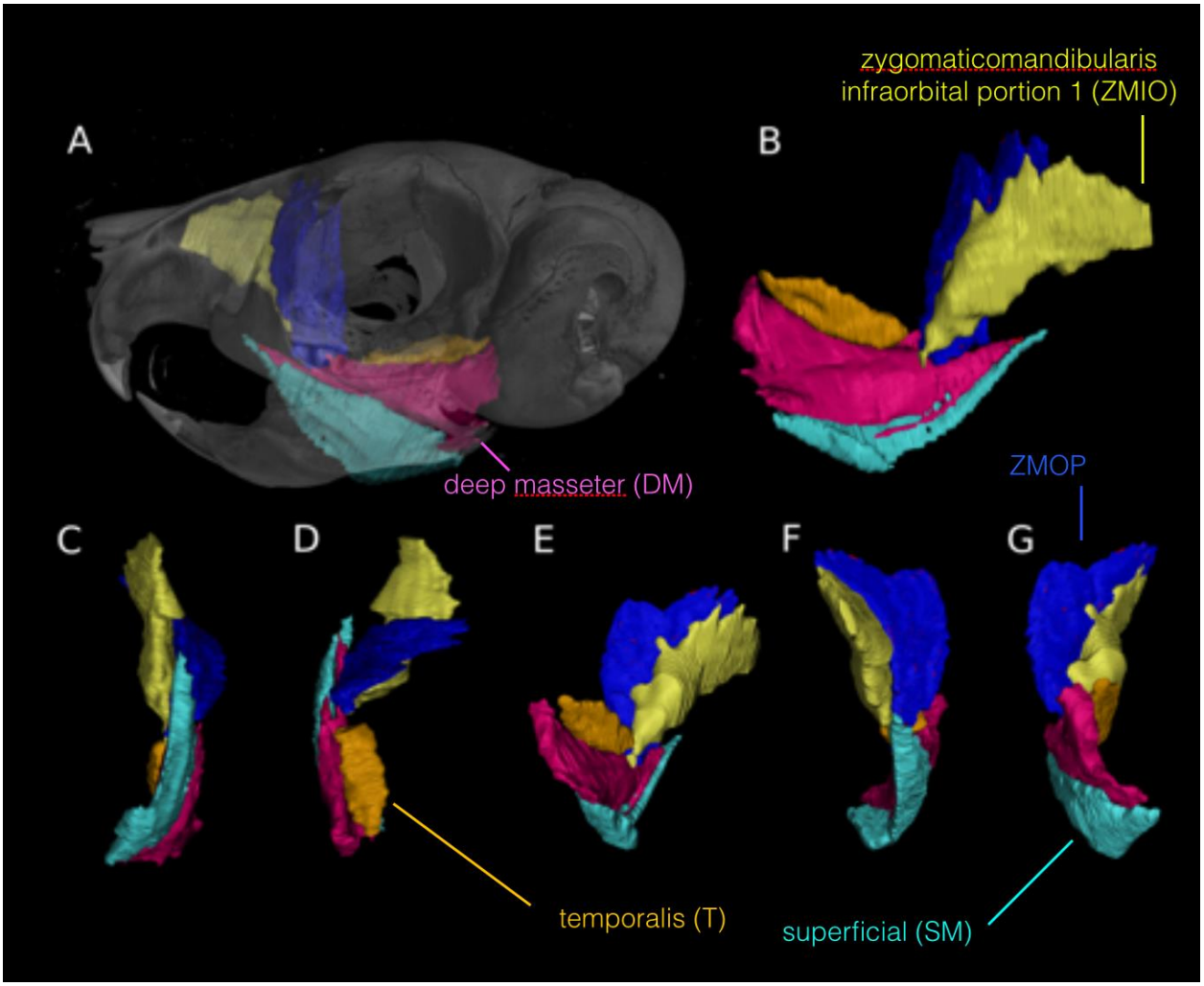

Figure 3.4. Adductor muscle reconstructions from iodine stained CT scans for *Jaculus jaculus* in A) lateral, B) medial, C) ventral, D) dorsal, E) posteromedial, F) anterior, and G) posterior views. Magenta = deep masseter, light blue = superficial masseter, yellow = ZMIO, dark blue = ZMOP, orange = temporalis.

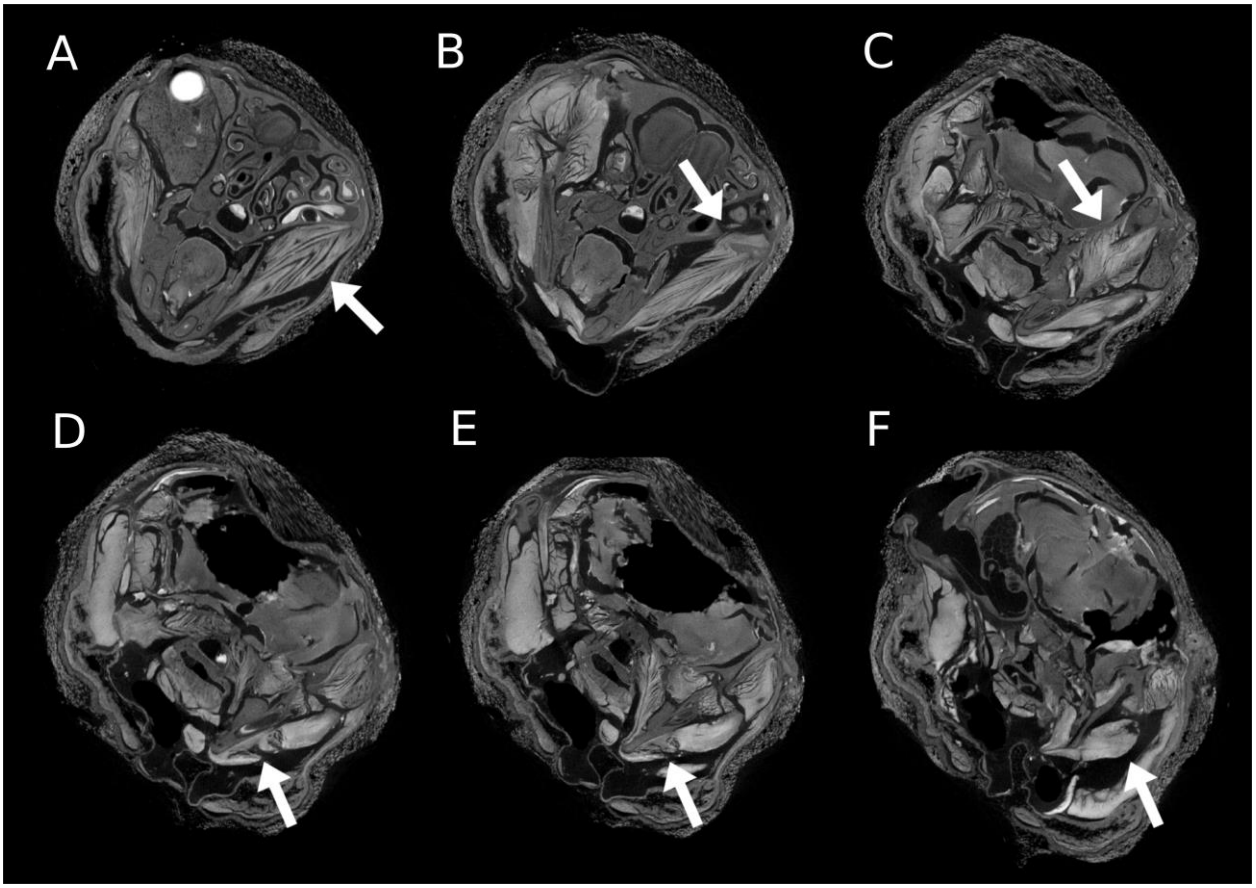

Figure 3.5. Iodine stained CT slices in approximately coronal view (slightly oblique) for *Heteromys desmarestianus* from anterior (A) to posterior (F), with dorsal at the top right and ventral at the bottom left. A) arrow points to left anterior deep masster, B) arrow points to split between anterior deep masseter ventral to the zygomatic plate and ZMOP, C) arrow points to medial temporalis attachments on the braincase with injury displacement, D-E) arrow points to ambiguous separation between the superficial masseter and ascending process of superficial masseter, F) arrow points to posterior swelling of posterior masseter onto accessory process of the angular.

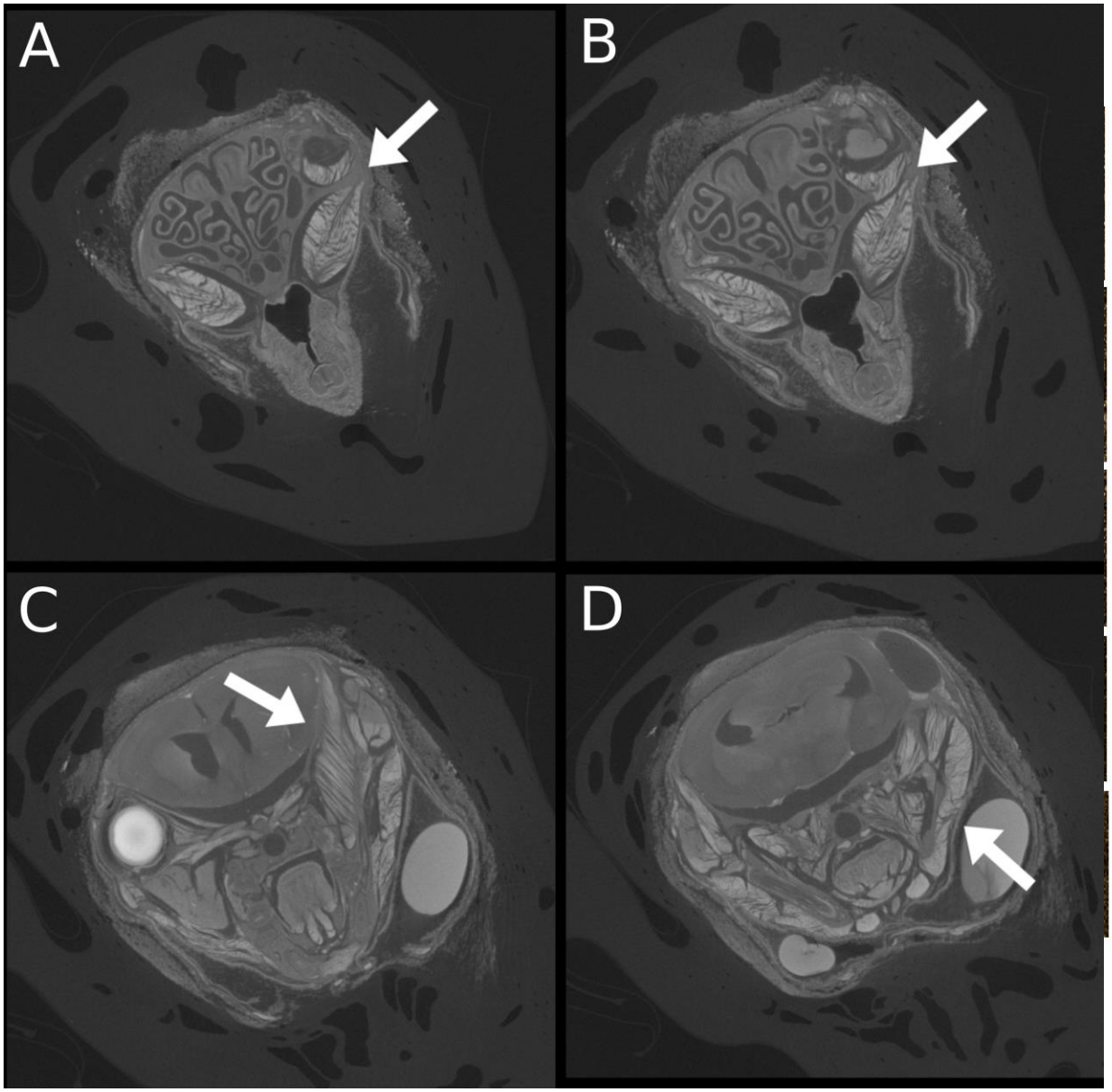

Figure 3.6. Iodine stained CT slices in approximately coronal view for *Chaetodipus formosus* from anterior (A) to posterior (D), with dorsal at the top left and ventral at the bottom right. A) arrow points to the bony split between the anterior deep masster and the ZMOP, B) arrow points to the split between anterior deep masseter and ZMOP posteroventral to the zygomatic plate, C) arrow points to medial temporalis attachments on the braincase, D) arrow points to the separation between the superficial masseter and the posterior masseter.

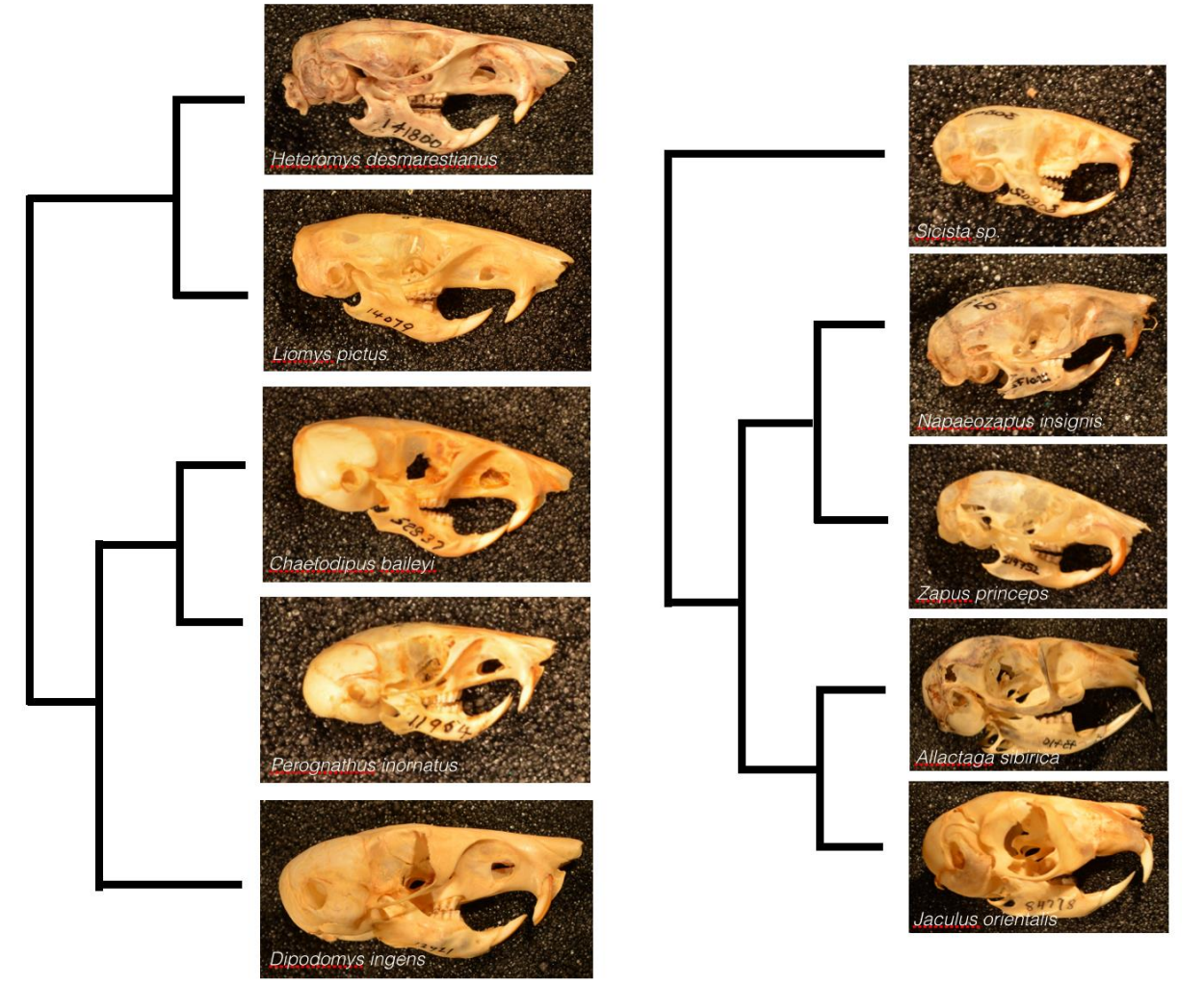

Figure 3.7. Phylogenetic relationships (modeled from Fabre et al. 2011) of heteromyid (left) and dipodoid (right) rodents under comparison.

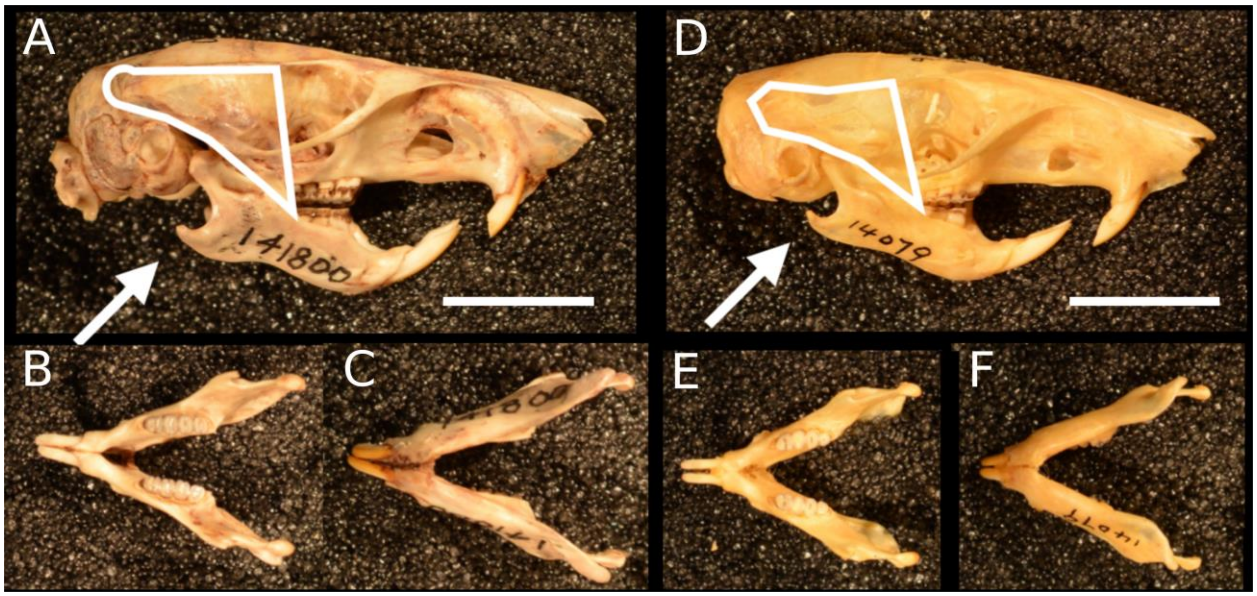

Figure 3.8. Skull morphology for A-C) *Heteromys desmarestianus* and D-F) *Liomys pictus* in right lateral view of the skull (A, D), and dorsal (B, E) and ventral (C, F) views of the mandible. Arrows point to accessory processes of the angular. White lines border temporalis attachment areas based on muscle scars. Scale bar = 10 mm. Mandible images not necessarily to scale.

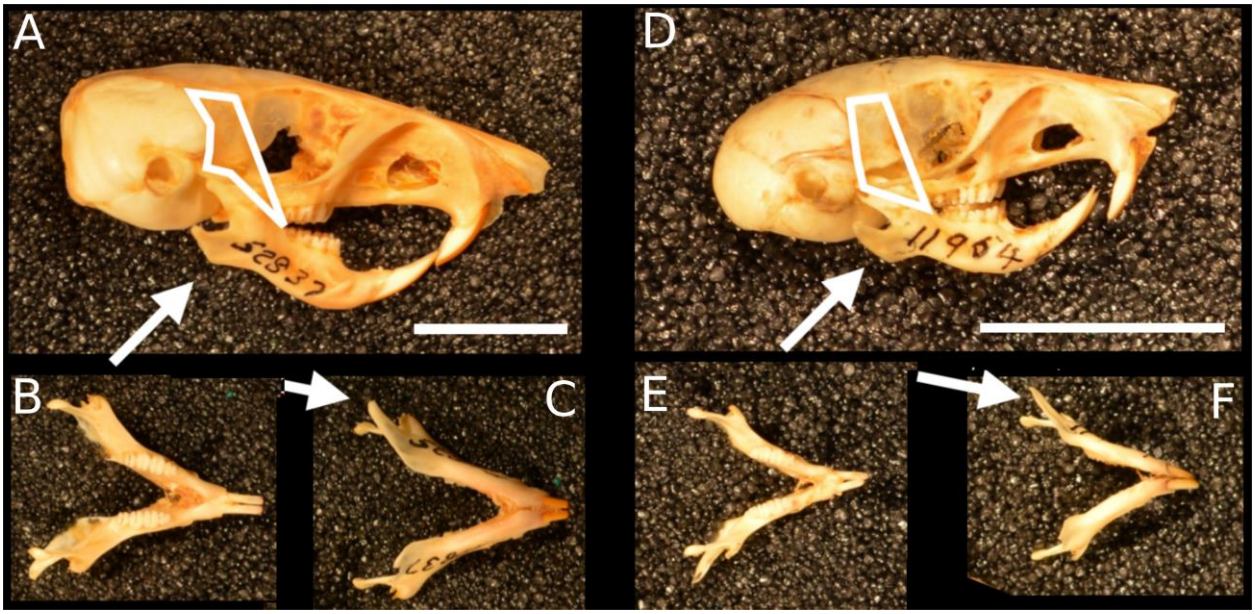

Figure 3.9. Skull morphology for A-C) *Chaetodipus baileyi* and D-F) *Perognathus inornatus* in right lateral view of the skull (A, D), and ventral (B, E) and dorsal (C, F) views of the mandible. Arrows point to accessory processes of the angular. White lines border temporalis attachment areas based on muscle scars. Scale bar = 10 mm. Mandible images not necessarily to scale.

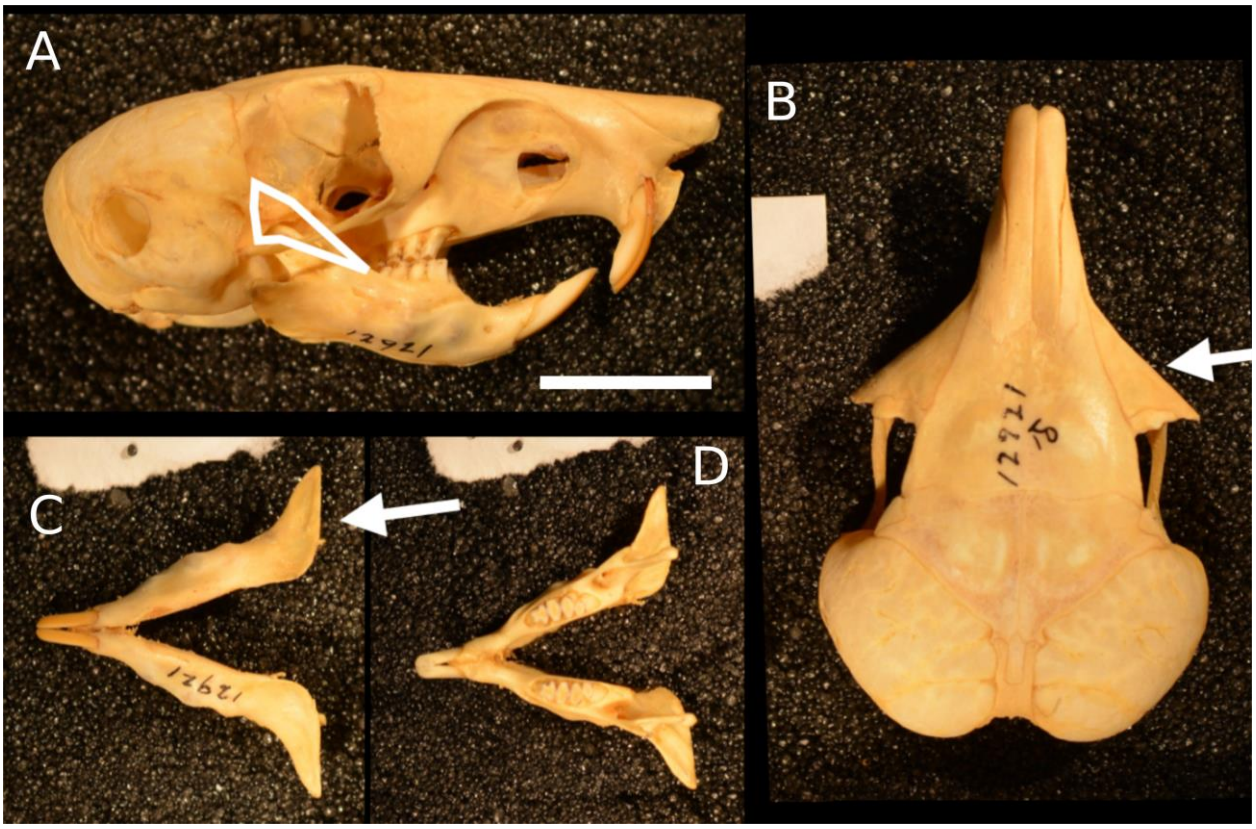

Figure 3.10. Skull morphology for *Dipodomys ingens* in right lateral view of the skull (A), dorsal cranial view (B), and dorsal (C) and ventral (D) views of the mandible. Arrows point B) external bulging of the anterior orbital fossa for the origination site of the ZMOP and C) to the accessory process of the angular. White lines border temporalis attachment areas based on muscle scars. Scale bar = 10 mm. Mandible images not necessarily to scale.

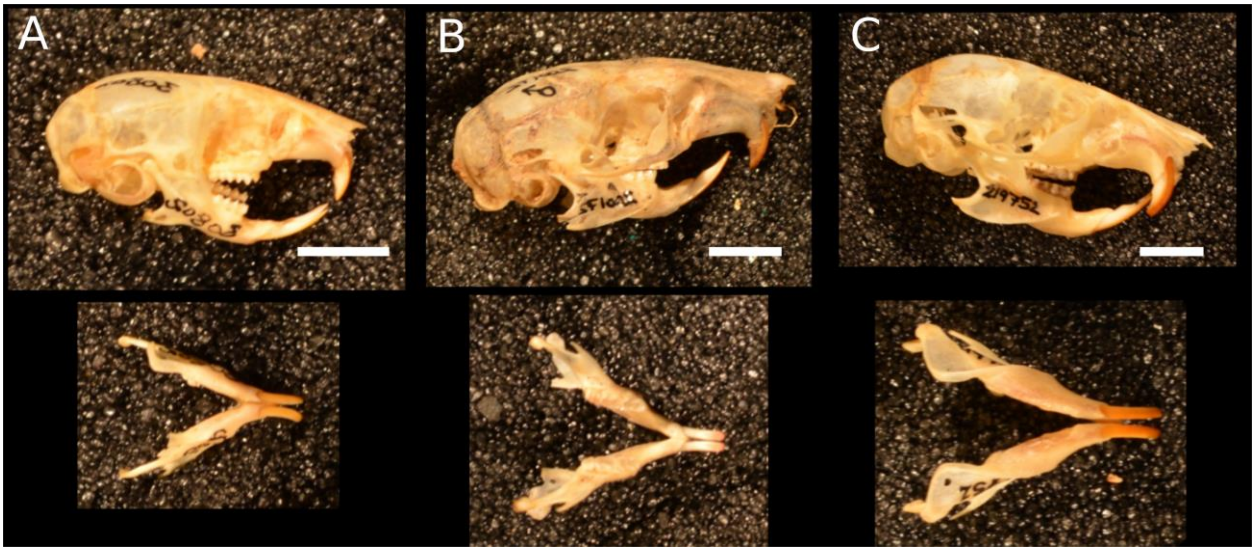

Figure 3.11. Skull morphology for A) *Sicista* sp. and B) *Napaeozapus insignis* and C) *Zapus princeps* in right lateral view of the skull and associated ventral and dorsal views of the mandible. Scale bar = 5 mm. Mandible images not necessarily to scale.

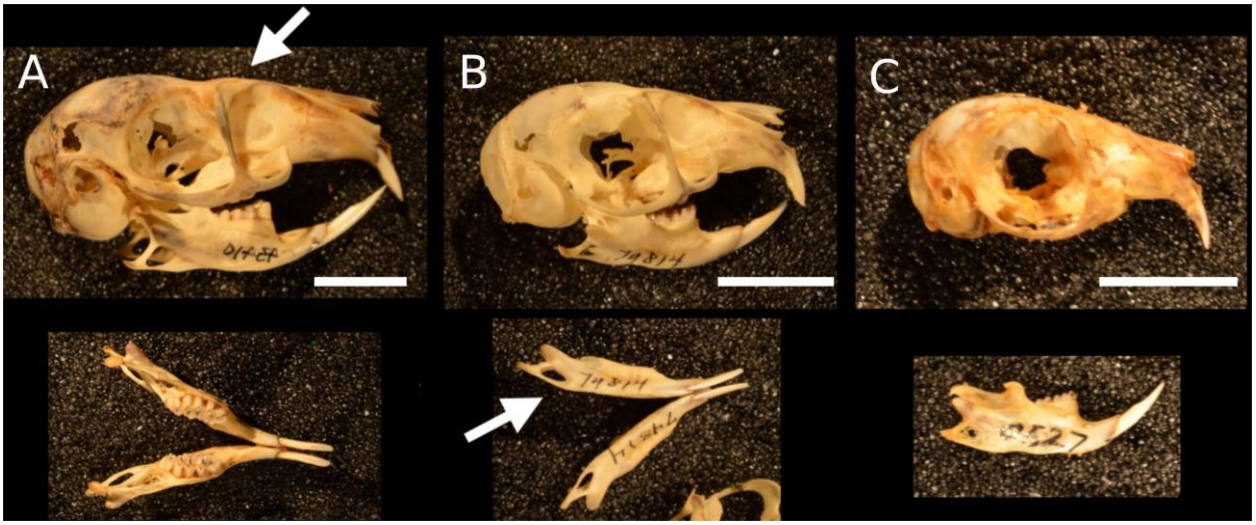

Figure 3.12. Skull morphology for A) *Allactaga sibiricus*. and B) *Allactaga tetradactyla* and C) *Pygeretmus pumilo* in right lateral view of the skull and associated dorsal, ventral, and lateral views of the mandible. Scale bar = 10 mm. Mandible images not necessarily to scale.

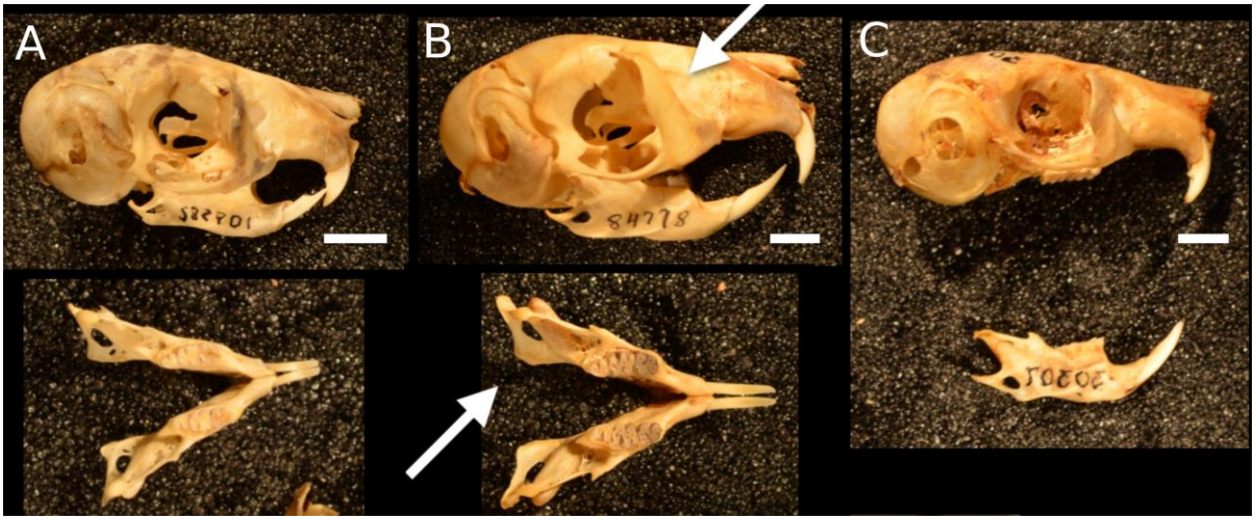

Figure 3.13. Skull morphology for A) *Jaculus jaculus*. and B) *Jaculus orientalis* and C) *Stylodipus telum* in right lateral view of the skull and associated ventral and lateral views of the mandible. White arrows point to bony swelling of the lateral infraorbital foramen wall for ZMOP originations (B, top) and medially inflected angular process (B, bottom). Scale bar = 5 mm. Mandible images not necessarily to scale in A-B.

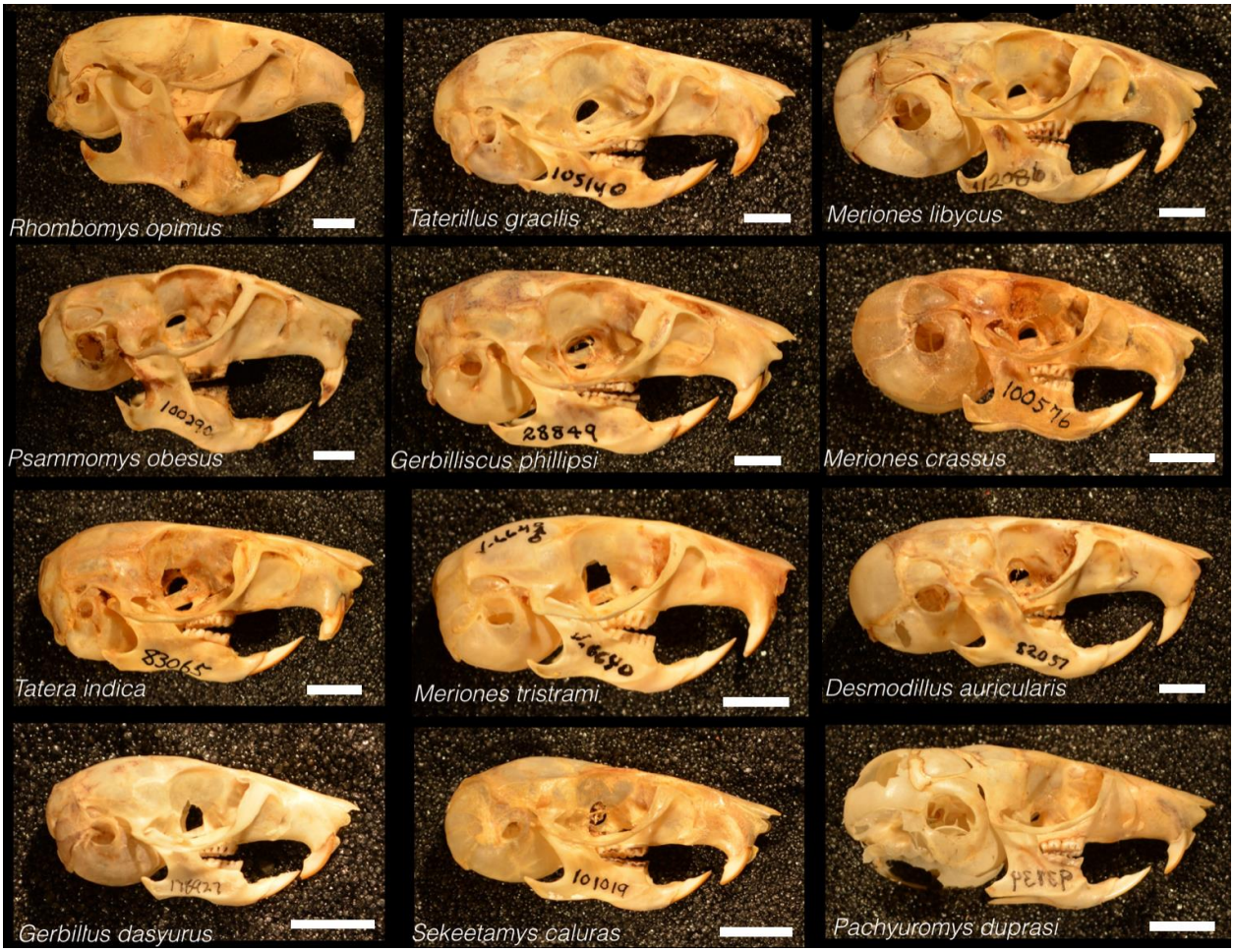

Figure 3.14. Skull morphology of Gerbillinae in right lateral view. Scale bar = 5 mm.

Appendix

Table A.1. Species list of sampled taxa with clade, morphotype, Field Museum of Natural History (FMNH) catalogue number, and sample size (not listed if 1). Continued on following pages.

Species names	Clade	Morphotype	FMNH #	Sample Size
Abrocoma_bennettii	Ctenohystrica	Hystricomorph	23148	
Abrothrix_longipilis	Muroidea	Myomorph	130256	
Aconaemys_sagei	Ctenohystrica	Hystricomorph	50762	
Aethomys_hindei	Muroidea	Myomorph	149720	
Akodon_aerosus	Muroidea	Myomorph	170460	
Alticola_roylei	Muroidea	Myomorph	103076	
Anomalurus_beecrofti	Anomaluromorpha	Hystricomorph	43659	
Aplodontia_rufa	Aplodontidae	Protrogomorph	6311, 6312, 6313	3
Apodemus_witherbyi	Muroidea	Myomorph	97442	
Apomys_abrae	Muroidea	Myomorph	62723	
Arborimus_longicaudus	Muroidea	Myomorph	51495	
Arvicanthis_niloticus	Muroidea	Myomorph	17229	
Arvicola_amphibius	Muroidea	Myomorph	112222	
Atherurus_africanus	Ctenohystrica	Hystricomorph	195178	
Auliscomys_pictus	Muroidea	Myomorph	21135	
Bandicota_bengalensis	Muroidea	Myomorph	104637	
Bathyergus_suillus	Ctenohystrica	Hystricomorph	99361	
Batomys_salomonseni	Muroidea	Myomorph	147931	
Beamys_hindei	Muroidea	Myomorph	219299	
Belomys_pearsonii	Sciuridae	Sciuromorph	114641	
Berylmys_bowersi	Muroidea	Myomorph	82975	
Brucepattersonius_iheringi	Muroidea	Myomorph	74895	
Bullimus_bagobus	Muroidea	Myomorph	61481	
Calomys_callosus	Muroidea	Myomorph	23374	
Cannomys_badius	Muroidea	Myomorph	112533	
Capromys_pilorides	Ctenohystrica	Hystricomorph	1140	

Carpomys_phaeurus	Muroidea	Myomorph	62291	
Castor_canadensis	Castorimorpha	Sciuromorph	180756, 138245, 14019	3
Cavia_porcellus	Ctenohystrica	Hystricomorph	88028, 88032, 88025	3
Cerradomys_maracajuensis	Muroidea	Myomorph	116761	
Chaetodipus_hispidus	Castorimorpha	Sciuromorph	6722, 6881, 6886	3
Chelemys_macronyx	Muroidea	Myomorph	132993	
Chinchilla_lanigera	Ctenohystrica	Hystricomorph	44345	
Chionomys_nivalis	Muroidea	Myomorph	35929	
Chiropodomys_gliroides	Muroidea	Myomorph	46721	
Chrotomys_mindorensis	Muroidea	Myomorph	142616, 150806, 142617	3
Clyomys_laticeps	Ctenohystrica	Hystricomorph	128349	
Coendou_mexicanus	Ctenohystrica	Hystricomorph	34993	
Coendou_pruinosus	Ctenohystrica	Hystricomorph	140261	
Coendou_rothschildi	Ctenohystrica	Hystricomorph	14181	
Colomys_goslingi	Muroidea	Myomorph	155977	
Crateromys_schadenbergi	Muroidea	Myomorph	62294, 62295	2
Cricetus_cricetus	Muroidea	Myomorph	6422	
Cryptomys_hottentotus	Ctenohystrica	Hystricomorph	56295	
Ctenomys_colburni	Ctenohystrica	Hystricomorph	134295	
Ctenomys_fulvus	Ctenohystrica	Hystricomorph	23225	
Ctenomys_magellanicus	Ctenohystrica	Hystricomorph	50742, 50744, 50745	3
Ctenomys_minutus	Ctenohystrica	Hystricomorph	98291	
Ctenomys_steinbachi	Ctenohystrica	Hystricomorph	51894	
Cuniculus_taczanowskii	Ctenohystrica	Hystricomorph	75126	
Dacnomys_millardi	Muroidea	Myomorph	84892	
Dasymys_incomtus	Muroidea	Myomorph	28635	
Dasyprocta_azarae	Ctenohystrica	Hystricomorph	52334	
Dasyprocta_leporina	Ctenohystrica	Hystricomorph	95778, 95790, 95791	3

Delomys_collinus	Muroidea	Myomorph	136938	
Dendromus_nyasae	Muroidea	Myomorph	163572	
Desmodillus_auricularis	Muroidea	Myomorph	38763	
Desmomys_harringtoni	Muroidea	Myomorph	28718	
Dicrostonyx_groenlandicus	Muroidea	Myomorph	200259	
Dicrostonyx_richardsoni	Muroidea	Myomorph	200270	
Dinaromys_bogdanovi	Muroidea	Myomorph	165342	
Dinomys_branickii	Ctenohystrica	Hystricomorph	34702	
Dipodomys_deserti	Castorimorpha	Sciuromorph	12961	
Dipodomys_merriami	Castorimorpha	Sciuromorph	125206, 125207, 125208, 125209	4
Dipodomys_microps	Castorimorpha	Sciuromorph	12987	
Dolichotis_salinicola	Ctenohystrica	Hystricomorph	54337	
Dremomys_rufigenis	Sciuridae	Sciuromorph	32282, 32281, 32283	3
Dryomys_nitedula	Gliridae	Myomorph	82165	
Echimys_chrysurus	Ctenohystrica	Hystricomorph	93267	
Eligmodontia_typus	Muroidea	Myomorph	133035	
Eliomys_melanurus	Muroidea	Myomorph	101510, 101519, 101523	3
Eliurus_webbi	Muroidea	Myomorph	173224	
Ellobius_fuscocapillus	Muroidea	Myomorph	112511	
Ellobius_talpinus	Muroidea	Myomorph	28944	
Eospalax_fontanierii	Muroidea	Myomorph	19070	
Eothenomys_melanogaster	Muroidea	Myomorph	36455	
Eremoryzomys_polius	Muroidea	Myomorph	19763	
Erethizon_dorsatum	Ctenohystrica	Hystricomorph	105057	
Euneomys_chinchilloides	Muroidea	Myomorph	133083	
Euryoryzomys_macconnelli	Muroidea	Myomorph	75275	
Euryzygomatomys_spinosus	Ctenohystrica	Hystricomorph	26637	
Exilisciurus_concinnus	Sciuridae	Sciuromorph	67746, 87471	2

Fukomys_mechowi	Ctenohystrica	Hystricomorph	81753	
Funisciurus_congicus	Sciuridae	Sciuromorph	81799, 81796, 81794, 81792, 81790	5
Galea_musteloides	Ctenohystrica	Hystricomorph	21510	
Galea_spixii	Ctenohystrica	Hystricomorph	20278	
Geocapromys_brownii	Ctenohystrica	Hystricomorph	34198	
Geomys_bursarius	Castorimorpha	Sciuromorph	123429, 123428, 123427	3
Georychus_capensis	Ctenohystrica	Hystricomorph	58659	
Geoxus_valdivianus	Muroidea	Myomorph	133124	
Gerbilliscus_kempi	Muroidea	Myomorph	25370	
Glaucomys_volans	Sciuridae	Sciuromorph	4753, 4757, 4756	3
Glis_glis	Gliridae	Myomorph	97654, 97671	2
Golunda_ellioti	Muroidea	Myomorph	83031	
Grammomys_dolichurus	Muroidea	Myomorph	17119	
Graphiurus_kelleni	Gliridae	Hystricomorph	151364	
Graphiurus_murinus	Gliridae	Hystricomorph	149344, 149346, 149347	3
Gymnuromys_roberti	Muroidea	Myomorph	169253	
Habromys_lophurus	Muroidea	Myomorph	41744	
Handleyomys_rostratus	Muroidea	Myomorph	14415	
Heimyscus_fumosus	Muroidea	Myomorph	167810	
Heliophobius_argenteocinere	Ctenohystrica	Hystricomorph	204997, 204995, 158272, 158274	4
Heterocephalus_glaber	Ctenohystrica	Hystricomorph	186440, 186441, 186442	3
Heteromys_desmarestianus	Castorimorpha	Sciuromorph	128429, 128431, 128432, 128433	4
Hodomys_alleni	Muroidea	Myomorph	47446	
Holochilus_brasiliensis	Muroidea	Myomorph	23307	
Hoplomys_gymnurus	Ctenohystrica	Hystricomorph	90122	
Hybomys_lunaris	Muroidea	Myomorph	149063	
Hydrochoerus_hydrochaeris	Ctenohystrica	Hystricomorph	26879, 34361, 125071, 36058, 68914	5
Hylaeamys_megacephalus	Muroidea	Myomorph	117108	

Hypogeomys_antimena	Muroidea	Myomorph	161571	
Hystrix_indica	Ctenohystrica	Hystricomorph	25724	
Hystrix_pumila	Ctenohystrica	Hystricomorph	62923	
Ictidomys_tridecemlineatus	Sciuridae	Sciuromorph	152087, 41094	2
Iomys_horsfieldii	Sciuridae	Sciuromorph	108898, 108900	2
Irenomys_tarsalis	Muroidea	Myomorph	134970	
Isthmomys_flavidus	Muroidea	Myomorph	14307	
Kannabateomys_amblyonyx	Ctenohystrica	Hystricomorph	94352	
Kerodon_rupestris	Ctenohystrica	Hystricomorph	20234	
Kunsia_tomentosus	Muroidea	Myomorph	122711	
Lagidium_peruanum	Ctenohystrica	Hystricomorph	20970, 52724, 52723	3
Lagidium_viscacia	Ctenohystrica	Hystricomorph	53672	
Lagostomus_maximus	Ctenohystrica	Hystricomorph	54340	
Lasiopodomys_brandtii	Muroidea	Myomorph	30910	
Lemmus_trimucronatus	Muroidea	Myomorph	7126	
Lemniscomys_striatus	Muroidea	Myomorph	86182	
Lenoxus_apicalis	Muroidea	Myomorph	52612	
Leopoldamys_edwardsi	Muroidea	Myomorph	39901	
Limnomys_bryophilus	Muroidea	Myomorph	148056	
Liomys_salvini	Castorimorpha	Sciuromorph	36715	
Lophiomys_imhausi	Muroidea	Myomorph	85244	
Loxodontomys_micropus	Muroidea	Myomorph	13654	
Lundomys_molitor	Muroidea	Myomorph	29257	
Macrotarsomys_ingens	Muroidea	Myomorph	161603	
Makalata_didelphoides	Ctenohystrica	Hystricomorph	140817	
Malacomys_longipes	Muroidea	Myomorph	148664	
Malacothrix_typica	Muroidea	Myomorph	38557	
Marmota_monax	Sciuridae	Sciuromorph	22239, 63957	2

Massoutiera_mzabi	Ctenohystrica	Hystricomorph	48806	
Mastomys_natalensis	Muroidea	Myomorph	128263	
Maxomys_rajah	Muroidea	Myomorph	76956	
Megadontomys_thomasi	Muroidea	Myomorph	47497	
Melanomys_chrysomelae	Muroidea	Myomorph	35208	
Melomys_burtoni	Muroidea	Myomorph	120706	
Menetes_berdmorei	Sciuridae	Sciuromorph	46654, 46653, 46652	3
Meriones_rex	Muroidea	Myomorph	77956, 77950, 77953	3
Mesembriomys_macrurus	Muroidea	Myomorph	120720	
Mesocricetus_auratus	Muroidea	Myomorph	90949	
Microcavia_niata	Ctenohystrica	Hystricomorph	53656, 53655, 53654, 53662	4
Microdipodops_megacephalu	Castorimorpha	Sciuromorph	52417	
Micromys_minutus	Muroidea	Myomorph	40581	
Microsciurus_alfari	Sciuridae	Sciuromorph	35193, 35194	2
Microtus_pennsylvanicus	Muroidea	Myomorph	106848	
Microtus_quasiater	Muroidea	Myomorph	52387	
Microtus_subterraneus	Muroidea	Myomorph	65380	
Microtus_townsendii	Muroidea	Myomorph	9338	
Millardia_meltada	Muroidea	Myomorph	35296	
Monticolomys_koopmani	Muroidea	Myomorph	162099	
Mus_triton	Muroidea	Myomorph	173403	
Muscardinus_avellanarius	Gliridae	Myomorph	74345	
Myocastor_coypus	Ctenohystrica	Hystricomorph	24344, 25258	2
Myodes_californicus	Muroidea	Myomorph	206855	
Myoprocta_acouchy	Ctenohystrica	Hystricomorph	50897	
Myoprocta_pratti	Ctenohystrica	Hystricomorph	88911	
Mysateles_prehensilis	Ctenohystrica	Hystricomorph	1141	
Nannosciurus_melanotis	Sciuridae	Sciuromorph	18038, 18039	2

Necromys_lasiurus	Muroidea	Myomorph	25196	
Nectomys_squamipes	Muroidea	Myomorph	25739	
Neodon_sikimensis	Muroidea	Myomorph	114330	
Neofiber_alleni	Muroidea	Myomorph	7911	
Neotoma_cinerea	Muroidea	Myomorph	91117	
Neotoma_floridana	Muroidea	Myomorph	6764	
Neotomodon_alstoni	Muroidea	Myomorph	55817	
Nephelomys_devius	Muroidea	Myomorph	43998	
Nesokia_indica	Muroidea	Myomorph	103749	
Nesomys_rufus	Muroidea	Myomorph	159477	
Nesoryzomys_indefessus	Muroidea	Myomorph	30841	
Neusticomys_monticolus	Muroidea	Myomorph	71220	
Niviventer_confucianus	Muroidea	Myomorph	36644	
Niviventer_tenaster	Muroidea	Myomorph	168785	
Notomys_alexis	Muroidea	Myomorph	104946	
Nyctomys_sumichrasti	Muroidea	Myomorph	73501	
Ochrotomys_nuttalli	Muroidea	Myomorph	200844	
Octodon_degus	Ctenohystrica	Hystricomorph	119756, 119757, 119768	3
Octodontomys_gliroides	Ctenohystrica	Hystricomorph	23642	
Oecomys_phaeotis	Muroidea	Myomorph	75223	
Oenomys_hypoxanthus	Muroidea	Myomorph	81920	
Olallamys_albicauda	Ctenohystrica	Hystricomorph	71128	
Ondatra_zibethicus	Muroidea	Myomorph	52412, 5422	2
Onychomys_arenicola	Muroidea	Myomorph	125257	
Onychomys_leucogaster	Muroidea	Myomorph	52778	
Orthogeomys_grandis	Castorimorpha	Sciuromorph	41766	
Orthogeomys_heterodus	Castorimorpha	Sciuromorph	34945	
Oryzomys_couesi	Muroidea	Myomorph	56028	

Oryzomys_palustris	Muroidea	Myomorph	201777	
Otomys_angoniensis	Muroidea	Myomorph	86198	
Otomys_orestes	Muroidea	Myomorph	16699	
Ototylomys_phyllotis	Muroidea	Myomorph	64565	
Oxymycterus_rufus	Muroidea	Myomorph	122697	
Pachyuromys_duprasi	Muroidea	Myomorph	84643	
Pappogeomys_tylorhinus	Castorimorpha	Sciuromorph	141793	
Paramelomys_moncktoni	Muroidea	Myomorph	54066	
Parotomys_littledalei	Muroidea	Myomorph	80885	
Pectinator_spekei	Ctenohystrica	Hystricomorph	1438	
Pedetes_capensis	Anomaluromorpha	Hystricomorph	38236, 38254, 38266	3
Perognathus_amplus	Castorimorpha	Sciuromorph	140708	
Perognathus_inornatus	Castorimorpha	Sciuromorph	11956	
Peromyscus_aztecus	Muroidea	Myomorph	41707	
Peromyscus_maniculatus	Muroidea	Myomorph	159895	
Petaurista_magnificus	Sciuridae	Sciuromorph	112560, 114367, 114366, 114363	4
Petromyscus_shortridgei	Muroidea	Myomorph	35306	
Phenacomys_intermedius	Muroidea	Myomorph	126822	
Phloeomys_pallidus	Muroidea	Myomorph	214419, 214420, 193967	3
Phyllotis_darwini	Muroidea	Myomorph	119493	
Podomys_floridanus	Muroidea	Myomorph	171196	
Praomys_delectorum	Muroidea	Myomorph	181200	
Prometheomys_schaposchni	Muroidea	Myomorph	92947	
Protoxerus_stangeri	Sciuridae	Sciuromorph	54428, 55776, 54481, 149005	4
Psammomys_obesus	Muroidea	Myomorph	84165	
Pteromys_volans	Sciuridae	Sciuromorph	92938	
Rattus_everetti	Muroidea	Myomorph	62333	
Rattus_exulans	Muroidea	Myomorph	142891	

Rattus_verecundus	Muroidea	Myomorph	128382	
Ratufa_affinis	Sciuridae	Sciuromorph	85940	
Ratufa_bicolor	Sciuridae	Sciuromorph	35432, 35440	2
Reithrodontomys_creper	Muroidea	Myomorph	128546	
Rhabdomys_dilectus	Muroidea	Myomorph	168126	
Rheithrosciurus_macrotis	Sciuridae	Sciuromorph	88615, 88616, 88617, 88614	4
Rhinosciurus_laticaudatus	Sciuridae	Sciuromorph	98523, 98525	2
Rhipidomys_leucodactylus	Muroidea	Myomorph	24831	
Rhizomys_pruinosus	Muroidea	Myomorph	84849	
Rhizomys_sumatrensis	Muroidea	Myomorph	39137	
Rhombomys_opimus	Muroidea	Myomorph	103552	
Saccostomus_campestris	Muroidea	Myomorph	38693	
Scapteromys_tumidus	Muroidea	Myomorph	98286	
Sciurillus_pusillus	Sciuridae	Sciuromorph	140797	
Sciurotamias_davidianus	Sciuridae	Sciuromorph	18923, 37777, 45963	3
Sciurus_carolinensis	Sciuridae	Sciuromorph	154676, 154675, 154679, 154678	4
Sciurus_niger	Sciuridae	Sciuromorph	196124, 214924	2
Sekeetamys_calurus	Muroidea	Myomorph	101028	
Sigmodon_hispidus	Muroidea	Myomorph	16509	
Spalacopus_cyanus	Ctenohystrica	Hystricomorph	23014, 23015, 23018	3
Spalax_leucodon	Muroidea	Myomorph	100996	
Spermophilopsis_leptodacty	Sciuridae	Sciuromorph	102903, 102904, 102905	3
Steatomys_parvus	Muroidea	Myomorph	187161	
Stenocephalemys_albipes	Muroidea	Myomorph	229694	
Stenocephalemys_griseicau	Muroidea	Myomorph	27817	
Stochomys_longicaudatus	Muroidea	Myomorph	74224	
Sundamys_infralutens	Muroidea	Myomorph	108936	
Synaptomys_cooperi	Muroidea	Myomorph	18303	

Tachyoryctes_ruandae	Muroidea	Myomorph	173304	
Tamias_ruficaudus	Sciuridae	Sciuromorph	137120, 137121, 137122	3
Tamiasciurus_hudsonicus	Sciuridae	Sciuromorph	5819, 5823, 5821	3
Tatera_indica	Muroidea	Myomorph	103282	
Taterillus_gracilis	Muroidea	Myomorph	105141	
Thomasomys_cinereiventer	Muroidea	Myomorph	71362	
Thomasomys_ischyrus	Muroidea	Myomorph	94990	
Thomomys_bottae	Sciuridae	Sciuromorph	12353, 12354, 12355	3
Thomomys_bulbivorus	Sciuridae	Sciuromorph	9446	
Thomomys_talpoides	Sciuridae	Sciuromorph	53886	
Thrichomys_fosteri	Ctenohystrica	Hystricomorph	18202	
Thryonomys_gregorianus	Ctenohystrica	Hystricomorph	108212, 160977, 161146	3
Toromys_rhipidurus	Ctenohystrica	Hystricomorph	87251	
Transandinomys_bolivaris	Muroidea	Myomorph	128491	
Trichys_fasciculata	Ctenohystrica	Hystricomorph	68751	
Trinomys_albispinus	Ctenohystrica	Hystricomorph	20402	
Trogopterus_xanthipes	Sciuridae	Sciuromorph	39834	
Tylomys_nudicaudus	Muroidea	Myomorph	71215	
Typhlomys_cinereus	Muroidea	Myomorph	41300	
Uromys_caudimaculatus	Muroidea	Myomorph	60964	
Voalavo_antsahabensis	Muroidea	Myomorph	188758	
Xerus_inauris	Sciuridae	Sciuromorph	38280, 38282, 38283	3
Zelotomys_hildegardeae	Muroidea	Myomorph	16953	
Zygodontomys_brevicauda	Muroidea	Myomorph	87992	
Zygogeomys_trichopus	Muroidea	Myomorph	51970, 51971, 51972	3
Zyzomys_argurus	Muroidea	Myomorph	120386	